Center of Diagnostics

University Medical Center Hamburg- Eppendorf

and

Leibniz Institute of Virology

Host factors and T cell responses in congenital cytomegalovirus infection and T cell diagnostics in SARS-CoV-2

Dissertation

Submitted to the

Department of Chemistry

Faculty of Mathematics, Informatics and Natural Sciences

University of Hamburg

In fulfillment of the requirements

For the degree of

Doctor of Natural Sciences (Dr. rer. nat.)

By

Luís Fonseca Brito

(born in Lisbon, Portugal)

Hamburg 2024

Prof. Dr. Wolfram Brune (First Reviewer)

Prof. Dr. Hans-Willi Mittrücker (Second Reviewer)

Date of oral defense: 24.01.2025

This study was conducted between November 2018 and July 2024 at the Center of Diagnostics of the University Medical Center Hamburg-Eppendorf and the Leibniz Institute of Virology under the supervision of Prof. Dr. Felix R. Stahl and Prof. Dr. Wolfram Brune.

Publications and presentations

Part of the work presented in this thesis was published in:

Cytomegalovirus (CMV) Pneumonitis: Cell Tropism, Inflammation, and Immunity

L. Fonseca Brito, W. Brune, and F. R. Stahl. International Journal of Molecular Science, August 2019

Inefficient Placental Virus Replication and Absence of Neonatal Cell-Specific Immunity Upon Sars-CoV-2 Infection During Pregnancy

A.-C. Tallarek, C. Urbschat, L. Fonseca Brito, S. Stanelle-Bertram, S. Krasemann, G. Frascaroli, K. Thiele, A. Wieczorek, N. Felber, M. Lütgehetmann, U. R. Markert, K. Hecher, W. Brune, F. R. Stahl, G. Gabriel, A. Diemert, and P. C. Arck. Frontiers in Immunology, June 2021

Performance of an interferon-γ release assay-based test for cell-mediated immunity to SARS-CoV-2

L. Fonseca Brito, S. Tödter, J. Kottlau, K. Cermann, A. Spier, E. Petersen, I. Schäfer, R. Twerenbold, M. Aepfelbacher, M. Lütgehetmann, and F. R. Stahl. Frontiers in Immunology, February 2023

Limited protection against early-life cytomegalovirus infection results from deficiency of cytotoxic CD8 T cells

L. Fonseca Brito, E. Ostermann, A. Perez, S. Tödter, S. Virdi, D. Indenbirken, L. Glau, A. Gieras, R. Brixel, R. Arens, A. Grundhoff, P. Arck, A. Diemert, E. Tolosa, W. Brune, F. R. Stahl. bioRxiv, July 2024

Delayed induction of noninflammatory SARS-CoV-2 spike-specific IgG4 antibodies detected 1 year after BNT162b2 vaccination in children
R. Kobbe, C. Rau, U. Schulze-Sturm, F. Stahl, L. Fonseca Brito, A. Diemert, M. Lutgehetmann, M.M. Addo, P. Arck, L.M. Weskamm. The Pediatric Infectious Disease Journal, October 2024

Parts of this work was presented at the following conferences:

Date	Conference	Type of presentation
September 2019	LIV Scientific Retreat	Oral presentation
September 2022	Annual meeting of the German Society for Immunology (DGfI) and the Austrian Society for Allergology and Immunology (ÖGAI)	Oral presentation
May 2023	LIV Scientific Retreat	Oral presentation
July 2023	DEEP-DV International Symposium	Poster presentation
September 2024	16th Mini Herpesvirus Workshop	Oral presentation

Contents

1 Abstract

Viral infections remain a significant cause of morbidity and mortality worldwide. Of these, congenital infection with human cytomegalovirus (HCMV) is the leading non-genetic cause of long-lasting disabilities in newborns. However, the precise mechanisms underlying increased susceptibility to congenital HCMV infection and disease are unclear.

While mouse models are the most used to study virus-host interactions, the murine cytomegalovirus (MCMV) is not able to cross the materno-fetal barrier and infect the fetus, and the mechanisms of fetal protection are incompletely understood. This thesis aimed to decipher cellular mechanisms at the materno-fetal barrier that prevent the fetus from being infected with MCMV. Primary placental cells and placenta trophoblast cell lines exhibited low susceptibility to infection with MCMV. This was associated with a low expression of the host factor neuropilin-1, and artificial expression of this protein increased cell susceptibility to infection. These results suggest a new mechanism of protection where cells that form the murine materno-fetal barrier exhibit low susceptibility to MCMV infection, resulting in protection of the fetus from vertical infection *in utero*.

T cells are important in clearing CMV infections, but their role in congenital CMV disease is unclear. In a mouse model of congenital disease, neonates exhibited a delayed expansion of MCMV-specific T cells which was associated with a low number of T cells in early life. Adoptive transfer of polyclonal or antigen-specific T cells into neonates were not protective due to a deficient CD8 T cell differentiation into cytotoxic phenotypes. This deficiency was associated with lower concentrations of gamma-chain cytokines critical for priming and maintenance of cytotoxic CD8 T cells. In a clinical cohort of HCMV-exposed newborns, low frequencies of highly cytotoxic CD8 T cell subsets were detected, in line with the increased susceptibility to HCMV disease in early life. In summary, deficient priming of CD8 T cells in congenital CMV infection can contribute to increased disease susceptibility.

Virus-specific T cell responses are generated upon viral infections, but their diagnostic potential is under-recognized. With the advent of the SARS-CoV-2 pandemic, this thesis aimed to establish cell-mediated immunity (CMI) tests that identify previous SARS-CoV-2 infections. A total of 522 individuals were enrolled in the early phases of

the pandemic and, using a certified chemiluminescence immunoassay, interferon-gamma release into supernatants was measured after T cell stimulations with spike and nucleocapsid peptide pools. Test performances were calculated applying cutoff values with the highest Youden indices and compared to a commercially available serologic test. CMI tests performed similarly to a commercially available SARS-CoV-2 antibody test and were less affected by confounding effects such as time from positive PCR result, diabetes and dyslipidemia. In conclusion, CMI tests are simple, cost-effective tests that accurately identify adaptive T cell immunity in SARS-CoV-2 convalescent individuals.

2 Zusammenfassung

Virusinfektionen sind weltweit nach wie vor eine wichtige Ursache für Morbidität und Mortalität. Die kongenitale Infektion mit dem humanen Cytomegalovirus ist die häufigste nicht-genetische Ursache für bleibende Schäden bei Neugeborenen. Die genauen Mechanismen, die einer erhöhten Anfälligkeit für HCMV-Infektionen und -Erkrankungen im frühen Leben zugrunde liegen, sind jedoch noch unklar.

Das murine Cytomegalovirus (MCMV) kann nicht die materno-fetale Barriere überwinden und den Fötus infizieren, und die Mechanismen des fötalen Schutzes sind nur unvollständig bekannt. Ziel dieser Arbeit war es, die zellulären Mechanismen an der materno-fetalen Barriere zu identifizieren, die eine Infektion des Feten mit MCMV verhindern. Primäre Plazentazellen und plazentare Trophoblastenzelllinien zeigten eine geringe Empfänglichkeit gegenüber einer Infektion mit MCMV. Dies war mit einer geringen Expression des Wirtsfaktors Neuropilin-1 verbunden, und die artifizielle Expression dieses Proteins erhöhte die Empfänglichkeit der Zellen. Zusammengenommen deuten diese Ergebnisse darauf hin, dass die Zellen, die die materno-fetale Barriere der Maus bilden, protektive Eigenschaften gegen eine MCMV-Infektion aufweisen und den Fötus vor einer vertikalen Übertragung *in utero* schützen.

T-Zellen spielen eine wichtige Rolle bei der Bekämpfung von CMV-Infektionen, aber ihre Rolle bei kongenitalen CMV-Erkrankungen ist unklar. In einem Mausmodell der kongenitalen Infektion zeigten Neugeborene eine verzögerte Expansion MCMV-spezifischer T-Zellen, was mit einer niedrigen Anzahl von T-Zellen in der frühen Lebensphase zusammenhing. Der adoptive Transfer von polyklonalen oder antigenspezifischen T-Zellen hatte keinen schützenden Effekt, da die CD8-T-Zellen nicht in zytotoxische Phänotypen differenzierten. Dieser Defekt war mit niedrigeren Konzentrationen von Gamma-Ketten-Cytokinen verbunden, die für das Priming zytotoxischer CD8-T-Zellen essentiell sind. In einer klinischen Kohorte von HCMV-exponierten Neugeborenen wurde eine geringe Frequenz hochzytotoxischer CD8 T-Zell-Subpopulationen festgestellt, was mit der erhöhten Anfälligkeit für HCMV-Erkrankungen im frühen Leben übereinstimmt. Diese Ergebnisse deuten darauf hin, dass ein unzureichendes Priming von CD8-T-Zellen während der kongenitalen CMV-Infektion zu einer erhöhten Krankheitsanfälligkeit beiträgt.

Virusspezifische T-Zell-Antworten werden bei Virusinfektionen erzeugt, aber ihr diagnostisches Potenzial ist noch nicht ausreichend erkannt. Mit dem Ausbruch der

SARS-CoV-2-Pandemie zielte diese Arbeit darauf ab, zellvermittelte Immunitätstests (CMI) zur Identifizierung früher SARS-CoV-2-Infektionen zu etablieren. Insgesamt wurden 522 Personen in den frühen Phasen der Pandemie rekrutiert, um die Interferon-gamma-Freisetzung in Überständen nach T-Zell-Stimulation mit Spike- und Nukleokapsid-Peptid-Pools mit einem zertifizierten Chemilumineszenz-Immunoassay zu messen. Die Testleistung wurde unter Verwendung der Schwellenwerte mit den höchsten Youden-Indizes berechnet und mit einem kommerziell erhältlichen serologischen Test verglichen. Diese CMI-Tests zeigten vergleichbare Ergebnisse wie die kommerziell erhältlichen SARS-CoV-2-Antikörpertests und wurden weniger durch Störfaktoren wie die Zeit nach einem positiven PCR-Ergebnis, Diabetes und Dyslipidämie beeinflusst. Zusammenfassendkann gesagt werden, dass CMI-Tests praktikable, kostengünstige Tests sind, die die adaptive T-Zell-Immunität bei rekonvaleszenten SARS-CoV-2-Patienten genau bestimmen.

3 Introduction

3.1 Immune system

The immune system is an intricate network of cells and molecules that cooperate to protect the host organism against infectious pathogens and tumors. To accomplish this vital function, strict mechanisms that differentiate “self” and “non-self” entities (antigens) must be engaged. Once a foreign antigen has been identified, the immune system triggers a range of responses to selectively eliminate it, while preventing damage to the surrounding healthy tissues. The immunity of vertebrates is classically divided into innate and adaptive, which differ in their response times to new and to repeated stimuli. The innate immune system is the first line of defense and provides rapid, non-specific responses to pathogens. In contrast, the adaptive system acts slower but is highly specific to antigens. B- and T cells make up the adaptive immune system and, upon encounter with their cognate antigens, can generate long-lived memory cell subsets allowing for a more efficient reaction to repeated stimuli. The correct coordination between the innate and adaptive systems is crucial to ensure not only a timely but also fine-tuned response against pathogens. An overactive response may lead to damage of healthy tissues and autoimmune diseases, while an insufficient response may lead to increased proliferation of pathogens and increased tissue damage.

3.1.1 T cells

T cells are part of the adaptive immune system, playing a central role in recognizing and responding to specific antigens. T cell development begins in the bone marrow, from which precursors migrate to the thymus for maturation. During this process, T cells commit to the expression of either the α- and β-chains of the T cell receptor (TCR) or the γ- and δ-chains, resulting in a major population of adaptive $\alpha\beta$ T cells or a minor population of innate-like $\gamma\delta$ T cells. The TCR is a highly variable molecule whose main function is to recognize peptides bound to major histocompatibility complex (MHC) molecules to initiate the adaptive immune response. To achieve this high variability, several recombination events occur during the maturation of T cells in the thymus, leading to a diverse amino acid sequences of TCRs, which can recognize virtually any antigen.

Mature αβ T cells migrate from the thymus to secondary lymphoid organs, including the spleen and lymph nodes. Here, these cells remain in a resting (naïve) state, characterized by the surface expression of molecules such as C-C chemokine receptor type 7 (CCR7) and CD62L, which are homing receptors for secondary lymphoid tissues[1] (Fig. 1A). αβ T cells express either CD4 or CD8 molecules on their surfaces, which ultimately determines their functions. CD4 is a co-receptor that binds directly to MHC class II molecules, which are almost exclusively expressed in antigen presenting cells (APCs) such as dendritic cells, macrophages, and B cells. Therefore, initially CD4 T cells preferentially interact with APCs and provide so-called “help” signals to other cells. The CD8 molecule interacts with MHC class I molecules (expressed on all nucleated cells), and the main function of CD8 T cells is to eliminate pathogen-infected or cancer cells.

Naïve T cells can recirculate between secondary lymphoid tissues and the bloodstream to increase the probability of a contact with APCs that potentially bear their cognate antigens on their surface MHC molecules. Upon an infection, activated APCs capture antigens in peripheral tissues and migrate to secondary lymphoid organs to present these antigens and activate T cells.

Activation of T cells is dependent on three types of signals provided by other cells (Fig. 1B). Initially, APCs expressing high levels of MHC present antigens to T cells through their TCR (signal 1). Recognition of the cognate antigen by the TCRs leads to a stable interaction with the peptide-MHC (pMHC) complex of the APC, resulting in signaling for proliferation and differentiation of the T cell[2]. Activated APCs additionally express co-stimulatory molecules such as CD80, CD86, CD70, and CD40 which provide additional survival and proliferation signals to, e.g., T cell (signal 2) (Fig. 1B)[3]. Activation through signals 1 and 2 are sufficient and necessary to generate effector T cells[4], while TCR stimulation lacking signal 2 can lead to anergic states or apoptosis[3]. Initial activation through signals 1 and 2 result in the increased expression of several cytokine receptors, and cytokine signaling (signal 3) finally optimizes T cell activation and influences the phenotype of the activated T cell[5,6] (Fig. 1B). Importantly, the differentiated T cell phenotype depends on the combination of multiple signals 1, 2, and 3, which are required for full activation[6]. Thus, highly variable effector T cell subpopulations are generated upon T cell activation as a result of different amounts of activation signals (Fig. 1C).

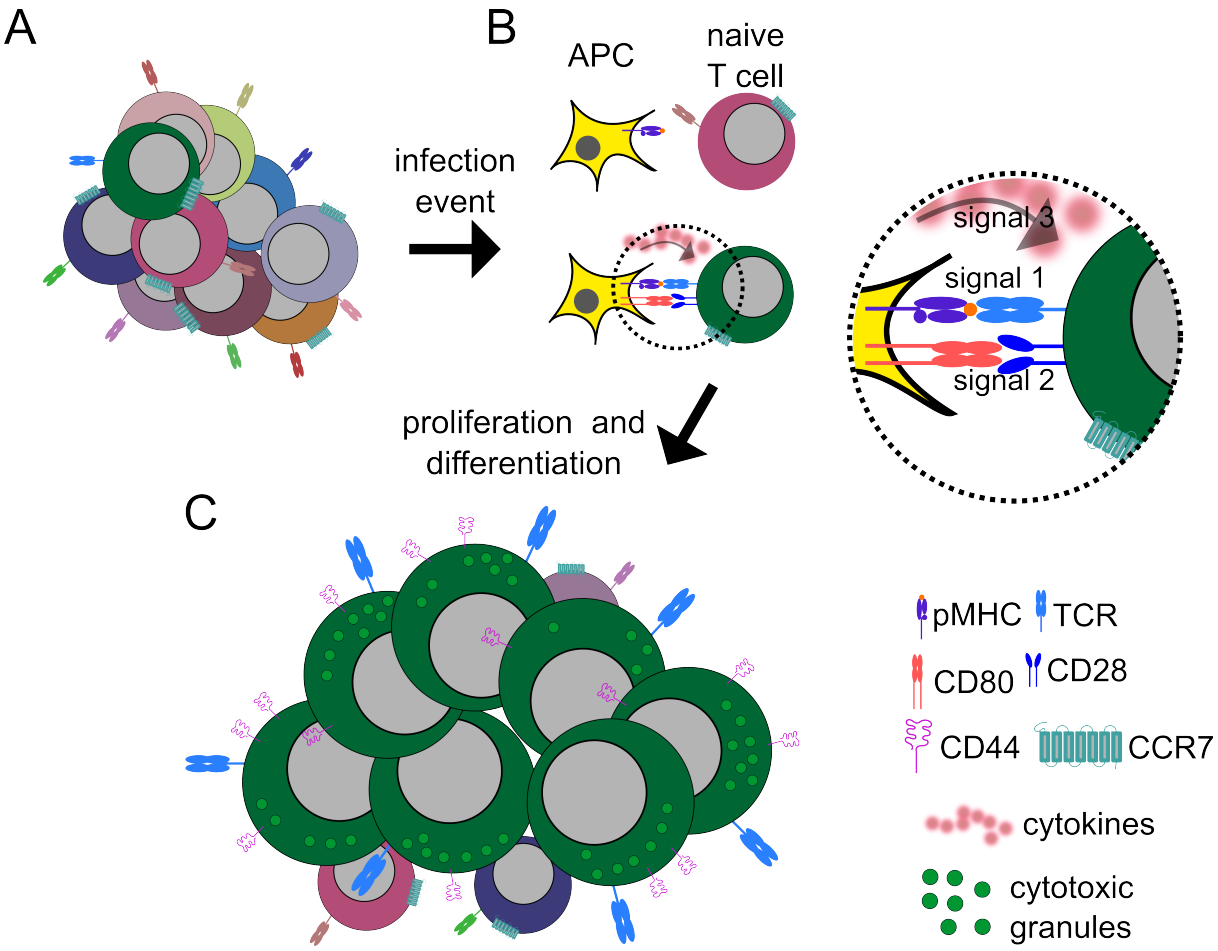

Figure 1. Generation of effector αβT cells. (A) Naïve T cells express diverse T cell receptors (TCR) specific against different pathogens (represented by different colors of the receptor). These cells localize preferentially in secondary lymphoid organs due to their high expression of homing molecules such as CCR7. (B) Upon infection, antigen-presenting cells (APCs) present antigens from the invading pathogen to all T cells. T cells specific against other pathogens do not recognize any antigen (upper panel), while T cells specific against the invading agent bind the peptide-MHC complex (pMHC) from the APC (lower panel). Additionally, APCs overexpress co-stimulatory molecules, e.g., CD80 (signal 2), and secrete cytokines (signal 3) that provide further activating signals to naïve T cells. (C) To increase the probability of an encounter with an infected cell, activated T cells proliferate over several days and differentiate into effector phenotypes. Differentiated cells become larger, express higher levels of CD44 and produce, e.g., cytotoxic granules that contain effector molecules and are released upon re-encounter with cognate antigen-bearing cells.

Cytokines influencing T cell responses vary depending on the activating pathogen. Viral and bacterial infections induce the production of interleukin- (IL-) 12 by dendritic cells, which in turn act on CD4 T cells to produce and secrete interferon-γ (IFN-γ), tumor necrosis factor-α (TNF-α), and IL-2. Thus, these CD4 T cells exhibit a T helper 1 (Th1) phenotype and act on CD8 T cells and macrophages to continue a cell-mediated immune response. Dendritic cell-derived IL-12 provides initial activation signals to CD8

T cells after TCR engagement and co-stimulation. Furthermore, IL-2 provides proliferation signals to activated CD8 T cells and enhances their differentiation into cytotoxic phenotypes. IFN-γ and TNF-α act directly on CD8 T cells to advance their differentiation into cytotoxic T cells[7,8]. Additionally, IFN-γ stimulates macrophages to increase their phagocytosis activity, leading to the engulfment of pathogens and rests of cells killed by CD8 T cells. Extracellular parasites and allergens initiate T helper 2 (Th2) responses by CD4 T cells after IL-4 stimulation and leads to a humoral response, i.e., mediated by soluble molecules. Stimulation of naïve CD4 T cells with IL-4 leads to their production of cytokines such as IL-4, IL-5 and IL-13, which enhance activation of B cells to secrete IgE antibodies, recruit eosinophils and increase mucus production, respectively. Alternatively, extracellular bacteria and fungi can lead to T helper 17 (Th17) phenotypes, which are characterized by secretion of IL-17 by CD4 T cells causing the recruitment of neutrophils.

T cells can be additionally classified according to their differentiation states[9]. In humans, both CD4 and CD8 naïve T cells express CCR7 and CD45RA surface markers, which are indicative of a naïve phenotype[10]. Upon activation, differentiation into effector cells leads to loss of CCR7 expression, leading to terminally differentiated T cells (TEMRA – T effector memory expressing CD45RA), whose populations undergo a contraction phase upon resolution of infection[11]. Additionally, subtypes of long-living, pathogen-specific $CCR7^{+}CD45RA^{-}$ central memory and $CCR7^{-}CD45RA^{-}$ effector memory cells remain in a resting state until a possible further contact with their cognate antigens, thereby allowing for a quicker response against recurring pathogens. Classification of T cell subtypes is less clear in mice. Here, naïve cells are classically characterized by the expression of CD62L in the absence of CD44, effector cells are $CD44^{+}CD62L^{-}$, while memory populations seem to simultaneously express both membrane markers.

The differentiation of CD8 T cells is orchestrated by the initial activation provided by APCs in combination with help signals from CD4 T cells[12]. In the case of viral infections, effector CD8 T cells acquire a cytotoxic phenotype and produce granules containing effector molecules such as granzymes and perforins (Fig. 2). Contact of effector or effector memory CD8 T cells with infected pathogens leads to release of these effector granules into the so-called immunological synapse. Here, perforin has been described to form large pores in the membrane of the antigen-bearing target cells, while

granzymes enter through these pores and initiate cell death pathways[13] (Fig. 2). Alternatively, central memory CD8 T cells secrete high amounts of activating cytokines, leading to more proliferation of antigen-specific T cells and a faster antiviral response.

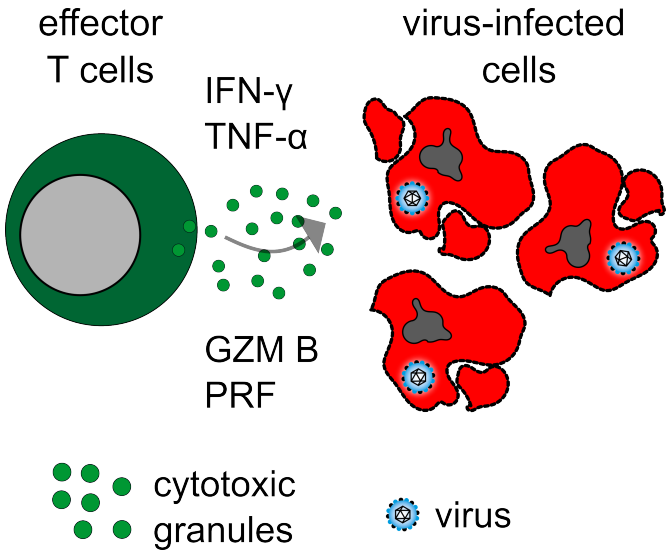

Figure 2. T cell-mediated cytotoxicity. Activated CD8 T cells can bear large amounts of effector molecules, e.g., interferon-γ (IFN-γ), tumor necrosis factor-α (TNF-α), granzyme B (GZM B), and perforin (PRF), in cytotoxic granules. Upon contact with cognate antigen-bearing cells, CD8 T cells polarize towards the infected cells and release the cytotoxic granules to elicit T cell-mediated cell death.

3.1.2 Early-life immunity in viral infections

The immune system undergoes dynamic changes throughout life, and early human development is characterized by an immature immune system[14], rendering this period particularly vulnerable to infections. Accordingly, infectious diseases are the leading cause of mortality and morbidity in under-five-year-old children[15,16]. Despite global efforts to reduce these factors, the reasons behind the increased susceptibility of children compared to adults remain under scrutiny[17].

Differences in the immune system during early life likely contribute to the heightened vulnerability of children[18-24]. The human fetus is especially at risk during infections[25], even though the placenta confers an effective protective barrier against infection of the fetus. Members of the TORCH (**T**oxoplasma, **O**thers, **R**ubella, **C**ytomegalovirus and **H**erpes Simplex) complex can circumvent this barrier and result in serious complications[26,27]. Thus, control of these pathogens by the immune system is crucial for the future health of the unborn child.

The timing of infection is a major determinant of the pregnancy outcome[28,29]**.** Early-pregnancy infection with CMV and Zika virus have been suggested to increase the likelihood of stillbirths[30,31], while infection at later stages can result in long-lasting symptoms[32]. These differences can partially be attributed to the immune responses against these pathogens, as the fetal immune system heavily relies on innate immunity in the first trimester of pregnancy[33,34]. Adaptive T- and B cells can first be detected around the end of the first trimester of pregnancy[33,35-37]. At this stage, T cells are reported to undergo homeostatic proliferation[38]. As a result, several T cells share the same TCR sequences and the range of antigens that can be recognized by T cells is limited in comparison to that of adults[36]. Consequently, insufficient T cell numbers and weaker antiviral responses from the existing T cells can contribute to a higher susceptibility to early-life infections.

3.2 Cytomegalovirus

3.2.1 Health burden of congenital infection

Congenital infection with human cytomegalovirus (HCMV) is the main non-genetic cause of permanent disabilities in newborns[39]. *In utero* infection with HCMV can lead to various complications including sensorineural hearing loss, mild to severe motor and developmental retardations, and stillbirths[30,40]. Notably, there are no effective preventive measures such as vaccines against congenital HCMV. Moreover, the available treatment options for the infected fetus are limited and often associated with severe side effects[41].

Despite the high seroprevalence of HCMV, routine screening for the virus during pregnancy is not commonly performed in most countries[39,42]. However, symptomatic congenital HCMV infection requires significantly longer hospital stays and treatment costs, placing a substantial economic strain on public health systems[43,44]. Therefore, understanding the pathophysiology, prevention, and treatment of congenital CMV (cCMV) infection is an urgent challenge.

3.2.2 HCMV disease

The prevalence of HCMV varies based on socioeconomic status and can reach up to 100% in underdeveloped countries[45,46]. CMV establishes latency in the infected host, leading to an increased seroprevalence with age[46,47]. The virus exhibits high organ

tropism and is shed through almost all body fluids[48]. Therefore, primary infection can occur through several pathways, facilitating viral transmission. Importantly, HCMV can be transmitted through breast milk feeding, and children infected with HCMV are believed to be an important virus reservoir due to their prolonged viral shedding[21].

In immunocompetent adults, HCMV infection commonly results in mild disease or no symptoms[49]. However, the virus can be lethal in immunocompromised individuals, especially after solid organ or hematopoietic stem cell transplantations. Transplant recipients, under immunosuppressive therapy to prevent organ rejection, face an increased risk of HCMV reactivation or primary infection [50,51]. The virus is a leading infectious agent post-transplantation, contributing to severe HCMV-related diseases, with symptoms including pneumonitis, hepatitis, retinitis and gastrointestinal disease [52-54]. Additionally, HCMV seems to increase the probability of graft-versus-host disease (GVHD)[55-57], thereby increasing the burden of opportunistic infections. Human immunodeficiency virus (HIV) patients represent another group of high-risk individuals for CMV infection. Indeed, CMV co-infection can significantly worsen the prognosis of HIV-infected patients, even in the presence of antiretroviral therapy[58,59].

Congenital and perinatal infections form another branch of clinically relevant HCMV infections. The incidence of *in utero* HCMV infection worldwide ranges from 0 to 6% [60,61]. Infection of the fetus can result from i) primary infection of the mother during pregnancy, where it is estimated that 20-40% of infections lead to a congenital infection [60]; or ii) HCMV reactivation/reinfection events which occur in approximately 1% of pregnancies of latently infected women [60]. Among congenitally infected children, approximately 10% develop long-lasting symptoms[62], the most common being sensorineural hearing loss, vision loss and mental retardation[63]. In extreme cases, death of the congenitally infected neonate can occur[64]. Treatment with antivirals poses great challenges due to potential side effects and is only recommended to babies who are symptomatic at birth[39]. However, asymptomatic neonates may still develop long-term sequelae, which commonly remain undiagnosed [65,66]. Prevention methods for congenital HCMV infection are limited, relying on behavioural recommendations for pregnant women, while vaccine and passive immunization attempts have not been successful to date[67-69]. Therefore, the knowledge gaps regarding risk factors combined with the lack of effective prevention and treatment options emphasize the urgency of the congenital HCMV infection problem.

3.2.3 Structure, genome and entry of cytomegaloviruses

Cytomegaloviruses (CMV) belong to the *Betaherpesvirinae* subfamily within the *Herpesviridae* family and have linear genomes of approximately 230 kilobase pairs (kbp) in size. The viral genome is encased within an icosahedral nucleocapsid, which is itself surrounded by tegument proteins that are important for genome delivery into the nucleus[70,71], expression of viral proteins[72] and immune evasion[73,74]. Tegument proteins are enveloped by a lipid bilayer derived from the host, which expresses several glycoproteins essential for viral entry into new host cells (Fig. 3).

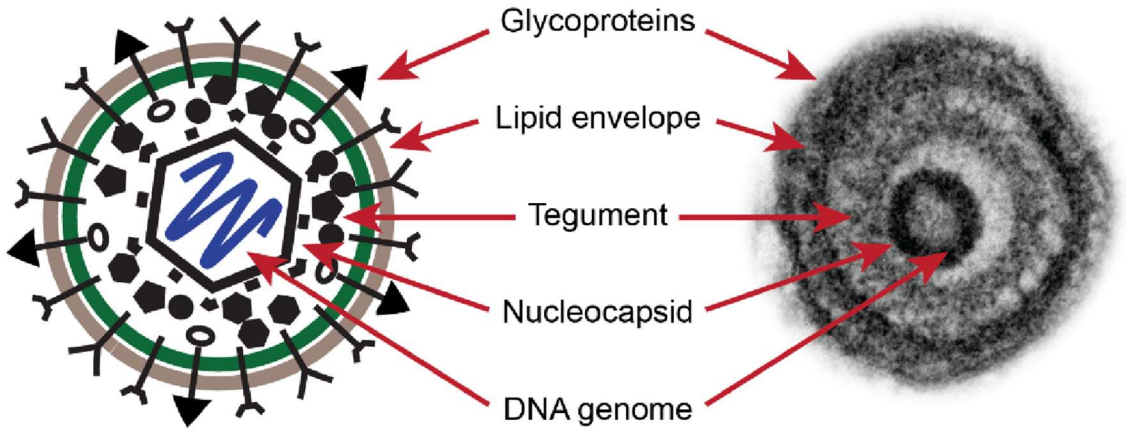

Figure 3. Cytomegalovirus structure. Adapted from Close et al.[75].

The large genome of CMV results in approximately 750 open reading frames (ORFs)[76], with only a small percentage of these genes being necessary for viral replication and structure[77,78]. Lytic CMV infection begins as the viral capsid is transported into the host cells' nucleus, initiating a temporally regulated expression of viral genes. The process starts with the transcription of immediate early (IE) genes, which act as both transcription factors and trans-activators of early (E) proteins. Early genes are important in triggering DNA replication, while late (L) genes initiate the assembly of the capsid. Replicated DNA is packaged into the capsid, which subsequently egresses the nucleus into the cytoplasm, where it associates with tegument proteins within the viral assembly compartment. Finally, capsids are enveloped with host-derived membranes from the endoplasmic reticulum and Golgi apparatus. Mature virions can then associate with secretory vesicles and be released into the extracellular space[79].

Cytomegaloviruses utilize glycoprotein complexes expressed on their envelope to facilitate their entry into host cells. In HCMV, the trimeric and the pentameric complexes are mainly involved in cell entry. The trimeric complex, consisting of viral glycoproteins H (gH), gL and gO, primarily facilitates HCMV infection of fibroblasts through the platelet-derived growth factor-α (PDGFR-α). Conversely, the pentameric complex, composed of gH and gL together with the unique long (UL)128, UL129, and UL131, is crucial to infect epithelial and endothelial cells as well as leukocytes such as monocytes and dendritic cells[80]. The HCMV pentameric complex primarily uses neuropilin-2 as a cell entry receptor[81]. Similarly, the murine CMV (MCMV) can employ two glycoprotein complexes for host cell entry. MCMV forms a trimeric complex with gH, gL, and gO similar to the HCMV trimeric complex, facilitating entry into fibroblasts and endothelial cells[82]. Additionally, another trimeric complex comprised of gH, gL and the MCMV chemokine 2 (MCK2) is homologous to the HCMV pentameric complex. MCK2 is essential for MCMV infection of macrophages[83,84], with MHC-I recently being identified as an entry receptor in MCK2-mediated infections[85].Moreover, a recent study suggests that neuropilin-1 (NRP1) may act as a receptor for MCMV[85,86] in MCK-2 independent infection, though its viral interaction partner remains elusive.

3.2.4 Mouse models of CMV infection

Cytomegaloviruses are notorious for their strict species specificity, with humans being the only known reservoir of HCMV. While HCMV infection cannot be modelled in other animals, established models using the related rhesus macaque CMV (RhCMV), MCMV and guinea pig CMV (gpCMV) provide valuable insights under controlled conditions[87-89]. Murine CMV is the most used animal model, sharing a significant portion of the genome and essential features with HCMV, such as myeloid cell infection facilitating viral spread to other organs[90], establishment of latency[91] and efficient immune evasion[92].

MCMV establishes latency in its natural host and is shed through various body fluids, making it challenging to track viral entry in newly infected mice. Salivary glands serve as a major reservoir for MCMV, and animal bites might also constitute a route for horizontal transmission. MCMV infection through the footpad (f.p.) has been proposed to mimic this[93]. The most used infection routes in mouse experiments involve direct application of the virus into the circulation of the animal, either intravenously (i.v.) or intraperitoneally (i.p.). However, systemic infection through these routes is unlikely to

represent a natural infection pathway. Infection through the oral route has been shown to be inefficient[94,95], though MCMV can be transmitted to mouse neonates through breast milk[96]. Alternatively, in several studies, infection is performed through mucosal tissues, e.g. the respiratory tract[94,95], leading to high infection efficiency and virus loads in both adult and neonatal mice[94,95,97].

In contrast to HCMV, MCMV does not infect the fetus during pregnancy even after systemic infection[98,99]. The mechanisms that lead to fetal protection are unknown, but likely involve a combination of viral factors, host immune responses, and anatomical materno-fetal barriers. Indeed, in a model of infection during immunodeficiency, viral DNA could be infrequently detected in fetuses[100]. Additionally, attempts to overcome anatomical barriers by directly applying the virus into the placenta or the fetal brain resulted in brain infection, developmental changes, but also high fetal loss[101,102].

Guinea pigs are the only small animal model where congenital infection is seen and are widely used in vaccine studies[103,104]. However, commercial anti-guinea pig antibodies are scarce hindering the investigation of e.g. immune responses in this model. Furthermore, the gestation period of guinea pig is three times longer than that of laboratory mice[105,106], significantly slowing down research output in this model. Although congenital CMV infection can also be studied in non-human primate models, these are significantly more expensive than small animals, have even longer gestation times, and are subject to considerably stricter ethical regulations. Hence, mouse models of congenital infection are still used to study immune responses and behavioral changes in the neonates.

At birth, mice display similarities to the neurological developmental stage of the human fetus in the second trimester of gestation[107]. Accordingly, mice infected within the first two days of life with MCMV develop neurological and behavioral changes[108]. Moreover, the immune system of neonatal mice significantly differs from that of adults, resulting in weaker responses against pathogens in early life. Consequently, modelling immune responses in congenital CMV disease in mice is well established and can be achieved by infecting them within the first hours of life[88].

3.2.5 T cell immunity to CMV

Infections with CMV are notable for inducing robust T cell-mediated immunity, resulting in profound changes in the general T cell phenotypes[109-111]. Human CMV can elicit

strong responses from both CD4 and CD8 αβ T cells against a broad range of viral antigens[112,113]. In chronically infected individuals, the proportion of HCMV-specific T cells can make up to 15% of total T cell populations[114]. These responses are characterized by the generation of polyfunctional T cells capable of simultaneously producing cytokines such as IL-2, TNFα, and IFN-γ, crucial for controlling viral infection[115-118]. However, as HCMV generally causes only mild symptoms in immunocompetent adults, investigating the determinants of T cell control in HCMV infection is challenging since the infection is usually not identified. Therefore, several studies focus on immunosuppression settings, where acute infection or latent HCMV reactivation are likely to occur. CD4 T cells have been found to be crucial in containing symptomatic HCMV reactivation in allogeneic stem cell transplantations[119]. Additionally, HCMV appears to induce the generation of cytotoxic CD4 T cells, which produce high levels of cytotoxic molecules[118,120] and are capable of lysing HCMV-peptide-loaded cells in an MHC-II dependent manner [121]. Similarly, CD4 T cells have been shown to play an important role in control of MCMV infection. Antibody-mediated depletion of CD4 T cells during MCMV infection leads to a general increase in the viral loads of most organs after systemic infection[122] CD4 T cells are particularly important in the control of MCMV infection in salivary glands, where a lack of cross-presenting dendritic cells hampers CD8 T cell responses and likely results in compensatory mechanisms by CD4 T cells[123]. Salivary-gland CD4 T cells are characterized by a high expression of IFN-γ and can exert cytotoxic functions, indicating that generation of CD4 T cells is not specific to HCMV infection and can also be observed in mouse models.

Besides CD4 T cells, CMV induces robust CD8 T cell responses in infected individuals. HCMV-specific CD8 T cells are polyfunctional and express high levels of cytotoxic molecules[116,124]. However, CD8 T cell responses in CMV infection deviate from the classical pattern described for other pathogens since, although CD8 T cells proliferate robustly during acute infection, clearance of HCMV is not followed by a general contraction of HCMV-specific CD8 T cells. Instead, HCMV leads to chronic expansion of CD8 T cells specific against viral peptides, e.g., pp65 (UL83), in a process called memory T cell inflation[125]. Consequently, in elderly individuals infected with HCMV, pp65-specific CD8 T cells can account for 20% of the total CD8 T cell pool. Similarly, mice infected with MCMV show memory inflation of CD8 T cells specific against viral antigens including M38 and m139[126,127]. In mice, depletion of CD8 T cells leads to the

most significant increase in viral loads[128], and reconstitution of these cells in stem cell transplantation models temporally coincide with the decrease of viral loads[128-130].

Knowledge about the T cell responses in congenital CMV infection settings is limited. Pregnant mothers can produce antiviral T cells which express high levels of cytotoxic molecules[131,132]. However, the production of these cells does not rule out transmission from the mother to the fetus. A comparison of blood from mothers and cord blood from their respective babies revealed a stronger CD8 response in the mothers, and the limited response in neonates could possibly account for the increased susceptibility to severe disease[133]. Moreover, the presence of high levels of CD4 TEMRA and CD8 TEMRA in pregnant women seems to correlate with protection against mother-to-fetus transmission[134]. Marchant and colleagues could show that HCMV can induce generation of specific CD8 T cells in the fetus, and these cells can produce cytotoxic molecules[135]. The extent to which these cells are able to exert control over HCMV infection is unknown. However, lack of *ex vivo* production of IFN-γ by T cells seems to predict the presence of long-lasting symptoms in congenitally infected newborns, indicating that T cell control is determinant in the pathogenesis of congenital HCMV infection[136].

Mouse models of congenital infection have shown that CD8 T cells play a crucial role in viral control in the brain of newborns[129], though neonatal T cells respond slower to MCMV than their adult counterparts[95,137]. Lung infection of newborn mice leads to the formation of granuloma-like structures called nodular inflammatory foci (NIFs)[95], where most of the virus-infected cells can be found. Infected epithelial cells and alveolar macrophages provide danger signals leading to substantial infiltration of immune cells, and T cells are arguably the most important cells in clearance of infected cells[138]. Additionally, IFN-γ secretion seems to play a determining role, as adoptive transfer of *Ifng*$^{-/-}$ T cells into *Rag2*$^{-/-}$ mice, lacking B and T cells, seems to lead to an impaired control of MCMV infection in comparison to treatment with wildtype T cells[138]. However, CD4 and CD8 T cells cooperate in the control of CMV infection, and presence of both types of cells significantly improves the reduction of viral loads. Importantly, adoptive transfer of antigen-specific CD8 T cells into neonates did not reduce lung viral loads, contrary to what has been extensively observed in adult models[95]. The reasons for this discrepancy in early-life T cell responses are not well understood and are addressed in this dissertation.

3.3 Immunological diagnostic tests

In the last century, several methods have been developed to detect immunological responses to antigens. These responses have been leveraged to create new diagnostic tools capable of detecting the presence of various acute and chronic infections or autoimmune diseases. The emergence of the Coronavirus disease 2019 (COVID-19) pandemic underscored the critical need for diagnostic tools to identify current or past infections which help control communal spread of the virus and identify correlates of protection[139-141]. Consequently, a method to detect T cell responses upon severe acute respiratory syndrome coronavirus type 2 (SARS-CoV-2) infection was evaluated in this dissertation.

3.3.1 SARS-CoV-2: structure, genome, and COVID-19 pandemic

SARS-CoV-2 is a member of the Coronaviridae family and was first identified in 2019, subsequently causing widespread morbidity and mortality worldwide, with over 770 million infections and over 6 million deaths [142] in the past four years. Infections with SARS-CoV-2 can lead to the Coronavirus disease 2019 (COVID-19), characterized by symptoms such as fever, cough, loss of smell and taste, and mild pneumonia[143]. Severe symptoms include hypoxia and dyspnea, while fatal cases often involve respiratory failure and septic shock[144,145]**.** Notably, the prevalence of severe symptoms is higher in older individuals, immunocompromised patients and pregnant women, while immunocompetent young individuals rarely suffer from severe COVID-19 [146]. Further long-lasting symptoms can develop several weeks after initial infection, leading to conditions encompassed in the umbrella term “long COVID-19”[147].

The genome of SARS-CoV-2 comprises 30 kbp of non-segmented, positive-sense single stranded RNA, and the virion is made up of four structural proteins: nucleocapsid (NC), membrane, envelope and spike (S) (Figure 4). SARS-CoV-2 enters host cells by binding of the S protein to host cell receptors. Although multiple receptors interact with S, the primary port of entry is the host angiotensin-converting enzyme 2 (ACE2)[148,149] The S protein binds to ACE2 via its receptor binding domain (RBD), initiating cleavage of S into two subunits by the host transmembrane protease, serine 2 (TMPRSS2). This cleavage exposes a fusion peptide, ultimately facilitating the fusion of the virus particle with the host cell membrane[148]. Subsequent release and uncoating of the viral RNA result in translation of two large ORFs, ORF1a and ORF1b. Proteins from these ORFs

form the non-structural proteins, responsible for the transcription of structural viral genes and new virus particles[150].

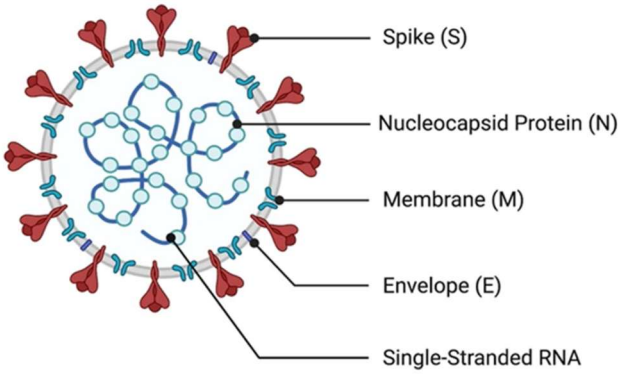

Figure 4. Structure of SARS-CoV-2. Adapted from Jamison et al.[151]

3.3.2 Diagnostic testing for SARS-CoV-2

Rapidly diagnosing acute SARS-CoV-2 infections was crucial to contain viral transmission. The gold standard for detection of acute SARS-CoV-2 infections is real-time polymerase chain reaction (RT-PCR) from upper respiratory tract samples due to its high sensitivity and specificity. This technique can detect acute infections up to two days before symptom onset[152,153]. However, limitations due to infrastructure requirements and need for expertise led to the development of other methods for direct viral detection, such as rapid antigen tests. These lateral flow tests, while exhibiting lower sensitivity and specificity, allow for quick detection by anyone, aiding in the prompt identification of infected individuals and breaking of transmission chains.

SARS-CoV-2 elicits a strong immune response which are necessary for viral clearance[154]. Accordingly, serologic tests were soon established in routine diagnostics to assess the presence of (previous) SARS-CoV-2 infections. SARS-CoV-2-specific antibodies are commonly measured with enzyme-linked immunosorbent assays (ELISA), where positive signals can be detected within two weeks of primary infection[155-157]. These tests exhibit high specificity and sensitivity and quantitative data (i.e. antibody titers) informs protection against severe disease and, to some extent, reinfection[158]. Vaccines against SARS-CoV-2 were developed in record times and contributed highly to the containment of COVID-19. The first widely distributed vaccines targeted the S protein, resulting in strong antibody responses and protection against severe COVID-19[159-161]. However, individuals with B cell deficiencies or treated

for autoimmune disorders may fail to mount robust antibody responses[162-164]. Additionally, declining antibody titers over time and genetic mutations leading to new SARS-CoV-2 variants can render the initially robust antibody responses ineffective, emphasizing the need for other immune correlates of protection.

Apart from antibody responses, SARS-CoV-2 infections were early shown to elicit strong T cell responses[165-168]. CD4 T cell responses were characterized by robust IFN-γ production[169], and their presence correlates stronger with protection than that of CD8 T cells and antibody-producing B cells[168]. Furthermore, SARS-CoV-2 infection leads to an increase in the frequency of T follicular helper cells, which help initiate antiviral B cell responses for antibody production[170]. CD8 T cells, though generated at lower frequencies than CD4 T cells, play a crucial role in clearing SARS-CoV-2-infected cells[166]. These cells also secrete high levels of IFN-γ upon stimulation with SARS-CoV-2 peptides[171], and their presence strongly correlates with improved protection from severe disease[168,172,173].

Using T cell responses for diagnostic use has been more challenging. The majority of studies involving these responses rely on complex flow cytometry experiments, where blood collected from infected or convalescent individuals is stained with multiple marker-specific antibodies before or after stimulations. While providing valuable insights, these methods are laborious, time-consuming and require high levels of expertise, making routine diagnostic tests involving T cells difficult to establish and standardize. Exceptionally, T cell responses can be used to diagnose latent *Mycobacterium tuberculosis* (Mtb) using interferon-gamma release assays (IGRA). In IGRA, blood from potentially infected individuals is stimulated with Mtb-derived peptides. In case of infection, Mtb-specific T cells secrete high amounts of IFN-γ, which can be detected in supernatants by ELISA or enzyme-linked immunospot assay (ELISpot) in the blood supernatants 16-24 hours after stimulation. The high sensitivity and specificity of these tests [174], together with the ease of handling, place them as a viable candidate for assessment of cell-mediated immunity (CMI) in other types of infections. Indeed, CMI tests have shown potential in the context of HCMV infections after transplantation [175-177]. Thus, I hypothesized that IGRA can be used to detect past SARS-CoV-2 infections and secreted IFN-γ values can be used as correlates of protection.

3.4 Aims of the study

This thesis is made of three sections:

Section 1: Identification of factors determining vertical transmission in mice

Contrary to HCMV, MCMV cannot cross the host placenta. The current hypotheses for this discrepancy include shorter gestational times and a different anatomy of the materno-fetal barrier between humans and rodents, but cellular mechanisms at the materno-fetal interface that modulate fetal susceptibility to MCMV are yet to addressed. Thus, this study aimed to identify cellular mechanisms of murine fetal protection against MCMV infection *in utero*. New findings in this regard could facilitate the development of tools to study MCMV-fetus interaction *in vivo*, which could additionally have a translational value.

Section 2: T cell immunity in congenital CMV disease

In case of congenital infection, neonates are at increased risk for long-lasting CMV disease. T cells are important for viral clearance in immunocompetent adults, but their role in congenital infection is still unclear. This study aimed to elucidate mechanisms that lead to a reduced immune response and protection to CMV disease in early life using mouse and human systems. The identification of these factors can potentially add to the lack of effective therapy in congenital HCMV disease.

Section 3: Establishment of a CMI test to assess previous SARS-CoV-2 infection

T cell responses are generated in case of SARS-CoV-2 infections but, contrary to antibodies, these adaptive responses are not currently used in routine diagnostics to assess previous infection. Moreover, these cells are important to control SARS-CoV-2 infection, but correlates of protection are challenging to study due to lack of standardized, quantitative diagnostic testing. Thus, this study aimed to establish a diagnostic test that quantifies T cell responses to SARS-CoV-2 antigens long after resolution of the infection and can be used to correlate to clinical features. This kind of diagnostic test can help in standardizing cell-mediated immunity testing against emerging respiratory viral infections, be used in case of known incapacity of antibody response, and be correlated to protection against disease.

4 Results

4.1 Section 1: Identification of factors determining vertical transmission in mice

4.1.1 Neuropilin-1 modulates MCMV infection susceptibility at the materno-fetal interface

Congenital infection with HCMV poses significant health problems, yet investigating the determinants of vertical transmission *in utero* remains highly challenging. Unlike HCMV, MCMV is not vertically transmitted to the offspring *in utero*, and the mechanisms of fetal protection in mice are not completely understood. Thus, the influence of cells at the materno-fetal barrier was investigated.

Previous findings in our lab and others[100] have revealed a role of maternal immunity in protecting against congenital MCMV infection. Systemic infection of immunocompetent (wildtype) mice and mice deficient in interferon-α (IFN-α) signaling (*Ifnar1*$^{-/-}$) with high viral loads resulted in no infected cells at the materno-fetal barrier, whereas sporadic infection of the visceral yolk sac and placenta cells was observed in mice lacking T-, B-, and NK cells (*Rag2*$^{-/-}$*Il2rg*$^{-/-}$), with no infection occurring within the fetal parenchymal tissue. These results indicated that immunodeficiency can predispose to congenital infection, while also highlighting the involvement of other tissue-specific factors that contribute to a protective effect.

The placenta is primarily composed of fetal cells derived from trophoblasts and acts as a materno-fetal barrier, separating the blood circulation of the mother from that of the fetus. Therefore, an absence of infection from cells at the materno-fetal barrier may contribute to fetal protection against *in utero* MCMV infection by reducing cell-to-cell spread in this tissue. To test this hypothesis, wildtype dams were mated with males expressing the enhanced green fluorescent protein (eGFP) under the β-actin promoter (GFP mice), and placentas were isolated at gestational day (gd) 12.5. This breeding strategy resulted in placenta preparations where eGFP^{+} cells originated from the fetus and eGFP^{-} cells were of maternal origin. Additional staining for the CD45 surface protein enabled the differentiation between hematopoietic cells (CD45^{+}) and non-hematopoietic cells (CD45^{-}). Most of the isolated cells exhibited a CD45^{-}eGFP^{-} phenotype, i.e., non-hematopoietic and of maternal origin (Fig. 5A and B). However,

approximately 17% of cells were eGFP$^+$(Fig. 15B). These freshly isolated primary cells were infected with an mCherry-expressing MCMV recombinant (MCMV-3DR, see materials and methods) and analyzed 24h post-infection (Fig. 5C-F). Interestingly, cells from the materno-fetal barrier showed low susceptibility to MCMV infection, with only 1.5% of cells expressing the mCherry reporter (Fig. 5C and D). Furthermore, the majority of MCMV-infected cells displayed an eGFP$^+$CD45$^-$ phenotype, indicating their fetal, non-hematopoietic origin (Fig. 5E and F).

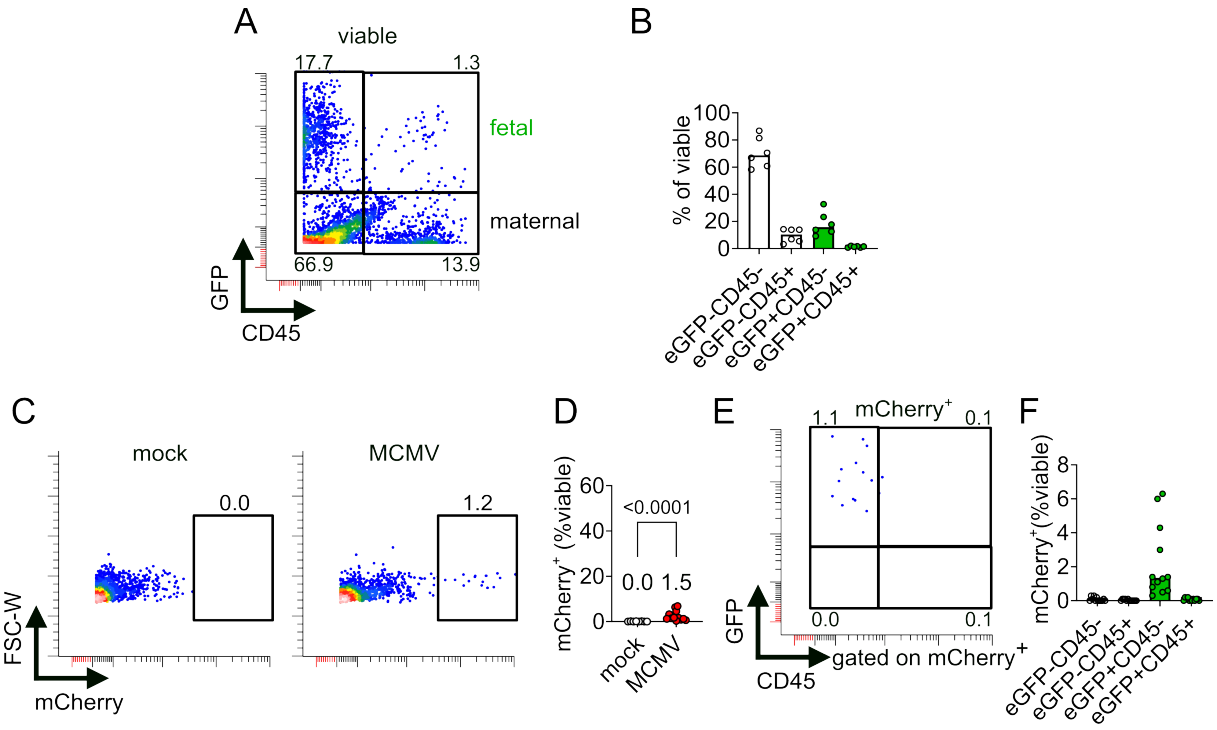

Figure 5. Primary placenta cells exhibit low susceptibility to MCMV infection. (A-G) Wildtype dams were mated with β-act-eGFP males and cells from the placenta were isolated at gestational day 12.5. (A and B) (A) Representative flow cytometry plot and (B) pooled analysis of freshly isolated placenta cells stained for the CD45 leukocyte marker. (C-F) Primary placenta cells were infected with MCMV with MOI 0.5 and analyzed 24h later. (C and D) (C) Representative flow cytometry plots and (D) pooled analysis of infected primary placenta cells. (E and F) (E) Representative flow cytometry plot and (F) pooled phenotypical analysis of MCMV infected cells. Numbers above and below the gates in (A), (C), and (E) indicate the percentage of the population from the total viable cells. Numbers in (D) indicate the median value for each group. eGFP, enhanced green fluorescent protein. The statistical difference in (D) was calculated with a Mann-Whitney U test and the p-value is provided above the graph. The gating strategy for (A) is provided in section 7.18.1.

Recently, neuropilin-1 (NRP1) has been described as a receptor for MCMV entry into endothelial cells[86]. Given the unknown expression of this molecule in cells at the materno-fetal barrier, a published single-nuclei RNA-sequencing experiment[178] was

reanalyzed for NRP1 expression. This approach allows for a high-throughput analysis of the transcriptomes within individual nuclei of an isolated tissue or organ. Using the Uniform Manifold Approximation and Projection (UMAP) dimensionality reduction method[179], thousands to millions of cells can be clustered based on the similarity of their transcriptomes, providing comprehensive insights into cellular phenotypes. In the study by Marsh and Blelloch[178], nuclei from primary placenta cells were annotated as fetal mesenchyme, endothelial, decidual stroma, trophoblast, and blood cells (Fig. 6A). Analysis of NRP1 expression of placentas isolated at gd12.5 revealed that NRP1 mRNA is only expressed in endothelial cells and fetal mesenchymal cells (i.e., fetal, non-hematopoietic cells) (Fig. 6B), suggesting that lack of NRP1 at the materno-fetal barrier might contribute to the protection against MCMV infection.

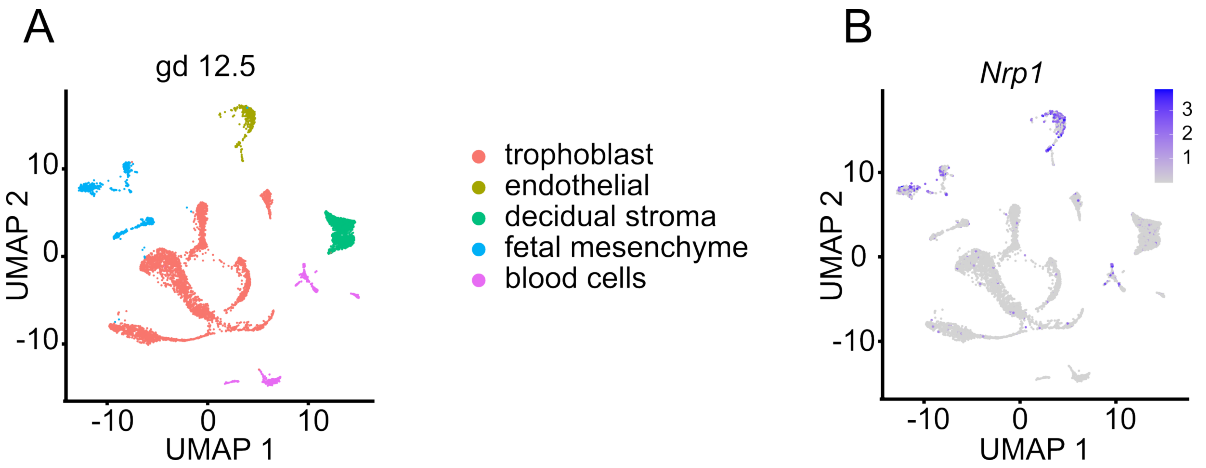

Figure 6. Low expression of neuropilin-1 at the materno-fetal barrier. (A and B) Neuropilin-1 (*Nrp1*) expression at the materno-fetal barrier was analyzed using a published single-nuclei RNA-sequencing dataset (GSE152248)[178]. (A) Transcriptomic phenotype and (B) relative expression levels of *Nrp1* transcripts in nuclei isolated from mouse placentas at gestational day (gd) 12.5.

To assess the impact of NRP1 expression on the susceptibility of the SM9-1 mouse placental trophoblast cell line to MCMV infection, cells were lentivirally transduced with either *Gfp* or *Nrp1-Gfp* constructs and subsequently infected with MCMV. Importantly, NRP1 protein expression was absent in SM9-1 and transduction with *Nrp1-Gfp* successfully increased the surface expression of this protein (Fig. 7A and B). SM9-1 trophoblasts are resistant to MCMV infection and, after 24h, only 1-2% of cells express mCherry as compared to 50% of 10.1 fibroblasts (Fig. 7C and D). The frequency of infected cells remained by 1-2% *Gfp*-transduced cells, while approximately 10-fold higher levels of MCMV-infected cells were present after transduction with *Nrp1-Gfp*-expressing lentiviral constructs (Fig. 7C and D). In summary, these findings indicate

that the lack of expression of NRP1 on SM9-1 placental cells contributes to their resistance to MCMV infection, and overexpression of NRP1 enhances susceptibility. Consistently, primary placenta cells are resistant to MCMV infection, while the effect of the expression of NRP1 in these cells remains to be addressed.

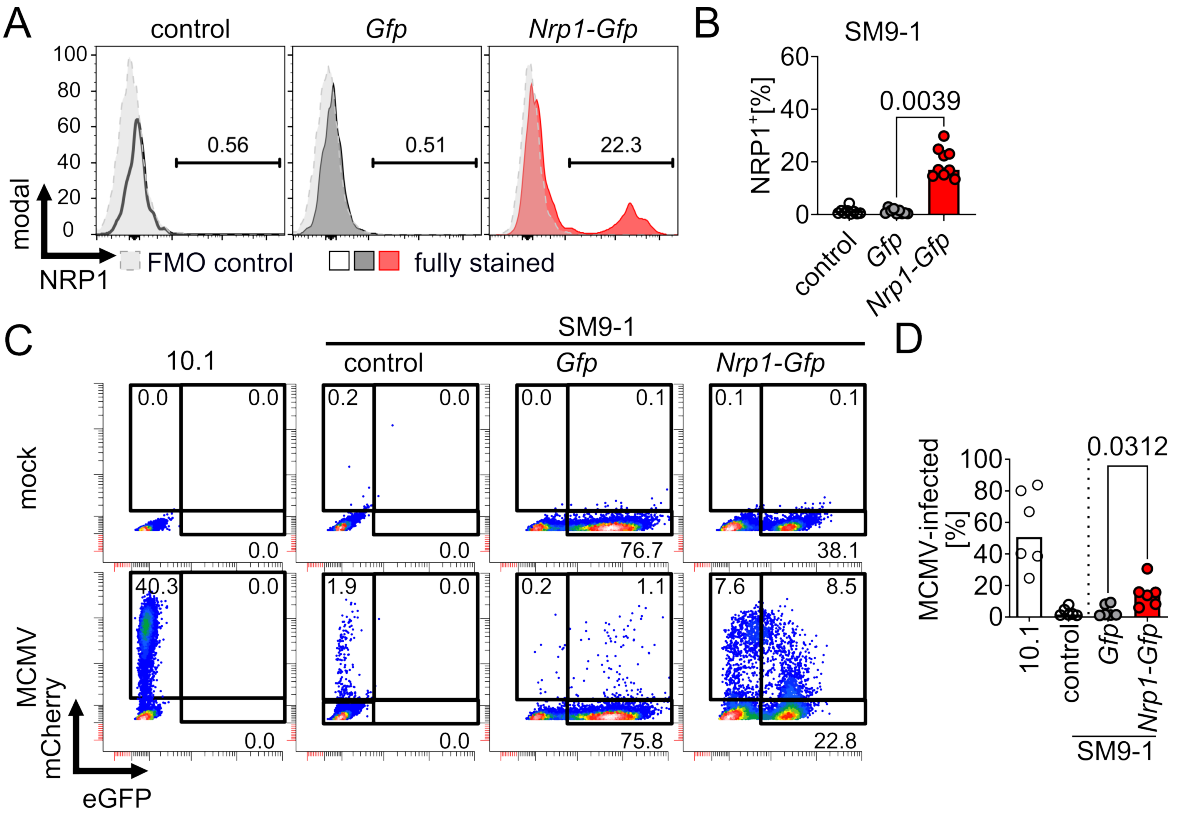

Figure 7. NRP1 expression increases susceptibility of the SM9-1 placenta trophoblast cell line to infection. (A and B) (A) Representative histograms and (B) pooled analysis of surface NRP1 expression of wildtype SM9-1 trophoblasts (control) and SM9-1 cells transduced with *Gfp*- or *Nrp1-Gfp*-encoding lentivirus. Counts in the Y-axes in (A) are normalized to the mode. (C and D) (C) Representative flow cytometry and (D) pooled analysis of MCMV infection of 10.1 fibroblasts and SM9-1 trophoblasts with and without transduction with Gfp- or *Nrp1-Gfp*-encoding lentiviruses (MOI 0.5). Data were acquired from at least three independent experiments (A and B, n=9; C and D, n=6). Statistical differences in (B) and (D) were calculated with Wilcoxon tests and the p-value are provided for the comparisons.

4.2 Section 2: T cell immunity in congenital CMV disease

4.2.1 Delayed expansion of MCMV-specific CD8 T cells in early life

Mouse fetuses are protected from *in utero* MCMV infection, and well-established mouse models of congenital HCMV disease employ neonatal infection within the first hours of life. To investigate the factors contributing to the higher risk of CMV disease in early life, a previously established lung infection model was used[95].

Neonatal and adult (6-12 weeks) mice were infected with MCMV and the frequencies of MCMV-specific T cells in the blood were tracked over time using either (i) peptide-MHC (pMHC) class I tetramer complexes targeting CD8 T cells specific to immunodominant MCMV peptides M38, M45 and m139[180] or (ii) pMHC class II tetramer complexes targeting CD4 T cells specific to the immunodominant M25 MCMV peptide[181]. MCMV-specific CD4 T cells could only be detected at low frequencies in blood, and the frequencies of these cells were similar across all time points in neonates and adults (Fig. 8A and B).

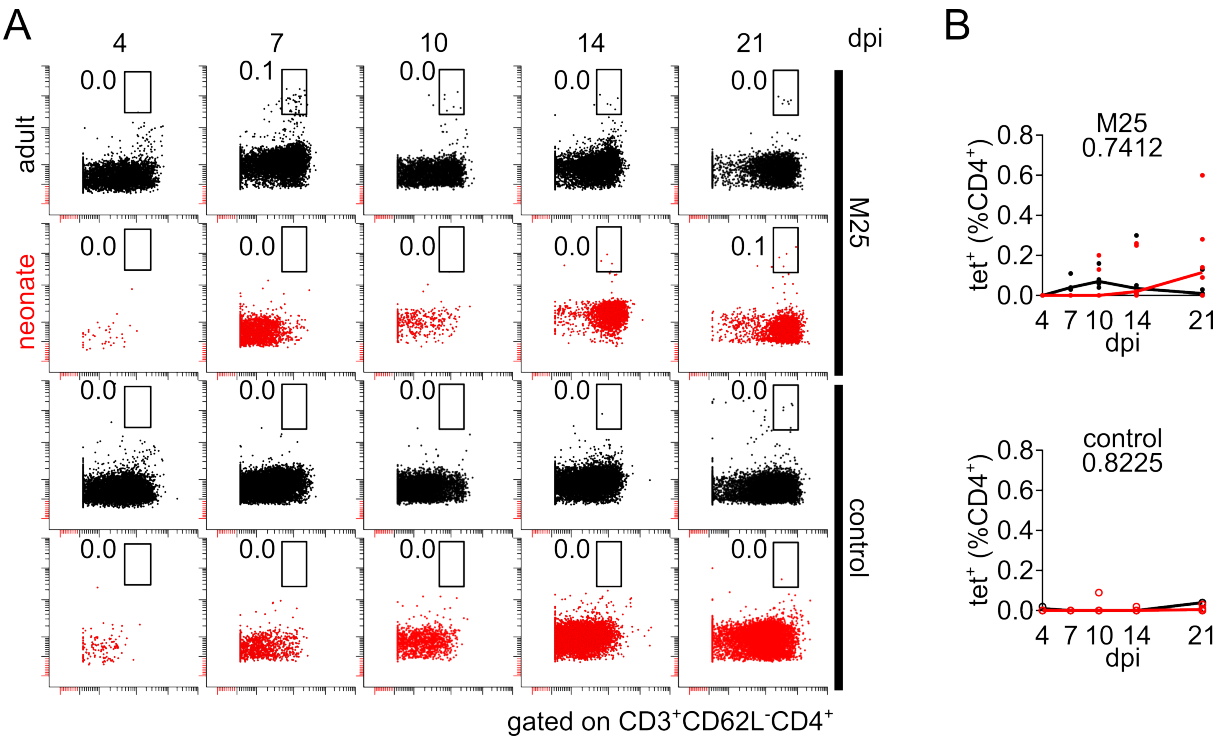

Figure 8. Expansion of MCMV-specific CD4 T cells in blood of neonates and adults. (A and B) Neonates (post-natal day 0) and adult mice (6-12 weeks) were infected through the respiratory tract with MCMV and blood and lungs were isolated at the indicated days post-infection (dpi). (A) Representative flow cytometry and (B) pooled analysis of MCMV-specific CD4 T cells in blood of MCMV-infected (M25, upper panels) and mock-infected (control, lower panels) animals. Numbers in (A) represent the

percentage of M25-specific cells of the total CD4 T cells. Data were acquired from two independent experiments. Statistical differences in (B) were calculated with 2-way ANOVAs and the p-values between adults and neonates are provided above each graph. The gating strategy for (A) is provided in section 7.18.2. Adapted from Fonseca Brito et al.[182].

In contrast, MCMV-specific CD8 T cells strongly expanded and were detected in adults as soon as seven days post-infection (dpi), whereas in neonates these tetramer$^+$ cells only appeared after 10 days and at significantly lower frequencies (Fig. 9A and B). Accordingly, control of viral loads was delayed in neonates compared to adults (Fig. 9C).

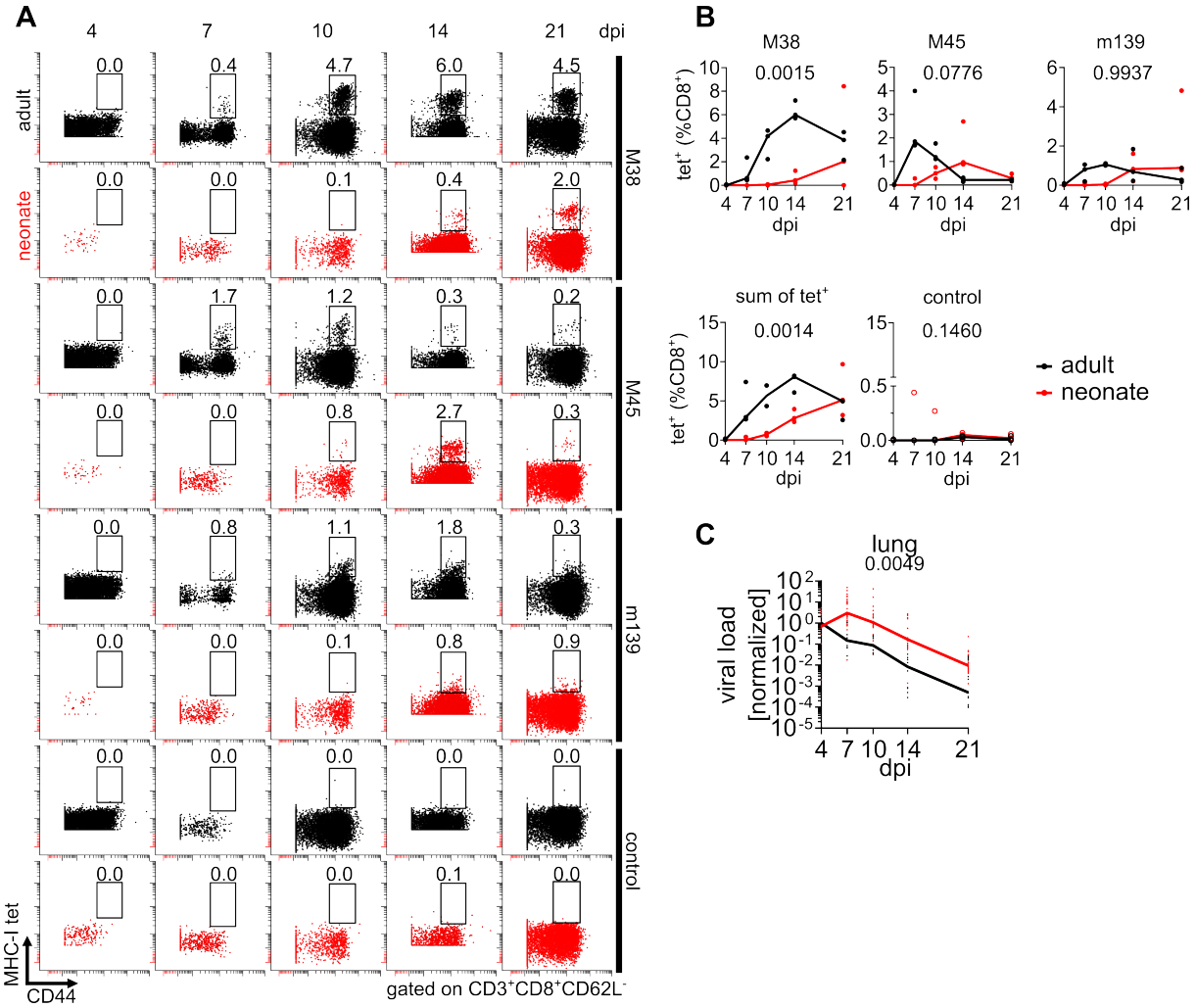

Figure 9. Expansion of MCMV-specific CD8 T cells. (A and B) (A) Representative flow cytometry plots and (B) pooled analysis of the frequencies of MCMV-specific CD8 T cells in the blood of mice after MCMV infection and staining with pMHC-I tetramers targeting the M38, M45 and m139 MCMV immunodominant peptides. Numbers above the gates represent the percentage of total CD8 T cells. (C) Lungs were isolated at the indicated time points and analyzed for viral load through luciferase activity. Data were acquired from three independent experiments (n=3). Lines in B and C connect the median values of each time point. Statistical differences were calculated with 2-way ANOVAs and the p-values

are provided above each graph. The gating strategy for (A) is provided in section 7.18.2. Adapted from Fonseca Brito et al.[182].

The composition of immune cells dynamically changes throughout life and might impact the expansion of MCMV-specific T cells. To describe the differences in the lymphocyte compartment in early life, spleens were collected within the first four weeks of life and analyzed for the presence of B cells (expressing the surface marker B220), NK cells (NK1.1$^+$) and T cells (CD3$^+$) (Fig. 10). The architecture of the spleen changed substantially within the first week of life. At post-natal day (PND) 0, very few T and B cells were present and the spleen was majorly comprised of red pulp (Fig. 10A). Quantification of spleen cells indicated an approximately 10,000-fold increase of (CD4 and CD8) T cells in the first seven days and a 10-fold increase in the number of B cells normalized to body weight (Fig. 10B and C), resulting in a larger proportion of white pulp in the spleen at PND 8 (Fig. 10A). In contrast, the number of NK cells remained fairly stable within the first 28 days of life. Taken together, T cells are present at low levels in the early-life immune system, resulting in a low number of naïve MCMV-specific T cells. Consequently, infection with MCMV in this vulnerable stage leads to a delayed expansion of these virus-specific T cells, leading to an impaired anti-viral control.

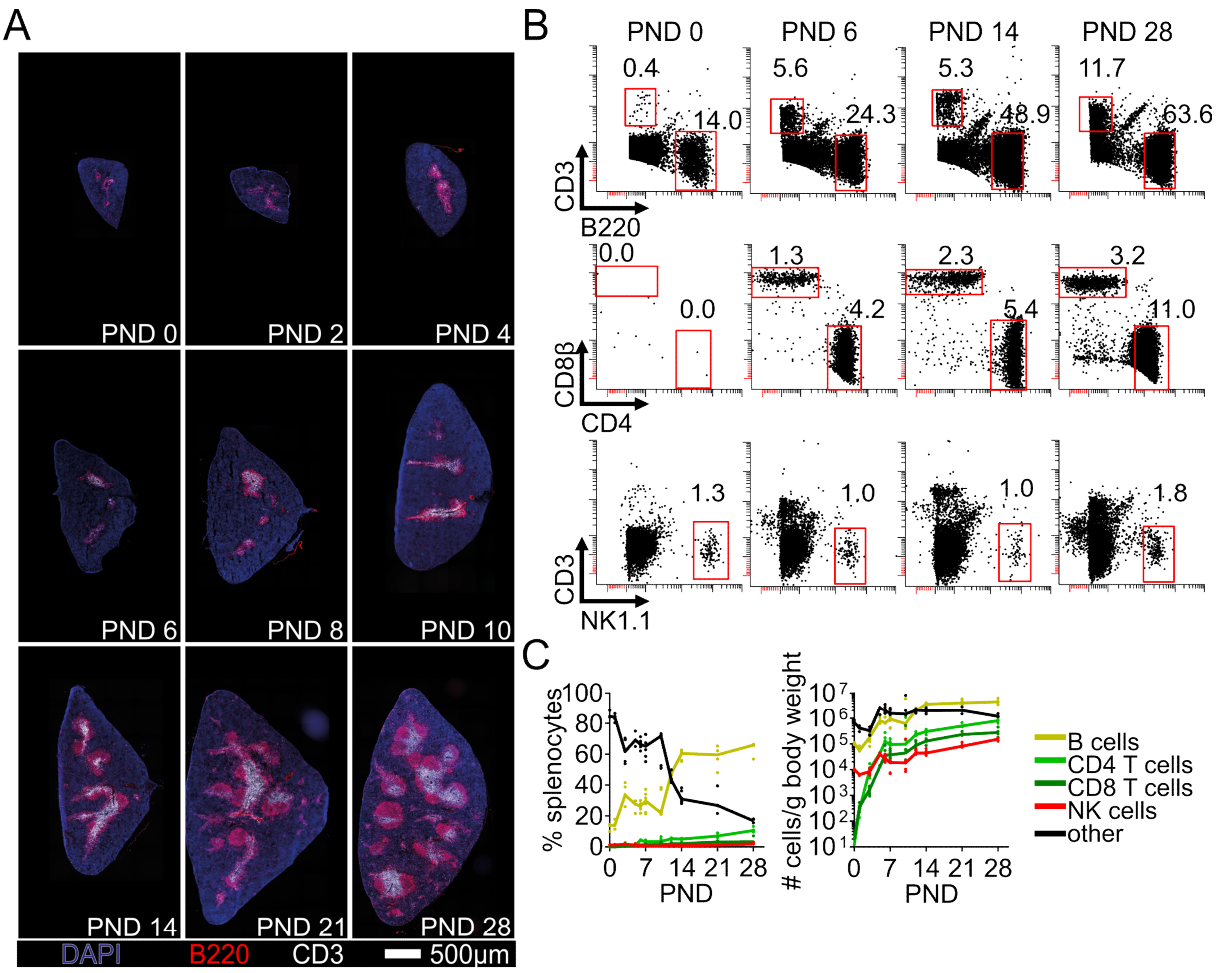

Figure 10. Early-life development of major lymphocyte populations. (A) Immunohistology of uninfected mouse spleens at the indicated post-natal days (PND). (B) Representative flow cytometry plots of major lymphocyte populations in the spleen. (C) Frequency (left panel) and number of cells normalized to body weight (right panel) of major lymphocyte populations in the spleen. Data were acquired from two or more independent experiments (n=3-7 per time point). Lines in C connect the median values in each time point. These experiments were performed by Silvia Tödter. Adapted from Fonseca Brito et al.[182].

4.2.2 Adoptive transfer of polyclonal antigen-inexperienced T cells does not protect against early-life MCMV infection

As low numbers of T cells impacted anti-MCMV control in early life, I hypothesized that compensating for this low number could improve anti-viral control. To test this, T cells were isolated from the spleen and lymph nodes of adult β-actin-eGFP (eGFP) mice and transferred into neonatal wildtype mice. This approach allowed to i) discriminate between adoptively transferred (eGFP$^+$) cells and neonatal endogenous cells (eGFP$^-$) and ii) exclude potential intrinsic differences in antiviral control between neonatal and adult T cells in the response against MCMV. To verify that adoptive T cell transfer

increased the total number of T cells in the neonatal system, $2x10^7$ eGFP$^+$ T cells were transferred into PND 0 mice and their spleens were collected and analyzed after 2 days (Fig. 11A-C). Notably, $2x10^7$ is an approximation to the total number of T cells in an adult mouse(Fig. 10C)[183] and was the highest number of T cells transferred into a neonate. Adoptive transfer of T cells led to an approximately 60-fold increase in the number of T cells in the spleen after two days (Fig. 11B), reaching numbers closer to those of a 28-day old mouse (Fig. 11B).

To assess whether higher T cells numbers at the time of early-life infection could be protective, up to $2x10^7$ eGFP$^+$ T cells were adoptively transferred into PND 0 mice infected with MCMV (Fig. 11D-G and Fig. 12). Transferred T cells were additionally labeled with a proliferation dye (eFluor 450), which enables the quantification of cell proliferation. At 7 dpi, eGFP$^+$ T cells adoptively transferred into mock-infected neonates showed little proliferation in the lungs (Fig. 11D and E), and levels of M38-, M45- and m139-specific CD8 T cells remained low (Fig. 11F and G). Conversely, in MCMV-infected animals, eGFP$^+$ T cells showed a higher expression of the CD44 surface marker, indicating acquisition of an effector phenotype, along with high proliferation levels (Fig. 11D and E), and significantly increased frequencies of MCMV-specific CD8 T cells (Fig. 11F and G).

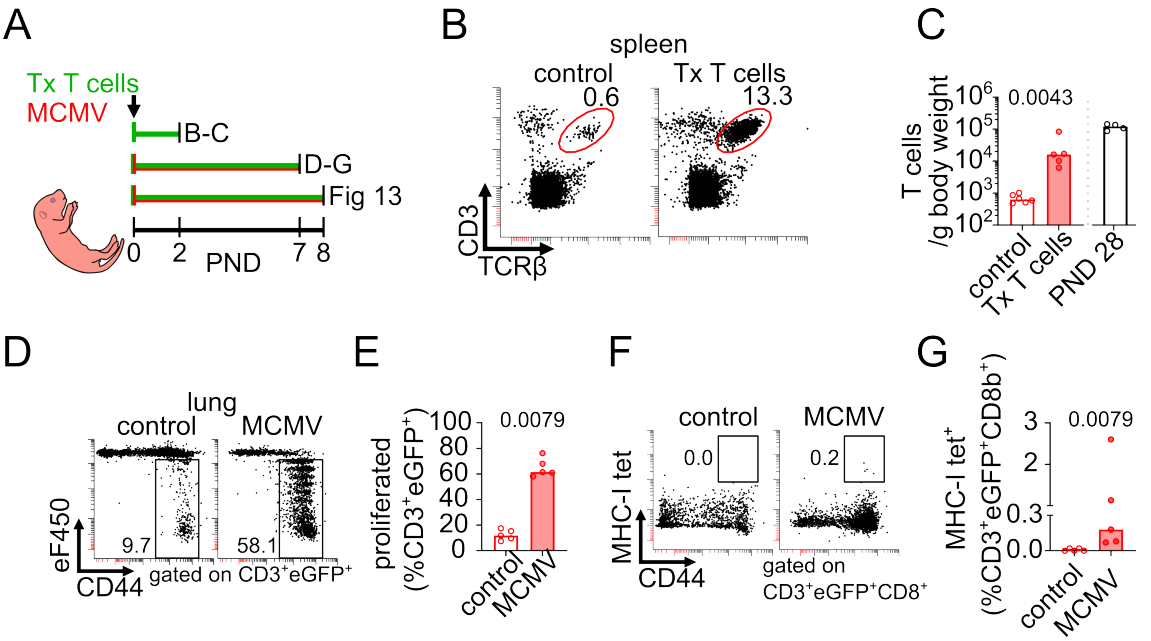

Figure 11. Adoptively transferred adult T cells can be activated and proliferate in neonates after MCMV infection. (A) Experimental setup for (B and C): $2x10^7$ adult polyclonal T cells from eGFP$^+$ mice were adoptively transferred (Tx) into neonatal mice and spleens were analyzed after 2 days; (D-G): Neonatal mice were infected with MCMV and, in parallel, adoptively transferred with 10^7 eGFP$^+$ adult T

cells previously stained with cell proliferation dye eFluor450. Control mice received cells but remained uninfected. Samples were analyzed 7 days post infection; (Fig. 12): Different numbers of adult eGFP⁺ T cells were adoptively transferred into simultaneously MCMV-infected neonatal mice and animals were analyzed after 8 days. (B and C) (B) Representative flow cytometry plots and (C) pooled analysis of spleen T cells 2 days after adoptive transfer. Cell numbers of post-natal day (PND) 28 animals from Fig. 10C are depicted for comparison. (D and E) (D) Representative flow cytometry and (E) pooled analysis of proliferation of adoptively transferred eGFP⁺ T cells. (F and G) (F) Representative flow cytometry and (G) pooled analysis of MCMV-specific eGFP⁺ T cells isolated from neonatal lungs. (B and C, n=5-6, D-G, n=5). Numbers within representative flow cytometry plots indicate the frequency of the gated populations. Statistical differences between groups were calculated with Mann-Whitney U (C, E and G) and the respective p-values are provided above each graph. Gating strategies for D and F are provided in section 7.18.3. Adapted from Fonseca Brito et al.[182].

Histological analysis of lungs from MCMV-infected neonates treated with 2x10^7 eGFP⁺ T cells indicated the preferential localization of transferred cells in nodular inflammatory foci (NIFs), sites of infection (Fig. 12A). However, the number of NIFs, NIF area or number of infected cells per NIF remained constant between T-cell- and buffer-treated animals (Fig. 12B). In line with this observation, lung viral loads remained similar at 8 dpi regardless of the number of adoptively transferred T cells (Fig. 12C). In summary, increasing the number of polyclonal, antigen-inexperienced T cells did not confer protection against early-life MCMV infection.

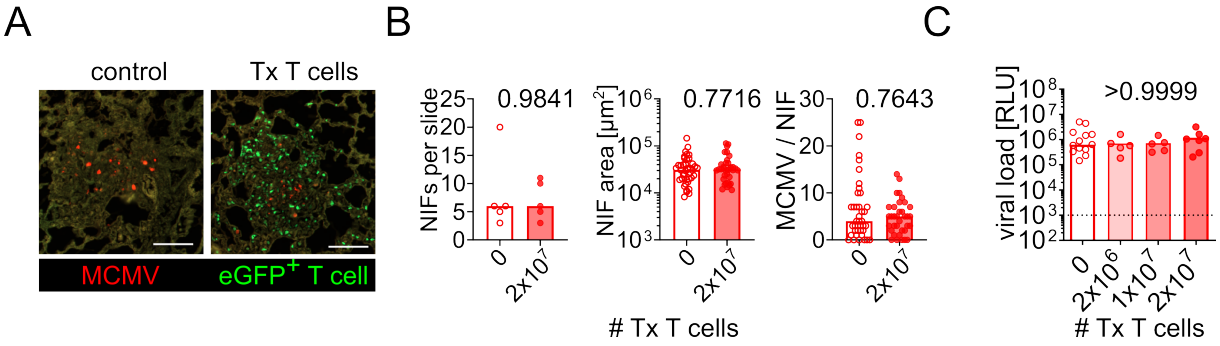

Figure 12. Adoptive transfer of adult naïve, polyclonal T cells into neonates is not protective against MCMV infection. (A and B) (A) Representative immunohistology of lung nodular inflammatory foci (NIFs) and (B) pooled quantitative analysis of lungs isolated from animals treated with buffer control or 2x10^7 eGFP⁺ polyclonal naïve T cells. (C) Quantification of lung viral loads after adoptive transfer (Tx) of different numbers of T cells. RLU, relative light units. Data were acquired from two or more experiments (n=5-13). Scale bars, 100 µm. Statistical differences were calculated with Mann-Whitney U tests (B) or a Kruskal-Wallis test (C) and the according p-values are provided above each graph. Adapted from Fonseca Brito et al.[182].

4.2.3 Adoptive transfer of antigen-specific T cells confers little protection in early-life MCMV infection

A polyclonal naïve T cell pool is comprised of cells specific to several pathogens beyond MCMV, and adoptive transfer of these cells might not sufficiently increase the frequency of MCMV-specific precursors. Therefore, the potential of naïve, antigen-specific T cells to protect against early-life MCMV infection was tested. For this, T cells from transgenic mice expressing only ovalbumin-specific CD4 T cells (OT-II mice) or ovalbumin-specific CD8 T cells (OT-I mice) were isolated. These mice were previously mated with eGFP and eCFP mice, respectively, to generate $CD4^+$ OT-II_{eGFP} and $CD8^+$ OT-I_{eCFP} T cells. This system allowed to track antigen-specific T cells in MCMV-infected neonates. For this, two MCMV-recombinants were used: (i) MCMV-4DR, which encodes the two ovalbumin peptides recognized by OT-I and OT-II T cells, and (ii) MCMV-2DR, which lacks these ovalbumin sequences (Fig. 13A). At PND 0, $5x10^6$ $CD4^+$ OT-II_{eGFP} and $5x10^6$ $CD8^+$ OT-I_{eCFP} T cells labeled with a proliferation dye were adoptively transferred into animals infected with either MCMV-2DR or MCMV-4DR (Fig. 13B). After eight days of infection, OT-I and OT-II T cells robustly proliferated in neonates infected with MCMV-4DR, but not MCMV-2DR (Fig. 13C and D).

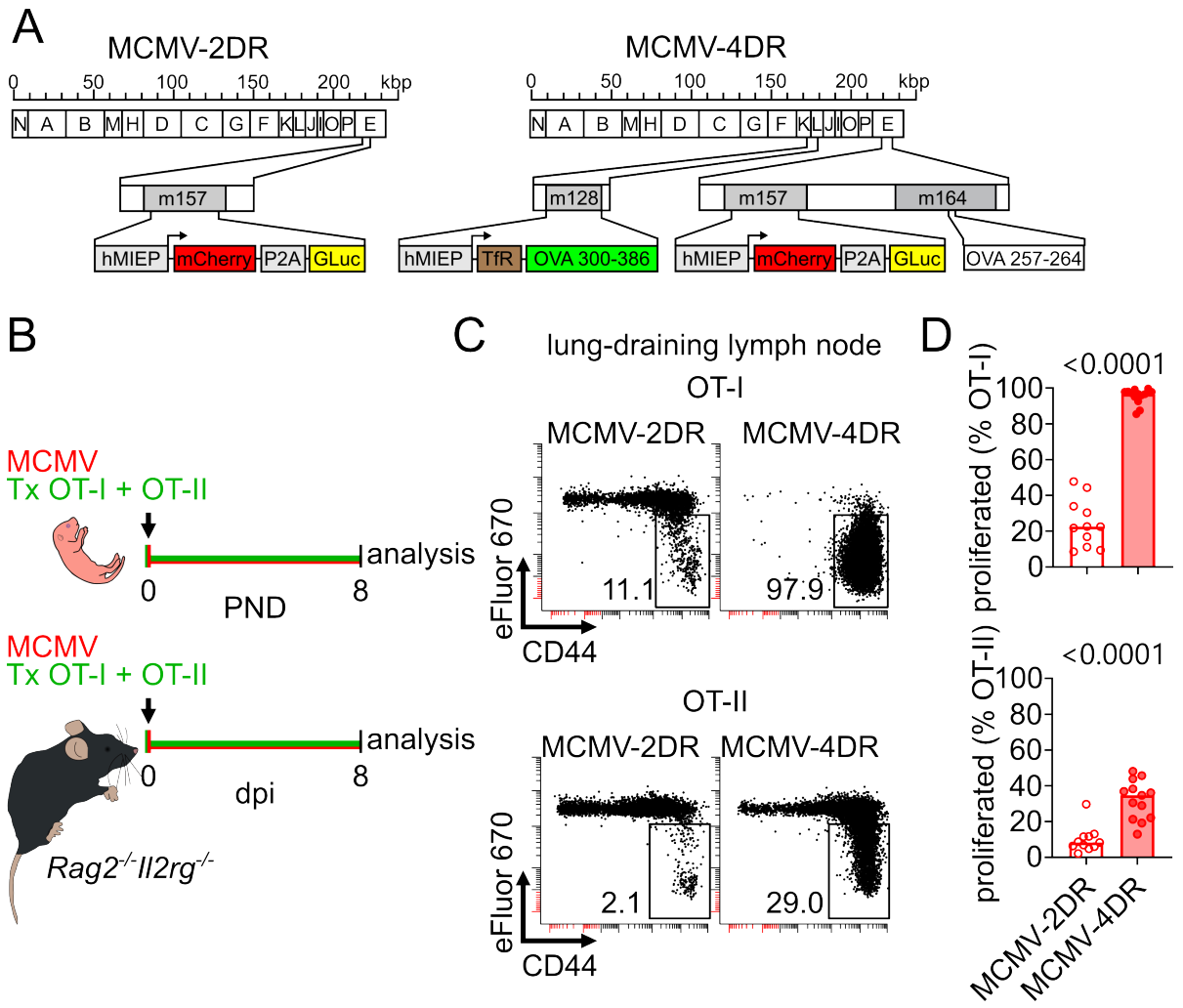

Figure 13. Adoptively transferred OT-I and OT-II cells are activated and proliferate in an antigen-specific manner. (A) MCMV-2DR expresses the *Gaussia* luciferase and mCherry reporters, whereas MCMV-4DR additionally encodes for sequences of the chicken ovalbumin that can be recognized by OT-I CD8 T cells (peptide residues OVA257-264) and OT-II CD4 T cells (OVA 323-339). (B) Experimental setup for (C-D): neonatal wildtype or adult *Rag2*$^{-/-}$*Il2rg*$^{-/-}$ mice were infected with weight-adjusted doses of MCMV-2DR or MCMV-4DR and received adoptive transfers of 5x10^6 OT-I$_{eCFP}$ and 5x10^6 OT-II$_{eGFP}$ cells previously labeled with the proliferation dye eFluor670. Control animals did not receive any T cells. The mice were analyzed at 8 dpi. (C and D) (C) Representative flow cytometry plots and (D) pooled analysis of OT-I and OT-II T cell proliferation within neonatal lung-draining lymph nodes. Data were acquired from 5 independent experiments (n=7-11). Scale bars, 100 µm. Statistical differences between groups were calculated with Mann-Whitney U tests and the p-values are provided for the respective comparisons. The gating strategies for (C) are provided in section 7.18.4. Adapted from Fonseca Brito et al.[182].

Histological analyses revealed a substantial increase of OT-I, but not OT-II cells, in NIFs of animals infected with MCMV-4DR (Fig. 14A and B). Numbers of MCMV-infected cells per NIF in MCMV-4DR were slightly lower after adoptive transfer of OT-

I and OT-II cells, but NIFs still harbored a significant number of infected cells (Fig. 14A and C). NIF areas remained similar to buffer control-treated animals (Fig. 14C).

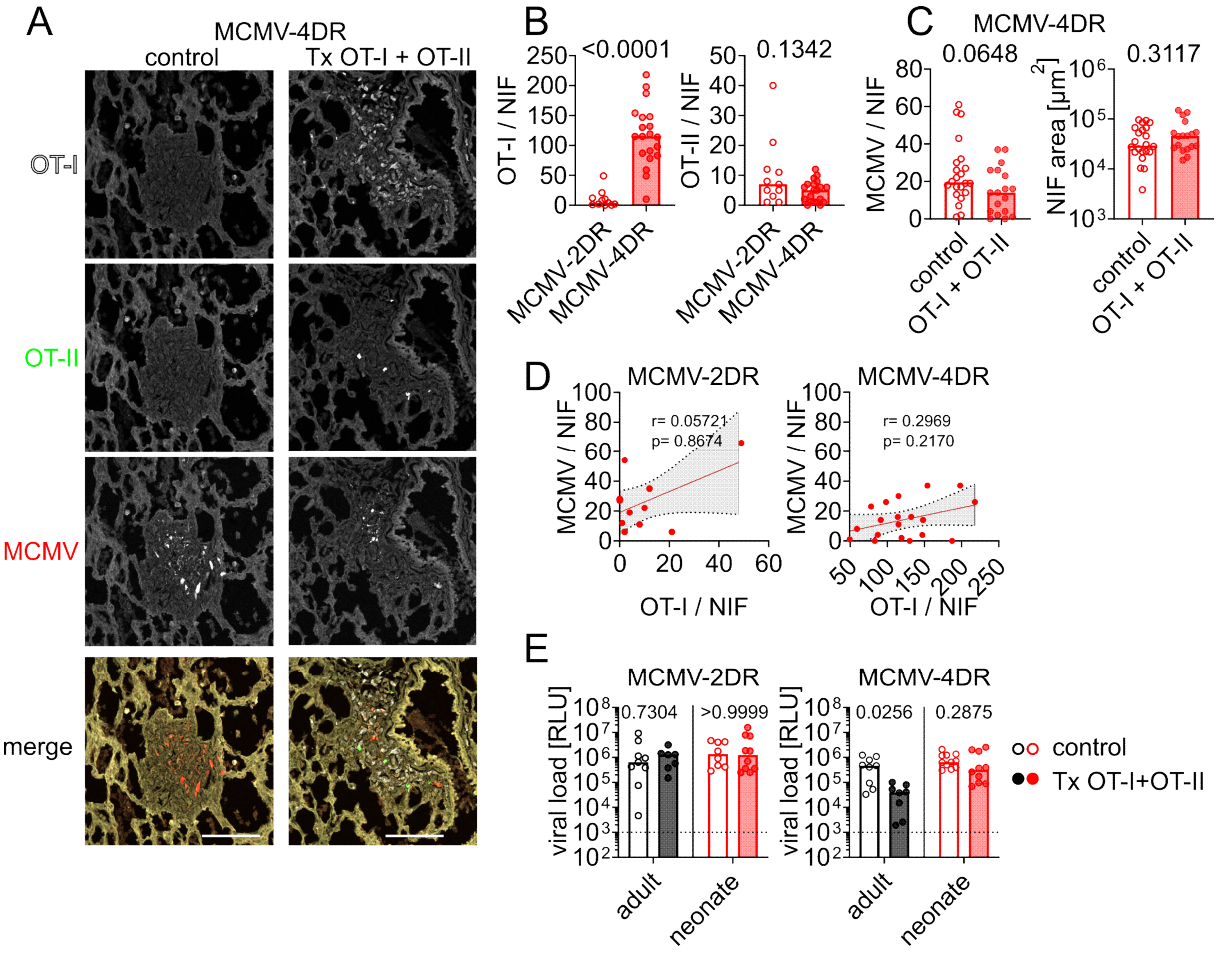

Figure 14. Adoptive transfer of adult, naive antigen-specific T cells does not protect neonates against MCMV infection. (A) Representative immunohistology of lungs from neonates infected with MCMV-4DR. (B) Quantitative analysis of OT-I and OT-II cells in nodular inflammatory foci (NIFs) of neonates infected with MCMV-2DR or MCMV-4DR. (C) Quantitative analysis of mCherry-expressing cells in NIFs of MCMV-4DR-infected mice. (D) Correlation of MCMV-infected cells and numbers of OT-I cells within a NIF. (E) Lung viral loads after infection with MCMV-2DR and MCMV-4DR with and without adoptive T cell transfers. Data were acquired from 5 independent experiments (n=7-11). Scale bars, 100 µm. Statistical differences between groups were calculated with Mann-Whitney U tests (B and C) and 2-way ANOVAs (E) and the p-values are indicated above the respective comparisons. Spearman correlation results in (D) are provided above the graphs. Adapted from Fonseca Brito et al.[182].

Moreover, the number of OT-I cells per NIF did not correlate with an improved control of MCMV infection within NIFs (Fig. 14D).

In parallel to the neonatal infections, adult *Rag2*$^{-/-}$*Il2rg*$^{-/-}$ were treated with the same number of cells and infected with weight-adjusted viral loads. These transgenic mice lack T, B and NK cells and were used as age controls of lymphopenia. Notably,

adoptive transfer with the same number of cells results in a treatment of approximately 20-fold fewer cells per body weight transferred into adults than neonates. When analyzing lung viral loads, treatment with buffer control or OT-I and OT-II cells yielded similar levels after infection with MCMV-2DR in both adults and neonates (Fig. 14E). However, after infection with MCMV-4DR, adult *Rag2*$^{-/-}$*IL2rg*$^{-/-}$ showed significant reduction of viral loads upon adoptive transfer of antigen-specific T cells as compared to buffer-treated animals, indicating an antigen-dependent effect of OT-I and OT-II cells (Fig. 14E). Conversely, there was no significant protection of MCMV-4DR-infected neonates after treatment with antigen-specific T cells (Fig. 14E). In summary, even high initial numbers of antigen-specific T cells failed to robustly protect neonates against MCMV infection. In contrast, adults treated with 20-fold less antigen-specific T cells per gram of body weight displayed a significant decrease in viral loads.

4.2.4 Effector CD8 T cells generated in early life express low levels of cytotoxic molecules

As high numbers of antigen-specific cells could not protect against early-life MCMV infection, I hypothesized that age-related factors in T cell activation and priming modulated differentiation and effector function of these cells. To understand these differences, the phenotypes of T cells primed in neonatal or in adult systems were compared (Fig. 15A). Twelve-week-old mice were infected with MCMV, and their lung T cells were isolated at 7 dpi. In parallel, naïve (CD44^{-}), polyclonal eGFP^{+} T cells from 12-week-old mice were adoptively transferred into PND 0 mice infected with MCMV and these eGFP^{+} cells were isolated from the lungs at 7 dpi. The cells were then phenotyped by single-cell RNA sequencing combined with TCR sequencing. This system allowed to isolate the effects of the neonatal environment on the activation and generation of antiviral T cells, while excluding intrinsic age-related differences in T cell function. In total, 6,023 T cells from all samples were analyzed (Fig. 15A). Cells from mock- and MCMV-infected samples separated from each other in the UMAP dimensionality reduction, indicating overall different transcriptomes between these samples (Fig. 15B). This separation was associated with the general expression of the *Ccr7* gene, indicative of a naïve phenotype in cells isolated from control uninfected animals (Fig. 15C). To screen general differences between the four groups, the pseudo-bulk transcriptomes were compared (Fig. 15D). Here, non-infected control neonates and adults exhibited similar phenotypes, as indicated by similar principal

component (PC) 2 values. In MCMV infection, adult and neonatal samples shifted along the PC 1 axis, indicating the acquisition of an effector phenotype (Fig. 15D). However, the phenotypes of MCMV-infected adults and neonates differed more than their control counterparts, indicating a generally different T cell response (Fig. 15D). Next, TCR clonotypes were defined as cells that share the same *Tra* and *Trb* genes and CDR3 amino acid sequences. Only up to 5% of cells from non-infected adults and neonates belonged to a clonotype represented by more than one cell (Fig. 15E), indicating a high repertoire diversity. By contrast, upon MCMV infection a high proportion of the cells expanded in both neonates and adults, leading to an increase in the proportion of clonotypes with more than one clone (Fig. 15E).

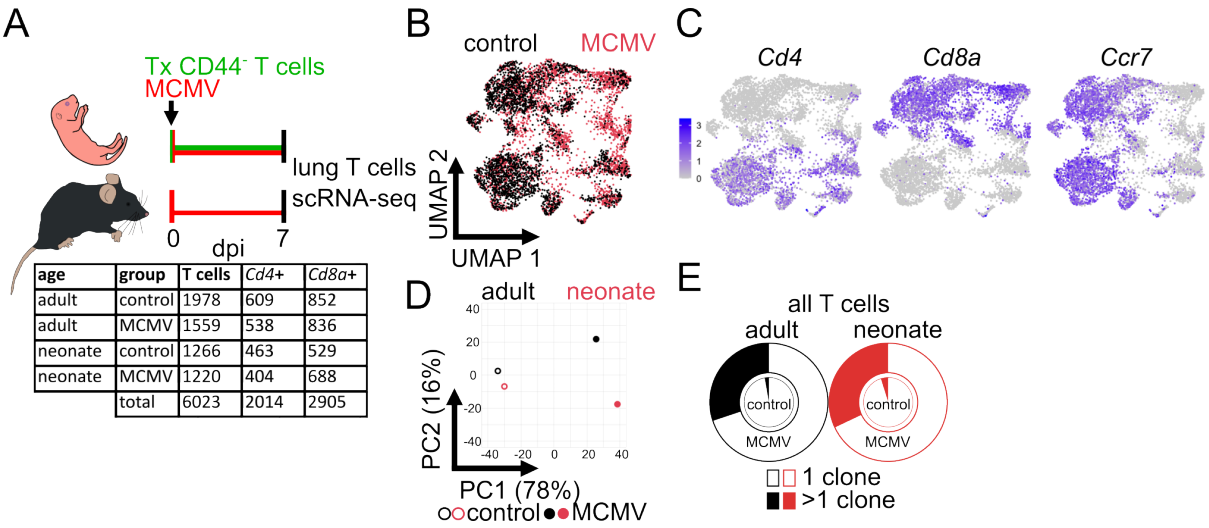

age	group	T cells	*Cd4+*	*Cd8a+*
adult	control	1978	609	852
adult	MCMV	1559	538	836
neonate	control	1266	463	529
neonate	MCMV	1220	404	688
	total	6023	2014	2905

Figure 15. Single-cell RNA sequence analysis of adult T cells primed in adults and neonates. (A) Experimental setup for Fig11-17: neonatal (n=3) and adult (n=3) mice were infected with weight-adjusted doses of MCMV. 10^7 adult eGFP$^+$ naïve (CD44$^-$) T cells were adoptively transferred (Tx) into neonates. Control animals were not infected with MCMV. After 7 days, adoptively transferred eGFP$^+$ lung T cells in neonates and endogenous lung T cells in adults were isolated and pooled for single-cell transcriptome profiling combined with T cell receptor (TCR) sequencing. The table indicates the final number of cells analyzed from each group after quality control. (B) UMAP dimensionality reduction of all cells with colors indicating infection status of mice from which the cells derived. (C) Relative gene expression plots. (D) Principal component analysis for the four different groups. The percentages indicate the proportion of the total variance in the overall dataset explained by the according principal component. (E) Relative distribution of T cells with identical TCRs indicating clonal enrichment. Data processing was performed by Dr. Sanamjeet Virdi. Adapted from Fonseca Brito et al.[182].

Upon differentiation, CD4 and CD8 T cells exhibit different phenotypes. Thus, *Cd4*$^+$*Cd8a*$^-$ (hereafter referred to as CD4) and *Cd4*$^-$*Cd8a*$^+$ (CD8) T cells were analyzed separately to increase the resolution of the datasets. CD4 cells were classified into (i)

naïve, based on the expression of *Tcf7*, *Ccr7* and *Sell*, (ii) cycling, expressing of *Mki67* and *Pclaf*, (iii) Treg, expressing *Foxp3* and *Il2ra*, and (iv) Th1, expressing *Cd44*, *Ly6c2* and *Cxcr6*[184,185] (Fig. 16A and B). CD4 subsets showed similar distribution between adults and neonates, both in steady state and after MCMV infection (Fig. 16C). Likewise, the distribution of cells isolated from infected animals was similar in the UMAP (Fig. 16D).

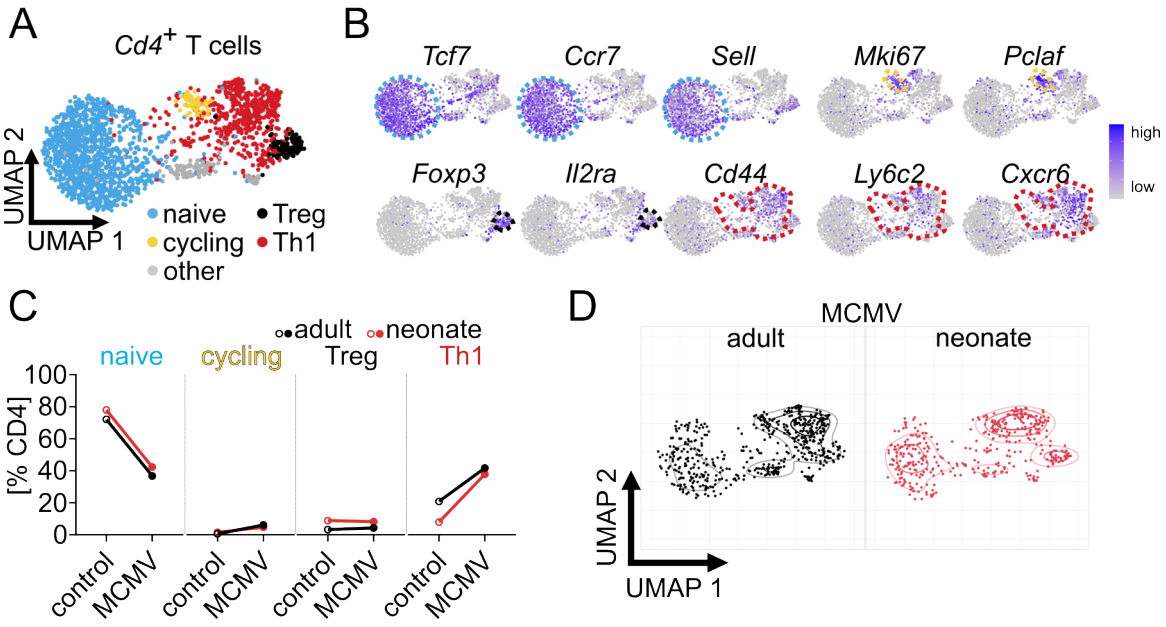

Figure 16. Phenotype of CD4 T cells primed in adults and neonatal lungs after MCMV infection. (A) UMAP dimensionality reduction and annotation of CD4 T cells. (B) Relative expression of genes used for classification of CD4 T cells into subpopulations. (C) Frequencies of each subpopulation within the four groups. (D) UMAP dimensionality reduction of CD4 T cells isolated from MCMV-infected animals. Data processing was performed by Dr. Sanamjeet Virdi. Adapted from Fonseca Brito et al.[182].

Surprisingly, while at steady state CD4 cells exhibited high clonotype diversity in both neonates and adults, T cells primed in MCMV-infected neonates expanded more strongly than in adults (Fig. 17A), and these expanded cells were largely of the Th1 phenotype (Fig. 17B). Th1 cells play a crucial role in controlling viral infections[186]. Comparison of these cells after priming in neonates and adults revealed a higher expression of *Ifng* in MCMV-infected neonates, resulting in a higher cytotoxicity signature of these cells in early life (Fig. 17C and D). In summary, slightly stronger CD4 T cell responses were observed in neonates upon MCMV infection.

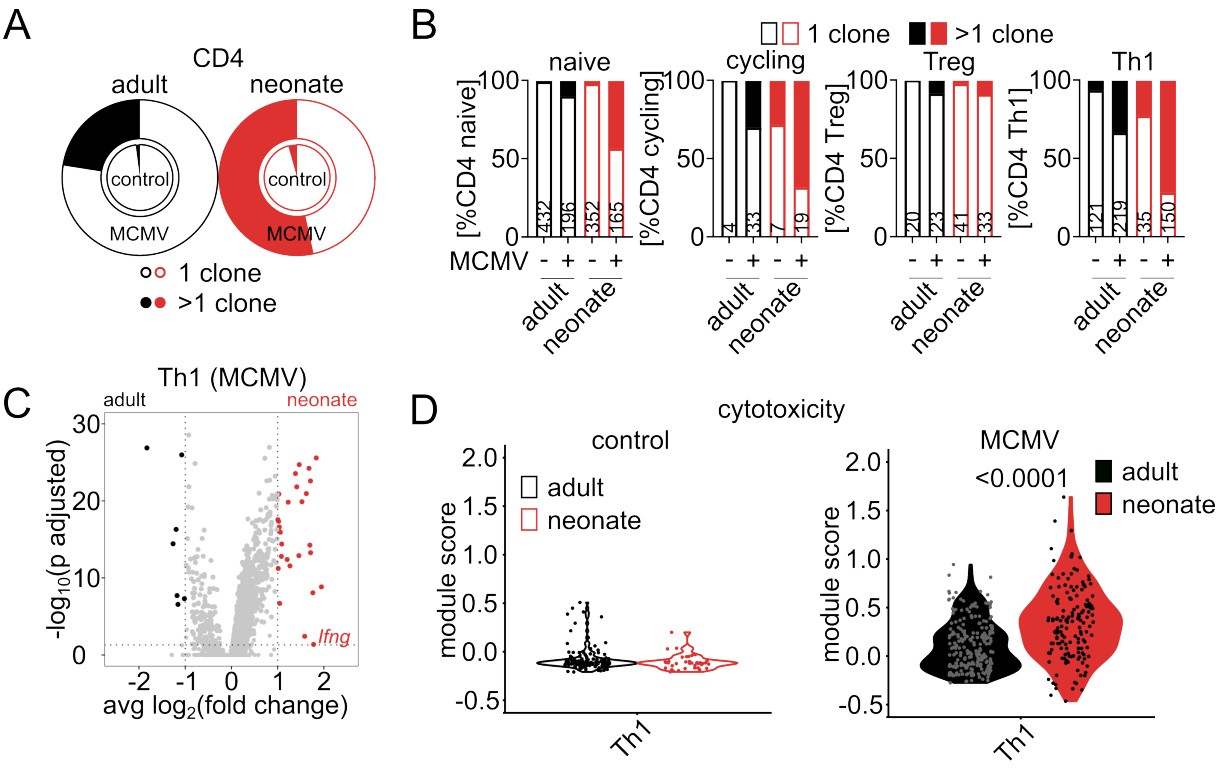

Figure 17. Expansion and differential gene expression of CD4 T cells isolated from adult and neonatal lungs after MCMV infection. (A) Frequency of the clonal and not clonal CD4 T cells within the four groups. (B) Relative distribution of clonal and not clonal CD4 T cell subpopulations within the four groups. (C) Differential gene expression of Th1 T cells obtained from MCMV-infected animals. (D) Cytotoxicity module scores of Th1 cells within the four groups. Statistical difference in (C) was calculated with a Mann-Whitney U test with Bonferroni correction. Differences in (D) were calculated with a Mann-Whitney U test and p-values <0.05 are given above the comparisons. Numbers within the bars in (B) represent cell numbers. Data processing was performed by Dr. Sanamjeet Virdi. Adapted from Fonseca Brito et al.[182].

Next, CD8 T cells were subject to similar analyses. Cells were classified into (i) naïve (*Tcf7*, *Ccr7* and Sell), (ii) cycling (*Mki67* and *Pclaf),* or (iii) effector (*Gzmb*, *Cd44* and *Ccl5)*[187,188] (Fig18 A and B). The proportions of these subsets were similar in adults and neonates (Fig. 18C). In non-infected animals, the majority of cells were naïve, while after infection the frequencies of these cells decreased due to differentiation into effector cells (Fig. 18C). However, a different distribution in the UMAP of effector cells was observed between infected adults and neonates, suggesting a different overall effector phenotype (Fig. 18D). Accordingly, analysis of differentially expressed genes within the effector subset indicated a higher expression of *Sell* in neonates, indicative of a less differentiated phenotype, while in adults, effector cells overexpressed several effector molecules such as *Gzma*, *Gzmk* and *Ccl5* (Fig. 18E). Moreover, contrary to the CD4 T cells, CD8 T cells in infected adults showed more expansion than in

neonates (Fig. 18F). In particular, almost 50% of effector cells from infected adults belonged to an expanded clonotype, whereas in neonates this frequency remained at 11% (Fig. 18G).

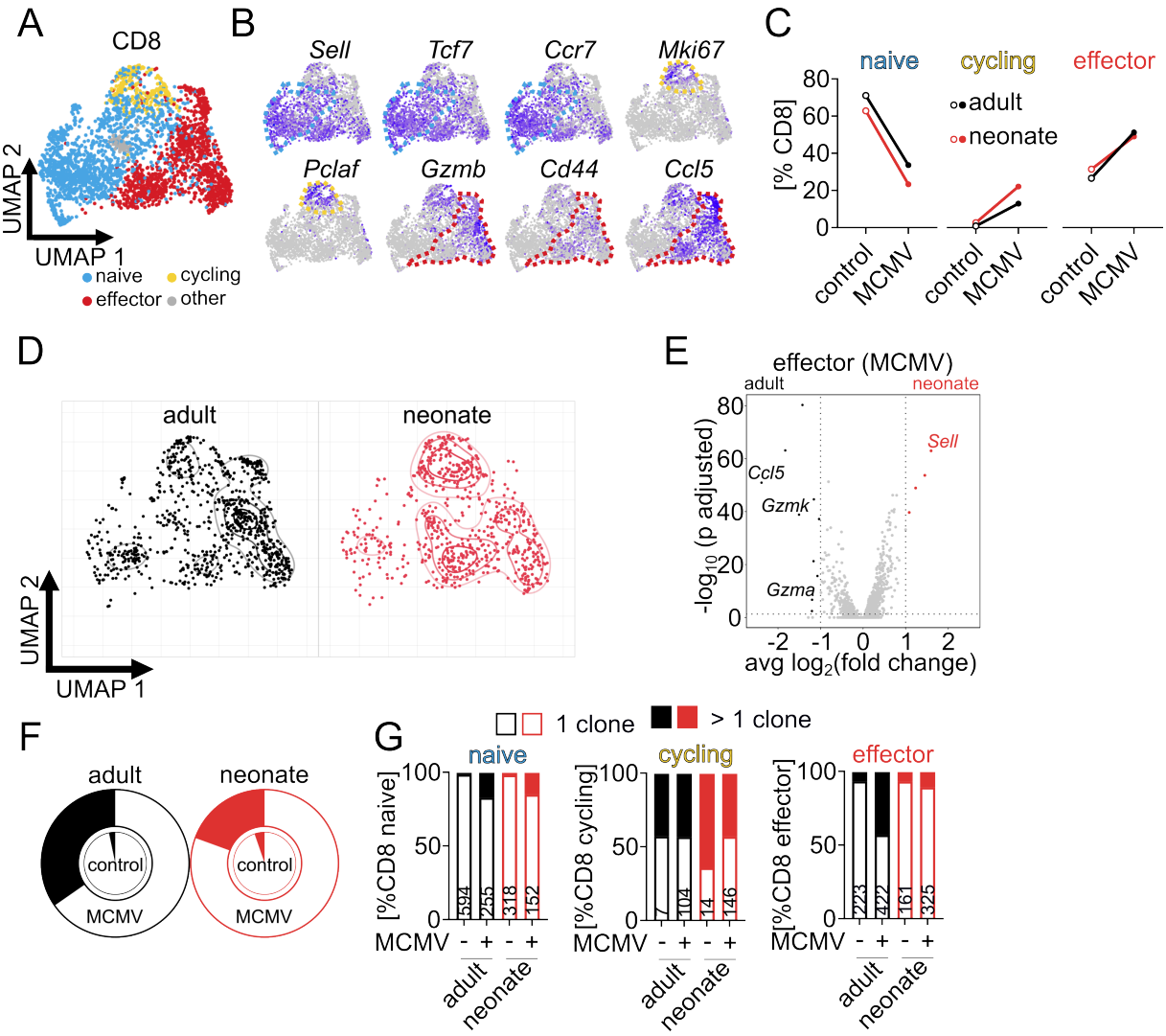

Figure 18. Phenotype and expansion of CD8 T cells primed in adult and neonatal lungs after MCMV infection. (A) UMAP dimensionality reduction and annotation of CD8 T cell subsets. (B) Relative gene expression of genes used to annotate CD8 T cell subsets. (C) Frequency of CD8 T cell subsets within the four groups. (D) UMAP dimensionality reduction of CD8 T cells isolated from MCMV-infected animals. Effector cells are highlighted in red. (E) Differential gene expression of effector CD8 T cells isolated from MCMV-infected animals. (F) Frequency of clonal and not clonal CD8 T cells within the four groups. (G) Relative distribution of clonal and not clonal CD8 T cell subsets within the four groups. Statistical differences in (E) were calculated with Mann-Whitney U tests with Bonferroni correction. Data processing was performed by Dr. Sanamjeet Virdi. Adapted from Fonseca Brito et al.[182].

These results indicated a stronger effector CD8 T cell response in adults. To further characterize these differences, effector cells were divided into four sub-clusters

exhibiting high expression of (i) *Gzmm, Eomes* and *Sell* ($T_{eff}1$), (ii) *Ly6a*, *Gzmb*, *Ifit1* and *Ifit3* ($T_{eff}2$), (iii) *Gzmk*, *Ccl5*, *Cxcr3* and *Cxcr6* ($T_{eff}3$) or (iv) *Ccl5*, *Gzma*, *Klrg1*, *Zeb2*, *Cx3cr1*, *S1pr5* and *Tbx21* ($T_{eff}4$) (Fig. 19A and B). All effector subsets were present within the four groups (Fig. 19C). However, $T_{eff}1$ frequencies were generally higher in both control and infected neonates, whereas CD8 T cells in infected adults preferentially acquired $T_{eff}3$ and $T_{eff}4$ phenotypes (Fig. 19C). These results were validated by flow cytometry, where neonates showed similar frequencies of effector cells (Fig. 19D), but lower frequencies of CCL5- and CXCR6-expressing effector CD8 T cells than MCMV-infected adults (Fig. 19E and F).

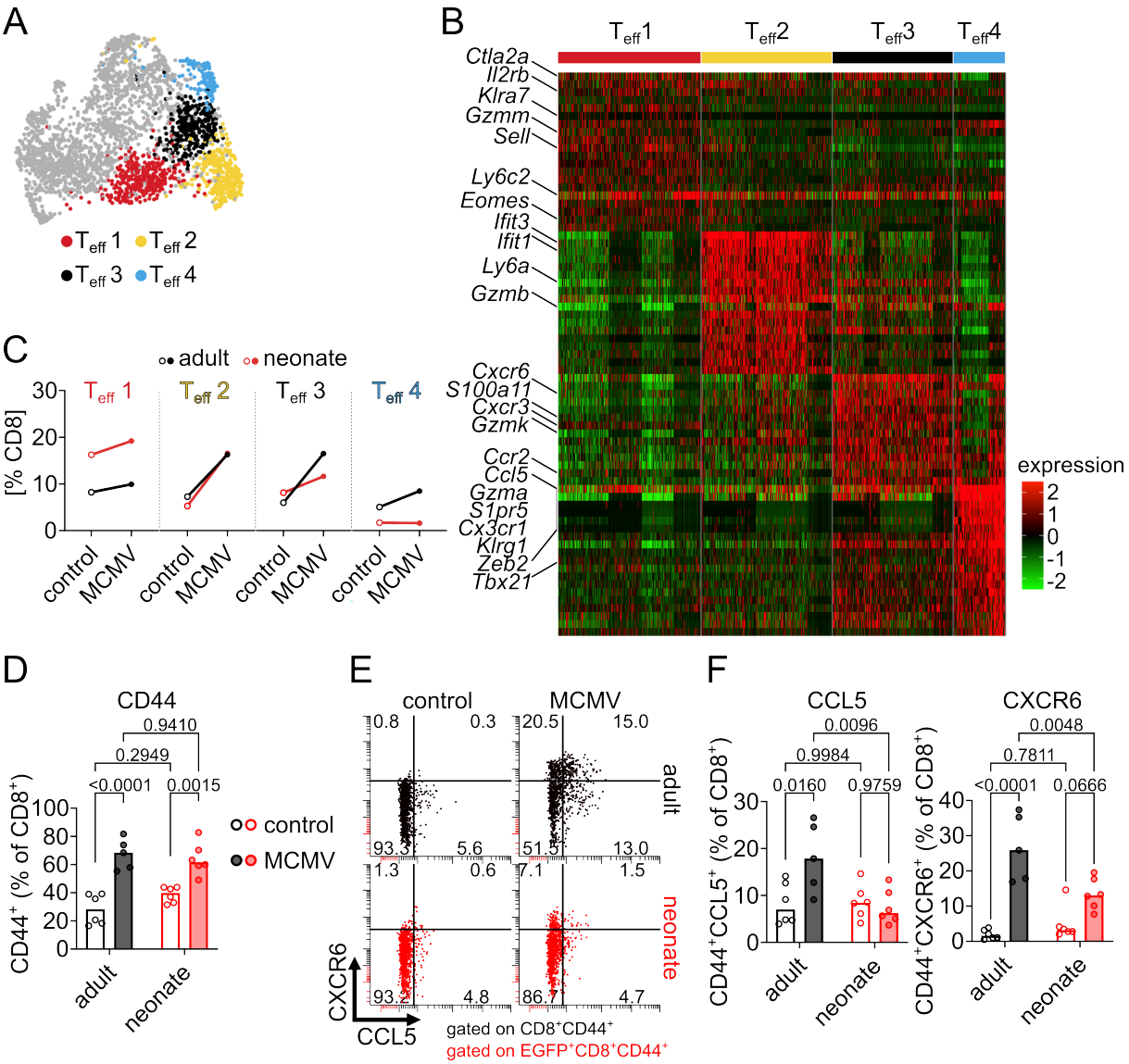

Figure 19. Differences between effector T cells primed in adults and neonates. (A) Subclassification of effector CD8 T cell clusters. (B) Heatmap of the top 20 marker genes of the effector CD8 T cell subclusters. (C) Frequencies of effector CD8 T cell subtypes within the four groups. (D) Flow cytometric analysis of effector ($CD44^+$) CD8 T cells in $eGFP^+$ or endogenous T cells isolated

from neonates and adults, respectively. (E and F) (E) Representative flow cytometry and (F) pooled analysis of CXCR6 and CCL5 expression within CD8 T cells isolated from neonates and adults. Data in (D-F) display results from two independent experiments. Statistical differences in (F) were calculated with 2-way ANOVAs and p-values are depicted for each comparison. Data processing in (A) and (B) was performed by Dr. Sanamjeet Virdi. Adapted from Fonseca Brito et al.[182].

Next, cytotoxicity signatures within these sub-clusters were analyzed. Non-infected animals displayed low levels of cytotoxicity in $T_{eff}1$-3, while $T_{eff}4$ were cytotoxic (Fig. 20A). After MCMV infection, $T_{eff}1$ maintained a low cytotoxic potential, whereas $T_{eff}2$-$T_{eff}4$ showed generally high cytotoxicity scores (Fig. 20A). Strikingly, in contrast to adults, the cytotoxicity score of $T_{eff}2$ isolated from infected neonates remained low, pointing out to a lower potential of eliminating virus infected cells (Fig. 20A). Thus, effector T cells isolated from MCMV-infected neonates generally exhibited lower cytotoxicity scores, as most of these cells belonged to the $T_{eff}1$ and $T_{eff}2$ subsets. In contrast, most adult effector CD8 cells showed high cytotoxic potential. Taken together, early-life MCMV infection leads to strong CD4 T cell responses in neonates. However, the generation of primarily cytotoxicity-deficient effector CD8 T cells might impair MCMV control and increase susceptibility to disease.

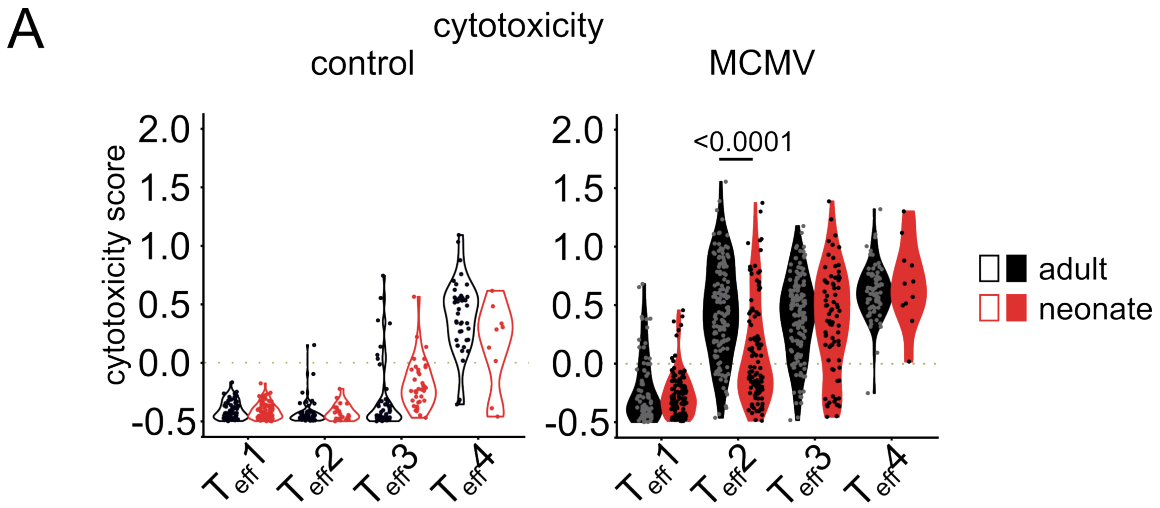

Figure 20. Lower cytotoxicity of effector T cells isolated from lungs of MCMV-infected neonates. (A) Cytotoxicity module scores from effector CD8 T cells isolated from control (left panel) and MCMV-infected (right panel). Dotted lines indicate a cytotoxicity threshold of 0. Statistical differences were calculated with a Mann-Whitney U Test and p-values <0.05 are depicted above each comparison. Data processing was performed by Dr. Sanamjeet Virdi. Adapted from Fonseca Brito et al.[182].

4.2.5 Deficient CD8 T cell priming in early life due to low levels of priming cytokines

The phenotype of effector CD8 T cells is highly influenced by the combination of the three different signals required for priming[189,190]. Adoptive transfer of polyclonal or antigen-specific T cells after MCMV infection led to robust antigen-specific proliferation, indicating that antigen presentation to TCRs occurred in both contexts (Fig. 11 and 13). Therefore, I hypothesized that differences in co-stimulatory and/or cytokine signaling during T cell priming might have an effect on the low cytotoxicity of effector CD8 T cells generated after early-life MCMV infection. Since naïve CD8 T cells can be primed in lungs[191] lung antigen-presenting dendritic cells (DCs) from uninfected 5-day-old mice were analyzed for their expression of co-stimulatory molecules important for priming of CD8 T cells, with adult 12-week-old mice serving as age controls. As not enough DCs per neonate can be isolated from their lungs at this time point, samples of three animals were pooled in every experiment. Lung conventional type I dendritic cells (cDC1) are the major subpopulation responsible for cross-presenting antigens to CD8 T cells[192]. These cells were characterized by their high expression of CD11b, MCH-II, and CD103[193], and were observed at a higher frequency in neonates (Fig. 21A and B). However, the frequencies of cDC1 expressing CD80 or CD86, the main co-stimulatory molecules of CD8 T cells, were lower in neonates than in adults (Fig. 21C and D). Furthermore, neonatal cDC1 expressed seemingly lower amounts of CD86 on their surfaces (Fig. 21C and E). Thus, the lower frequencies of CD80- and CD86-expressing cDC1 in early life, combined with low expression of CD86, likely contribute to a different priming of CD8 T cells in MCMV infection.

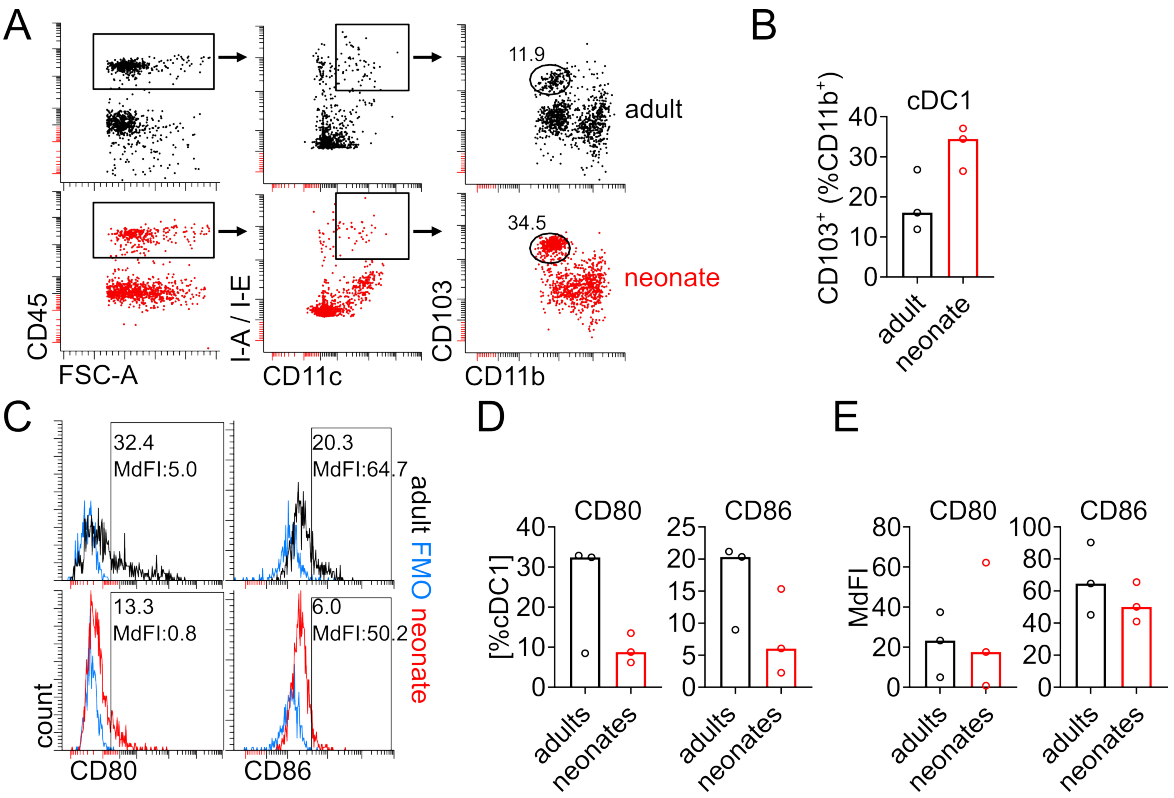

Figure 21. Phenotype of antigen-presenting cells in the lungs of adults and neonates. (A) Gating strategy and representative flow cytometry plots of lung-resident dendritic cells from adults (12 weeks) and neonates (post-natal day 5). (B) Frequency of lung-resident conventional Type 1 dendritic cells. (C) Representative histograms of expression of CD80 and CD86 on cDC1. (D and E) (D) Frequency and (E) median fluorescence intensity (MdFI) of CD80 and CD86 on lung-resident cDC1 isolated from adult and neonatal mice. Data were acquired from three independent experiments, with three mice pooled per group and per experiment. Adapted from Fonseca Brito et al.[182].

Next, cytokine signaling during CD8 T cell priming was addressed during MCMV infection. A 14-analyte multiplex ELISA was employed to quantify the concentrations of IFN-α, IFN-β, IFN-γ, IL-1β, IL-2, IL-6, IL-7, IL-10, IL-12p70, IL-15, IL-18, IL-27, IL-33 and TNF-α in lungs. After five days, non-infected adults displayed higher levels of these cytokines than control neonates, where several cytokines remained undetected (Fig. 22A-J). MCMV infection induced higher expressions of IL-2, IL-7, and IL-15 in adults but not in neonates (Fig. 22B). Moreover, levels of IL-27, IL-33, and IFN-α remained significantly higher in adults than neonates after MCMV infection (Fig. 22C-F). In contrast, levels of IL-10, IFN-β, and IL-1β were similar between adults and neonates after MCMV infection. Surprisingly, neonates exhibited higher levels of IFN-γ in their lungs, while IL-6 levels were also higher in these animals (Fig. 22H-J). Altogether, low levels of IL-2, IL-7, and IL-15 combined with low levels of co-stimulatory cDC1 result

in priming conditions that lead to low cytotoxicity of effector CD8 T cells in early-life MCMV infection.

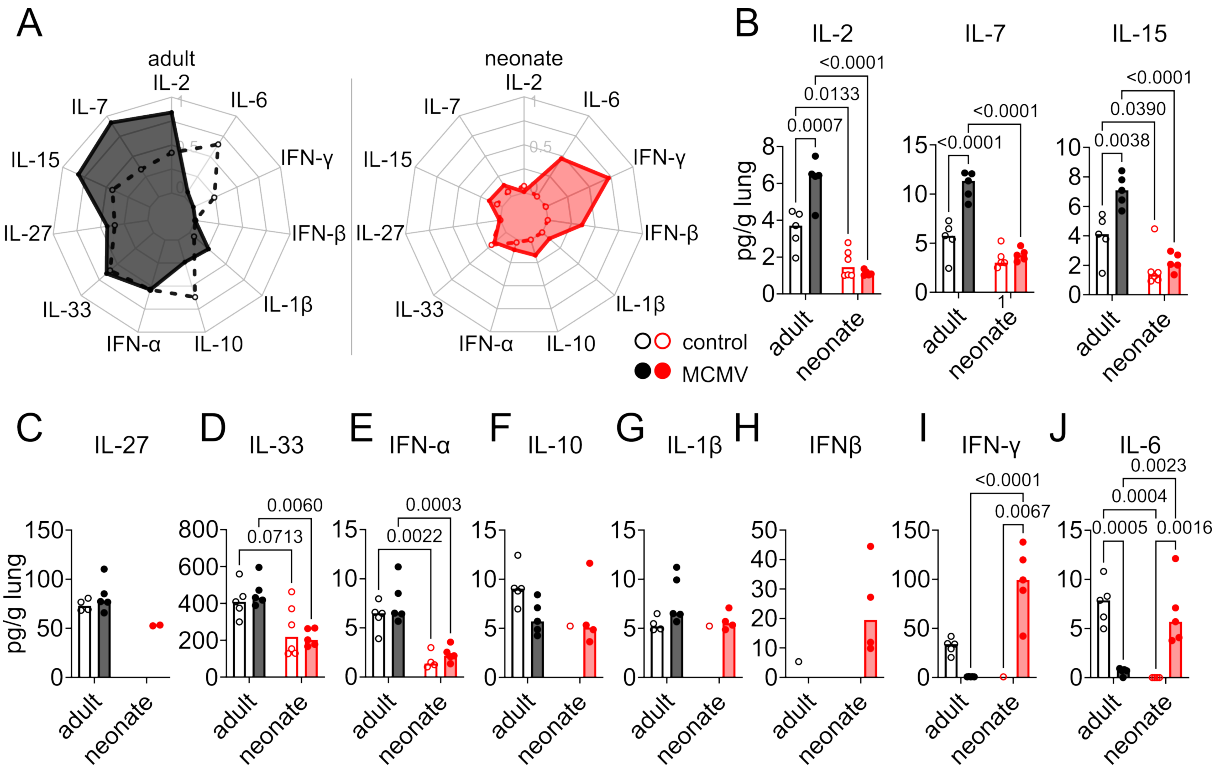

Figure 22. CD8 T cell-priming cytokines in the lungs of MCMV-infected adults and neonates. (A) Normalized concentration of cytokines in lungs of 12-week-old adults or neonates at 5 days post-infection. (B-J) Concentration of cytokines in lungs of steady-state or MCMV-infected neonates or adults at 5 dpi. Data were acquired from two independent experiments (n=6). Statistical differences were calculated with 2-way ANOVAs and the p-values <0.1 are provided for each comparison. Adapted from Fonseca Brito et al.[182].

4.2.6 T cells primed in adult systems protect neonates against MCMV infection

Priming of CD8 T cells in neonatal systems led to cells expressing low mRNA levels of cytotoxic molecules. Thus, I hypothesized that CD8 T cells primed in adults could improve antiviral control in neonates, as these cells are highly cytotoxic (Fig. 20A) and can clear MCMV infection within a few days[95,138]. To test this, T cells primed in adult systems were adoptively transferred into MCMV-infected neonates. For this, adult wildtype mice were infected with MCMV, their lung CD44$^+$ effector T cells were isolated at 7 dpi and adoptively transferred into neonates, who were infected in parallel with MCMV (Fig. 23A). After eight days, a significant increase in the frequency of T cells was observed in effector T cell-treated animals (Fig. 23B and C). Moreover, adoptive

transfer of effector T cells led to a general increase of effector T cells in the lung (Fig. 23D and E).

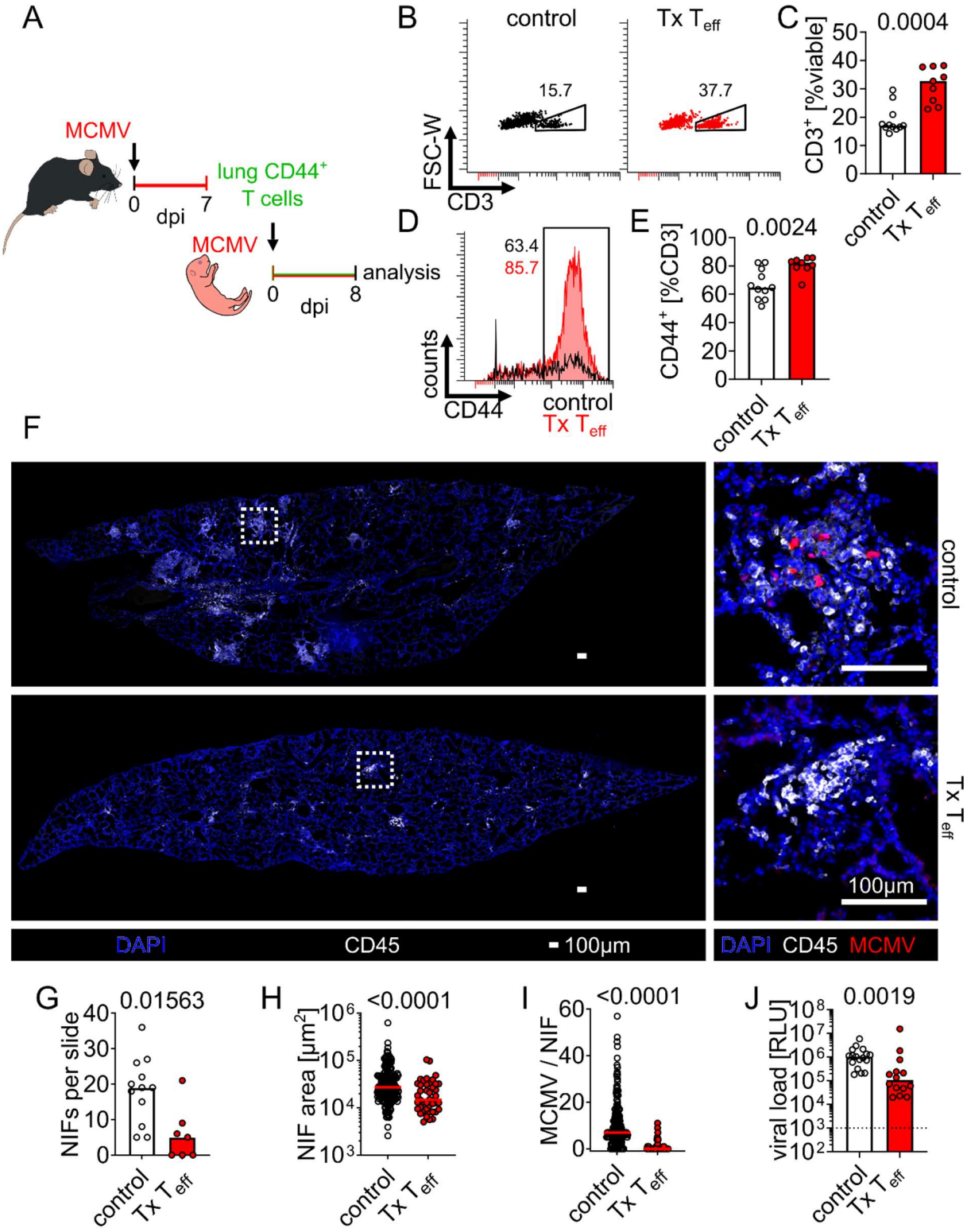

Figure 23. Protective characteristics of T cells primed in MCMV-infected adults. (A) Experimental setup for (B-J): Lung CD3+CD44+ effector T cells were isolated from adult mice at 7 dpi and 8x106 cells were adoptively transferred into neonates infected, in parallel, with MCMV. Control mice did not receive T cells. Mice were analyzed at 8 dpi. (B and C) (B) Representative flow cytometry and (C) pooled

analysis of T cell frequency in lungs of neonates at 8 dpi. (D and E) (D) Representative histogram and (E) pooled analysis of frequency of effector T cells in lungs of neonates at 8 dpi. (F) Representative immunohistology of whole lung slices (left panels) and nodular inflammatory foci (NIF, right panels). Dotted squares indicate the zoomed area in the right panels. (G-I) Quantitative analysis through immunohistology of (G) number of NIFs per lung slide (H) NIF area, and (I) MCMV-infected cells per NIF. (J) Quantification of lung viral loads. Data were acquired from four independent experiments (n=11-14) Statistical differences were calculated with Mann-Whitney U tests and the p-values are provided above each comparison. Adapted from Fonseca Brito et al.[182].

Accordingly, in lung histological analyses there was a robust decrease of NIFs per lung slide, inflammation area and MCMV per NIF, with several NIFs of effector T cell-treated animals being free of infected T cells, contrary to buffer-control treated animals (Fig. 23F-I). In line with these observations, lung viral loads were significantly lower in animals treated with effector T cells primed in adult systems (Fig. 23J). Taken together, these data suggest that with effective T cell priming, MCMV can be effectively controlled in early life.

4.2.7 Low frequency of highly differentiated, highly cytotoxic CD8 T cells in congenital HCMV infection

To validate the observations made in mouse models, peripheral blood from a clinical cohort of human congenital CMV infection was analyzed. Women with an HCMV infection during pregnancy were enrolled in this study. Since only 30-70% of mothers with a primary infection are expected to transmit HCMV to the fetus[194], non-infected controls are intrinsically included in this cohort. A total of 23 neonates were analyzed in this study, of which 19 (83%) were not infected and 4 (17%) were $HCMV^+$. Among them, 10 (43%) babies were of male sex and 13 of female (57%) with a median gestational age of 271 days (IQR 260-278 days). Blood populations of $HCMV^+$ and $HCMV^-$ babies were compared using seven multiparameter flow cytometry panels (Table 3) spanning a total of 101 populations of i) general blood subsets, ii) effector T cells, iii) invariant T cells, iv) Tregs, v) B cells, vi) innate lymphoid cells (ILCs) and vii) NK cells. Interestingly, significant differences between $HCMV^+$ and $HCMV^-$ babies were only found in $\alpha\beta$ T cell subpopulations, except for the frequencies of $\gamma\delta$ T cells and NK cells (Fig. 24A).

A

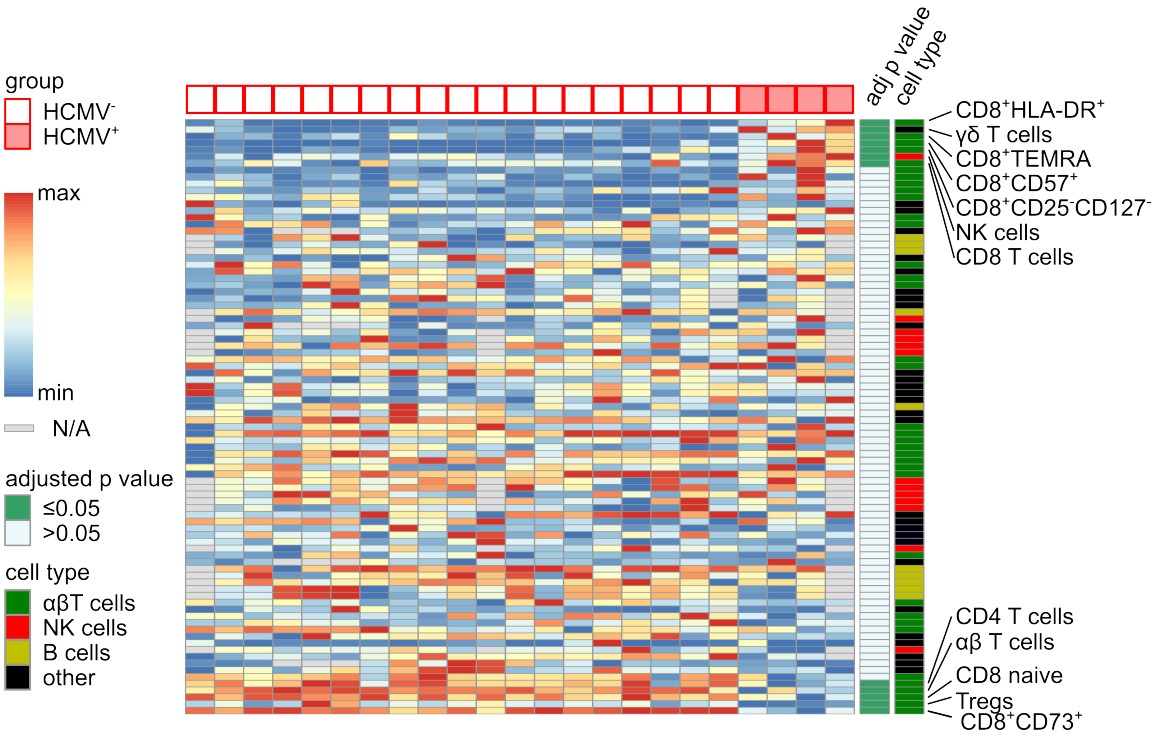

Figure 24. Immune phenotyping of peripheral blood from HCMV-exposed neonates. (A) Heatmap of frequencies of all peripheral blood populations (rows) measured in HCMV-exposed neonates (columns). Subpopulations with adjusted p-values <0.05 are depicted. Values are normalized to minimum and maximum values. Adjusted p-values for comparison of HCMV$^-$ and HCMV$^+$ donors were calculated using a Mann-Whitney U test with false discovery rate correction. Data was acquired by Romy Hackbusch and all panels except NK cells (see section 7.18, Table 3) were analyzed by Prof. Eva Tolosa, Dr. Anna Gieras, Dr. Kati Tillack and Romy Hackbusch. Data processing was performed by Laura Glau. Adapted from Fonseca Brito et al.[182].

To compare these effects with adults, peripheral blood T cell subpopulations of 10 immunocompetent HCMV$^+$ and HCMV$^-$ adults were analyzed. Notably, the general phenotypes in adult and neonatal samples were substantially different, with neonatal T cells presenting a largely naïve phenotype (Fig. 25A and B).

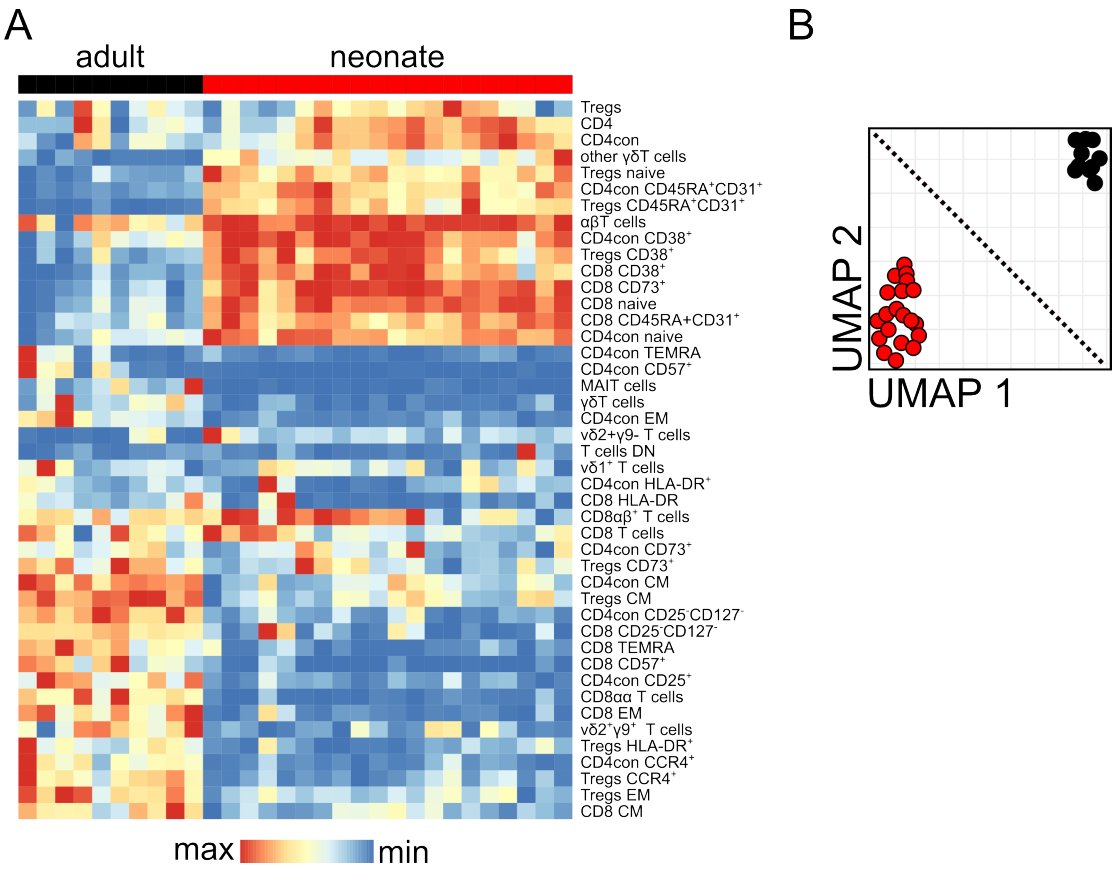

Figure 25. Comparison of T cell subpopulation frequencies between adults and neonates. (A) Normalized frequencies of T cell subpopulations in adult and neonatal donors. (B) UMAP dimensionality reduction of adult and neonatal samples. con, conventional; TEMRA, terminally differentiated effector memory; MAIT, mucosal-associated invariant T; EM, effector memory; DN, double-negative; CM, central memory. Data was acquired by Romy Hackbusch and all panels except NK cells (see section 7.18, Table 3) were analyzed by Prof. Eva Tolosa, Dr. Anna Gieras, Dr. Kati Tillack and Romy Hackbusch. Data processing was performed by Laura Glau. Adapted from Fonseca Brito et al.[182].

Samples derived from HCMV$^+$ and HCMV$^-$ donors segregated in principal component analyses of both adults and neonates (Fig. 26A and B). Moreover, in the total of 44 T cell subpopulations that were investigated, 7 subpopulations were significantly different in adults (HCMV$^-$ vs. HCMV$^+$), while in neonates there were 15 significantly different subpopulations (Fig. 26C and D).

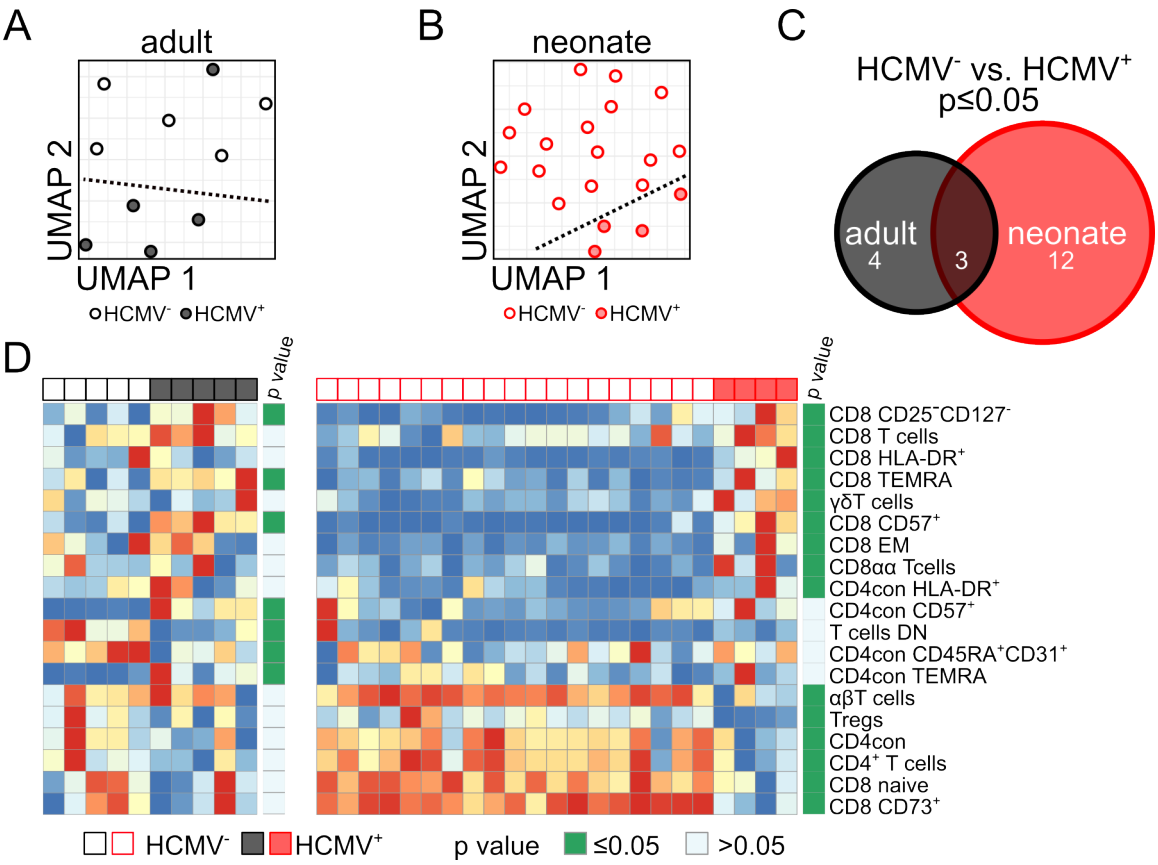

Figure 26. T cell phenotypes in HCMV⁺ and HCMV⁻ adults and neonates. (A) UMAP dimensionality reduction of al adult samples stratified by HCMV serostatus. (B) UMAP dimensionality reduction of all neonatal samples stratified by HCMV serostatus. (C) Numbers of subpopulations significantly different between HCMV- and HCMV+ donors in adults and neonates. (D) Normalized frequencies of the 19 subpopulations significantly different in either neonates or adults after HCMV infection. TEMRA, terminally differentiated effector memory; EM, effector memory; con, conventional; DN, double-negative. Data was acquired by Romy Hackbusch and all panels except NK cells (see section 7.18, Table 3) were analyzed by Prof. Eva Tolosa, Dr. Anna Gieras, Dr. Kati Tillack and Romy Hackbusch. Data processing was performed by Laura Glau. Adapted from Fonseca Brito et al.[182].

HCMV infection led to a decrease in the ratio of CD4 and CD8 T cells in adults and neonates (Fig27A-D). Frequencies of effector memory (EM) and terminally differentiated (TEMRA) CD8 cells were higher in HCMV-infected adults and neonates when compared to uninfected individuals (Fig27E-H). However, these frequencies were significantly lower in neonates than in adults. Moreover, upon HCMV infection, the frequency of the HCMV-induced CD57-expressing CD8 T cells[109,195] significantly increased in adults and neonates, with neonates showing significantly lower frequencies of these cells than adults (Fig. 27I and J). Taken together, HCMV infection affects the effector T cell phenotype of adults and neonates. However, virus-induced

CD8 TEMRA and CD8$^+$CD57$^+$ T cells can be detected at lower frequencies in neonates, likely impacting the control of acute HCMV infection in early life.

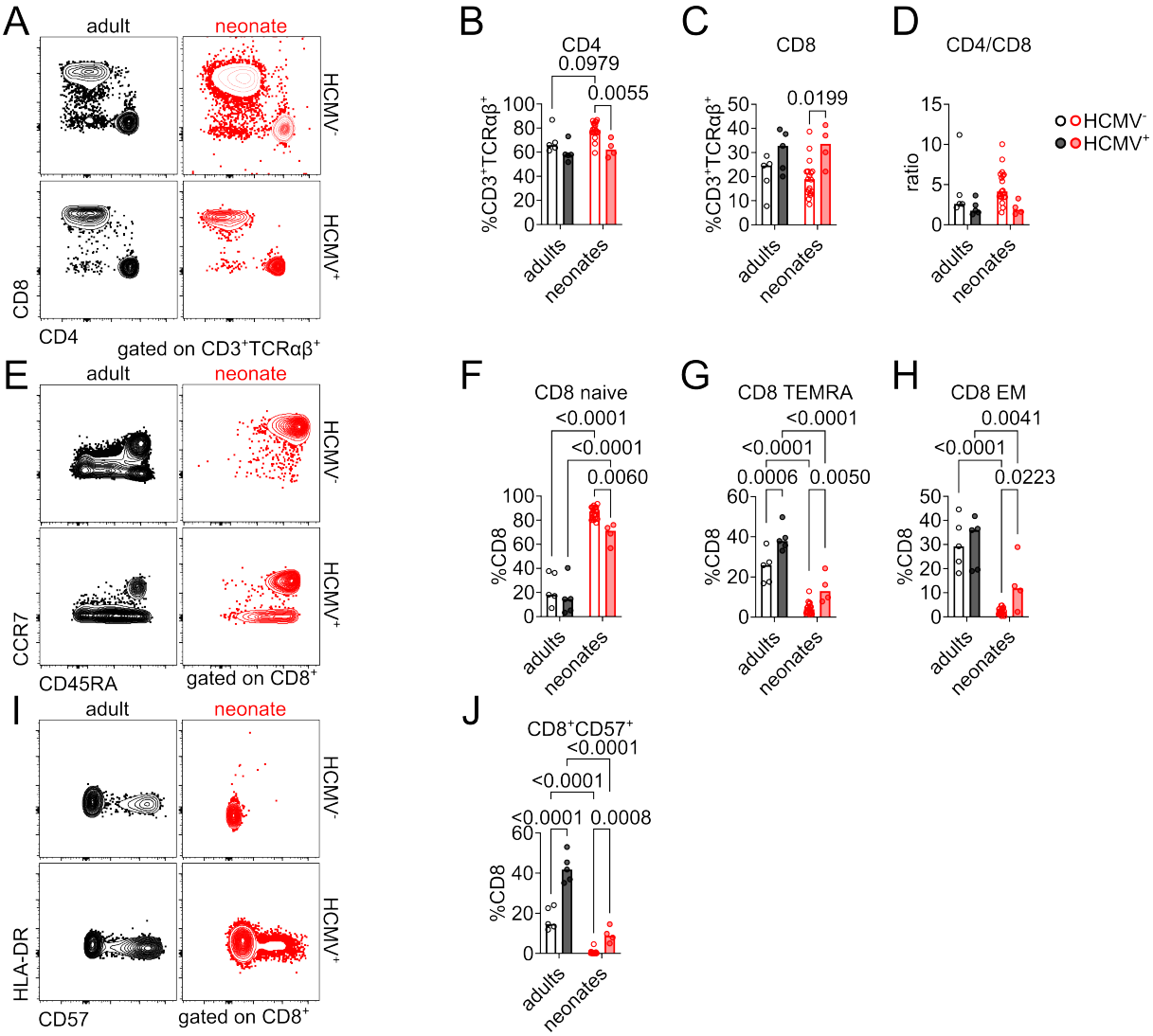

Figure 27. Proportion of effector CD8 T cells in HCMV$^+$ and HCMV$^-$ adults and neonates. (A-D) (A) Representative flow cytometry plots and (B-D) pooled analysis of CD4 and CD8 T cells. (E-H) (E) Representative flow cytometry plots and (F-H) pooled analysis of CD8 T cell differentiation status. (I-J) (I) Representative flow cytometry plots and (J) pooled analysis of CD57 expression of CD8 T cells. Statistical differences were calculated with 2-way ANOVAs and the p-values <0.1 are provided above each comparison. Data was acquired by Romy Hackbusch and gatings were done by Prof. Eva Tolosa, Dr. Anna Gieras, Dr. Kati Tillack and Romy Hackbusch. Adapted from Fonseca Brito et al.[182].

4.3 Section 3: Establishment of a CMI test to assess previous SARS-CoV-2 infection

4.3.1 SARS-CoV-2 diagnostics: cohort characteristics

Antibody testing emerged early during the SARS-CoV-2 pandemic and is well-established in routine laboratory diagnostics. By contrast, tests assessing T cell responses are less frequent in diagnostics, even though they might inform on protection against severe disease[196,197]. Therefore, interferon-γ release assays (IGRA) were evaluated as a potential SARS-CoV-2 diagnostic tool to assess T cell-mediated immunity (CMI). In collaboration with the Hamburg City Health Study[198,199], blood donors were recruited from 16th November 2020 to 28th April 2021. At the end of this period, Hamburg totaled 71,465 cases from a population of more than 1.8 million people. This low incidence enabled the recruitment of individuals without a history of SARS-CoV-2 infection and with a low probability of asymptomatic infection. In total, 549 individuals participated, of which 394 had a positive PCR test for SARS-CoV-2 at least 2 months prior to blood collection and 155 had no positive test until blood collection (Fig. 28A). At the end of 2020, Germany employed a state-wide vaccination program against SARS-CoV-2. Nevertheless, at the time of blood collection, most individuals were not yet vaccinated (Fig. 28A). Twenty-five vaccinated individuals (11 SARS-CoV-2^{-} and 14 SARS-CoV-2^{+}) were excluded due to the high heterogeneity of the group regarding the number of vaccines and time from vaccination to blood drawing. Moreover, two donors were excluded since no response was detected in positive control samples. Therefore, 144 healthy controls and 378 convalescent donors were included in the final analysis. Within the convalescent group, CMI was measured at a median of 298 days after the first PCR-positive test. The healthy control group comprised 38% females and 62% males with a median age of 53 (IQR 49-59), while in the convalescent group, 48% individuals were female with a median age of 55 (IQR 51-60) (Fig. 28B).

A

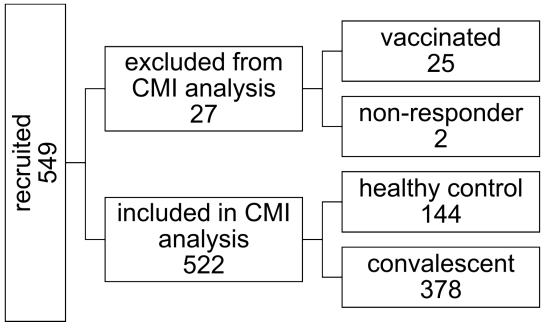

B

	healthy control	convalescent
days since) PCR$^+$	-	298 (229, 319)
age [years]	53 (49, 59)	55 (51, 60)
female sex [%]	37.5	48.4

Figure 28. Characteristics of the cohort used to establish an IFN-γ release assay for SARS-CoV-2 infection. (A) 549 individuals were recruited through the Hamburg City Health Study[198,199] and tested for cell-mediated immunity (CMI) to SARS-CoV-2. Samples were excluded due to prior vaccination (n=25) or negative results in positive controls (n=2). The remaining 522 samples were included and comprised of 144 healthy controls and 378 convalescent individuals. (B) Cohort characteristics of individuals included in CMI analysis. Data depict median values and interquartile ranges. Adapted from Fonseca Brito et al.[200].

4.3.2 Cell-mediated immunity (CMI) tests are suitable for SARS-CoV-2 routine laboratory diagnostics

To assess the suitability of CMI tests as a diagnostic tool for SARS-CoV-2, whole peripheral blood was stimulated with either i) phosphate buffer saline (negative control), ii) PMA and ionomycin (positive control), iii) nucleocapsid or iv) spike peptide sequences from the wildtype variant first detected in Wuhan, China in December 2019[201]. After 24h of stimulation, supernatants were collected and IFN-γ concentration was measured. IFN-γ concentrations in negative controls were significantly different between healthy control and convalescent groups (0.0437 IU/mL and 0.0509 IU/mL, respectively; $p < 0.0001$). In positive control samples, there were no differences, with most values above the upper limit of detection (Fig. 29A and B). To account for the variation of background IFN-γ values, the ratio to negative control was additionally calculated (Fig. 29C).

In stimulations with nucleocapsid and spike peptide pools, healthy controls showed lower concentrations of IFN-γ in comparison to convalescent donors, indicating a specific IFN-γ release in case of previous SARS-CoV-2 infection (Fig. 29D and E). Receiver operating characteristic (ROC) curves were applied to assess the quality of each test (Fig. 29D-G). Absolute values of nucleocapsid stimulations yielded an area under the curve (AUC) of 0.9357, whereas for spike this value was 0.8334, indicating

a slightly better performance of nucleocapsid. Accounting for the background values led to a reduction in the AUC in both nucleocapsid and spike (Fig. 29F and G). For comparison, a commercial antibody test used in routine laboratory diagnostics and targeting nucleocapsid was included. For this test, a higher AUC of 0.9616 was obtained (Fig. 29H). Next, cutoff values with the highest Youden indices of the different CMI tests were calculated. Optimal thresholds resulted in absolute values of spike showing a sensitivity of 89% and specificity of 69%, and nucleocapsid showing a sensitivity of 89% and specificity of 87% (Fig. 29I). Additionally, in the ratios to the negative control, the sensitivity of spike and nucleocapsid decreased to 88% in both tests, while the specificity of spike increased to 74% and of nucleocapsid to 91%. Cutoff values for the antibody test were provided by the manufacturer and led to a specificity of 94% and sensitivity of 94% (Fig. 29I). Taken together, CMI tests showed good performance and are suitable for diagnostics of SARS-CoV-2.

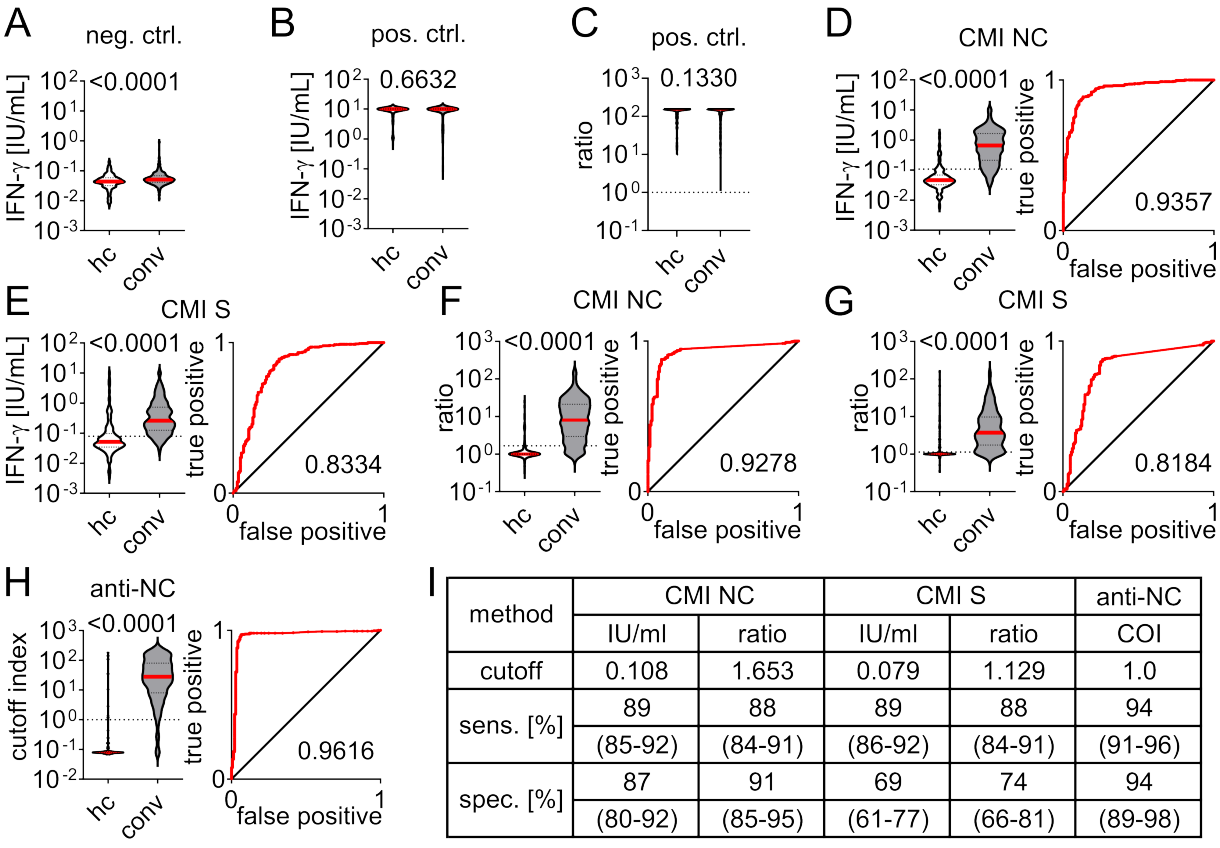

I

method	CMI NC		CMI S		anti-NC
	IU/ml	ratio	IU/ml	ratio	COI
cutoff	0.108	1.653	0.079	1.129	1.0
sens. [%]	89	88	89	88	94
	(85-92)	(84-91)	(86-92)	(84-91)	(91-96)
spec. [%]	87	91	69	74	94
	(80-92)	(85-95)	(61-77)	(66-81)	(89-98)

Figure 29. Cell-mediated immunity (CMI) tests detect past SARS-CoV-2 infections. (A and B) Interferon (IFN)-γ supernatant concentration in response to (A) buffer control and (B) PMA/ionomycin (positive control). (C) Ratio of positive control samples to the respective negative controls. Dotted lines indicate ratio of 1. (D and E) IFN-γ concentration in supernatants in response to stimulation with peptide pools spanning sequences of the SARS-CoV-2 (D) nucleocapsid (NC) and (E) spike (S) (left panels) and respective receiver operating characteristic curves (right panels). (F and G) Ratios of IFN-γ

concentrations to the according negative controls after stimulation with (F) NC and (G) S. (H) Anti-NC antibody titers provided as cutoff indices (COI). (I) Test performance characteristics for all CMI and antibody tests. Cutoffs were determined as the highest Youden indices or provided by the commercial manufacturer (anti-NC). Sensitivities (sens.) and specificities (spec.) are provided as median and interquartile ranges. Differences between healthy control (hc) and convalescent (conv) groups were determined by Mann-Whitney U tests and the p-values are provided above each graph. Adapted from Fonseca Brito et al.[200].

4.3.3 Comparisons between CMI and antibody tests

Next, the different tests were compared with each other. Applying the cutoff values calculated in Fig. 29I, the majority (>84%) of healthy control and convalescent samples were either true negatives or true positives (Fig. 30A), respectively. To allow for the combined comparison between all CMI tests and anti-nucleocapsid test, a t-SNE (t-distributed stochastic neighbor embedding) dimensionality reduction approach including the results of the ratios to negative control of spike and nucleocapsid and anti-nucleocapsid results was employed (Fig. 30B). Notably, only ratios were considered in this analysis since they already account for the variation in baseline IFN-γ values which significantly differ between healthy controls and convalescent donors (Fig. 29A). With this approach, samples are positioned into two main groups that generally reflect the classification into healthy control (PCR^-) and convalescent donor (PCR^+) (Fig. 30C). Using this dimensionality reduction approach enabled the identification of a cluster of samples that was only positive for spike, possibly indicating cross-reactivity with other coronaviruses[165,166] and accounting for the lower specificity of spike CMI tests (Fig. 30C).

Next, the distribution of each sample according to the negative or positive status as calculated by the respective cutoff values was analyzed. Applying a scoring system where each positive test equals 1, 77% of samples had either a score of 0 or 6, indicating full concordance between all the parameters analyzed (Fig. 30D).

To identify possible confounding effects, test results were contextualized to several parameters obtained from diagnostic laboratories and self-filled questionnaires (Tables 1 and 2). Of the 12 parameters analyzed, six affected anti-nucleocapsid antibody tests (days from positive PCR, age, body-mass index, cystatin C levels, previous diabetes and dyslipidemia diagnosis). In contrast, CMI tests were only impacted by the number of white blood cells (Table 2, Fig. 31A and B), while spike CMI tests correlated with

age (Table 2). Interestingly, a cluster in the t-SNE contained samples with positive PCR and anti-nucleocapsid results but negative results for all CMI measures (Fig. 31C). A comparison of the number of white blood cells between individuals that were false negative for CMI and true positive revealed a significantly higher number of WBC in donors with false negative CMI tests (Fig. 31B).

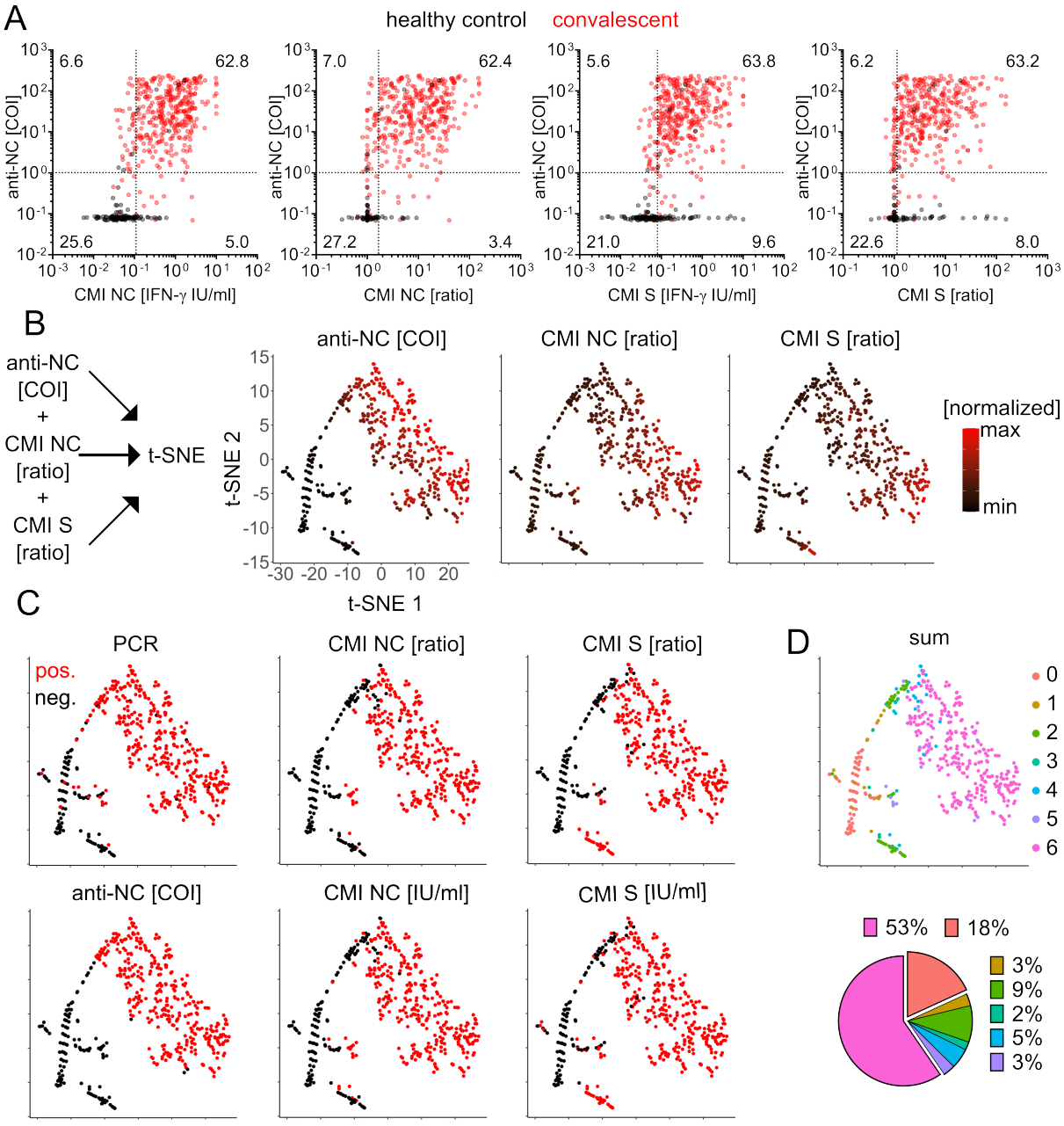

Figure 30. Comparisons of CMI and commercial antibody tests. (A) Absolute values and ratios measured for each CMI test and anti-NC antibody test. Dotted lines indicate cutoff values as indicated in Fig. 29I and numbers in each quadrant indicate percentages. (B) Dimensionality reduction of CMI and anti-NC results. (C) Test results as positive (pos) or negative (neg). after application of cutoff values as

indicated in Fig. 25I. (D) Concordance between results of all tests by summing each result (neg.=0 and pos.=1). Adapted from Fonseca Brito et al.[200].

Table 1. Potential confounders for SARS-CoV-2 CMI and antibody tests.

parameter		n	CMI NC IU/ml		CMI NC ratio		CMI S IU/ml		CMI S ratio		n	anti-NC COI	
			median (IQR)	*p*	median (IQR)	*p*	median (IQR)	*p*	median (IQR)	*p*		median (IQR)	*p*
sex	female	183	0.6640 (0.1930, 1.500)	0.6246	8.406 (2.504, 20.62)	0.6655	0.2410 (0.124., 0.7870)	0.6502	3.554 (1.692, 10.49)	0.6349	170	30.18 (7.668, 81.619	0.7898
	male	195	0.6510 (0.2320, 1.700)		7.738 (3.462, 21.81)		0.2960 (0.1260, 0.7280)		3.831 (1.754, 9.554)		186	26.83 (9.295, 81.34)	
diabetes	yes	24	0.4555 (0.2430, 1.593)	0.7803	6.419 (3.738, 17.34)	0.8857	0.2590 (0.09698, 0.6925)	0.6320	3.854 (1.492, 7.391)	0.7326	21	50.86 (19.69, 146.8)	***0.0254***
	no	336	0.6795 (0.2083, 1.670)		8.710 (2.808, 21.52)		0.2615 (0.1250, 0.7650)		3.697 (1.742, 10.45)		322	26.55 (7.913, 80.00)	
dyslipidaemia	yes	77	0.5030 (0.2040, 0.2100)	0.4917	7.738 (2.857, 20.81)	0,7756	0.2480 (0.1245, 0.7865)	0.9261	3.600 (1.777, 9.410)	0.6651	73	45.12 (16.49, 99.57)	***0.0230***
	no	285	0.7030 (0.2100, 1.670)		8.631 (2.961, 21.31)		0.2620 (0.1245, 0.7480)		3.815 (1.715, 10.41)		273	24.13 (7.320, 77.55)	
smoker	yes	32	0.5235 (0.2778, 1.270)	0.6997	7.132 (2.950, 16.380)	0.4194	0.2485 (1.563, 0.5490)	0.9848	3.531 (2.359, 6.802)	0.6610	31	26.98 (13.63, 69.17)	0.9355
	no	343	0.6810 (0.2120, 1.670)		8.843 (3.000, 21.81)		0.2610 (0.1240, 0.7730)		3.815 (1.692, 11.04)		327	28.10 (7.800, 81.89)	
HCMV	positive	17	0.7030 (0.2820, 2.000)	0.4046	8.843 (4.100, 28.38)	0.5507	0.4220 (0.1895, 0.8840)	0.7471	4.015 (2.675, 13.60)	0.9614	17	66.71 (26.01, 83.03)	0.0705
	negative	14	0.4170 (0.2278, 1.595)		6.415 (3.504, 24.54)		0.3240 (0.1748, 1.230)		4.985 (2.688, 18.92)		10	28.99 (5.998, 54.80)	

Number of samples (n) included for each analysis is provided. Statistical differences were calculated with Mann-Whitney U tests. HCMV, human cytomegalovirus; IQR, interquartile range. Comparisons with a p-value <0.05 are provided in bold and italic. Data was acquired by the HCHS. Adapted from Fonseca Brito et al.[200].

Table 2. Correlation of cohort characteristics with SARS-CoV-2 CMI and antibody measurements

parameter	n	CMI NC IU		CMI NC ratio		CMI S IU		CMI S ratio		n =	anti-NC COI	
		Spearman r	*p*	Spearman r	*p*	Spearman r	*p*	Spearman r	*p*		Spearman r	*p*
days since PCR+	365	-0,05616	0,2845	-0,0488	0,3525	-0,03444	0,5119	-0,02643	0,6147	347	-0,1987	***0,0002***
age (years)	378	0,06803	0,1869	0,06021	0,2429	0,1162	***0,0239***	0,1114	***0,0303***	360	0,2914	***<0,0001***
BMI (kg/m2)	352	0,01633	0,7601	0,02976	0,5779	0,01789	0,7381	0,02701	0,6135	336	0,2199	***<0,0001***
WBC (counts/µl)	370	-0,3027	***<0,0001***	-0,3059	***<0,0001***	-0,251	***<0,0001***	-0,2532	***<0,0001***	352	-0,01431	0,789
PCR Ct value	178	0,1238	0,0996	0,1044	0,1655	0,09298	0,2171	0,08094	0,2828	171	0,04558	0,5538
creatinine (mg/dl)	368	-0,01182	0,8212	-0,01016	0,8461	-0,04805	0,358	-0,05293	0,3112	351	0,04649	0,3852
cystatin C (mg/dl)	352	-0,07122	0,1825	-0,09972	0,0616	-0,0734	0,1694	-0,1075	0,0439	339	0,1236	0,0229

Number of samples (n) included for each analysis is provided. PCR, polymerase chain reaction; BMI, body mass index, WBC, white blood cells; Ct, cycle threshold. Correlations with a p-value <0.05 are provided in bold and italic. Data was acquired by the HCHS. Adapted from Fonseca Brito et al.[200].

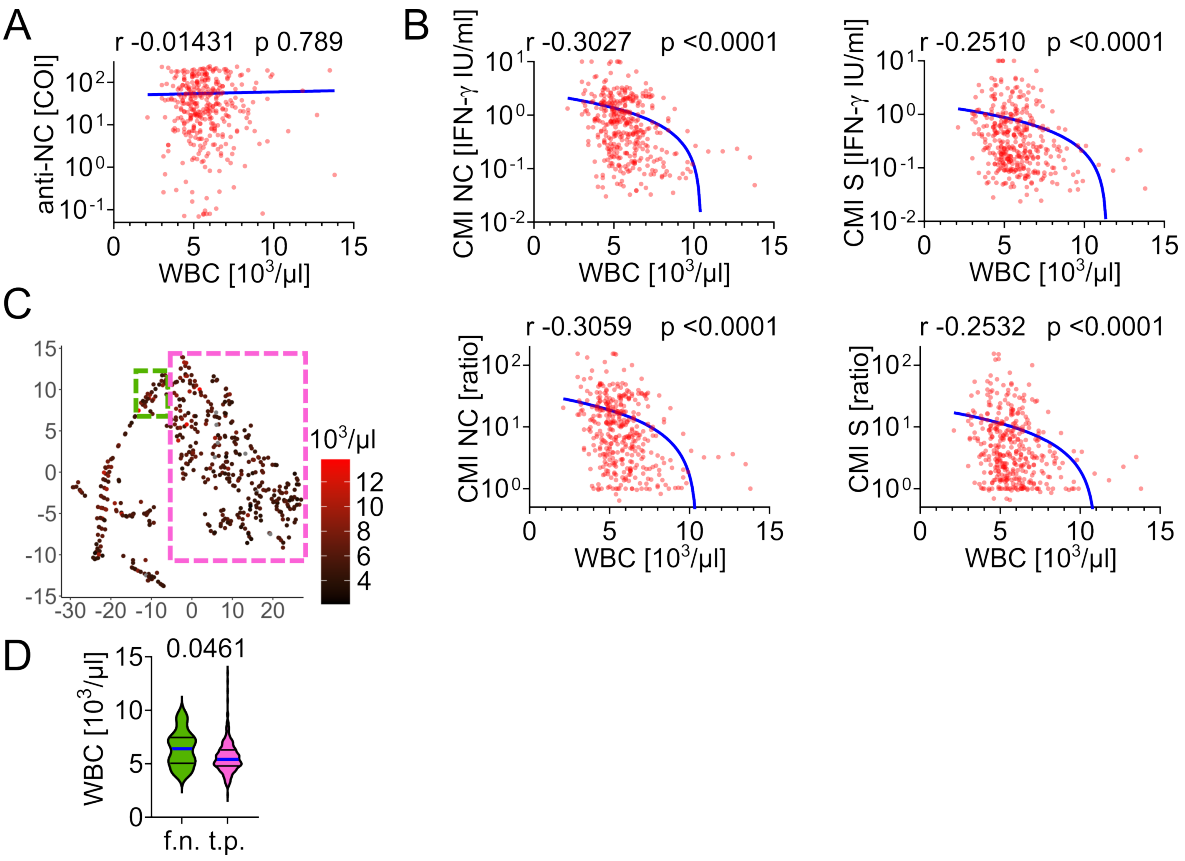

Figure 31. Confounding effect of white blood cell counts on CMI tests. (A and B) Correlation of (A) anti-nucleocapsid antibody and (B) CMI tests with the numbers of white blood cells in the blood. (C) Absolute number of WBC at the time of blood sample collection. Individuals with a score of 6 (true positives, t.p.) in Fig. 30D are framed in pink, and a fraction of individuals positive for PCR and anti-nucleocapsid, but negative for all CMI (false negatives, f.n.) are framed in green. (D) Comparison of WBC counts between the two groups. Spearman correlation results in A and B are provided above each graph. Statistical differences in (D) were calculated with Mann-Whitney U test and the p-values is provided. WBC counts were provided by the HCHS. Adapted from Fonseca Brito et al.[200].

The time from the first positive PCR test to blood collection was significantly correlated with anti-nucleocapsid tests, but not CMI tests (Table 2, Fig. 32A). However, IFN-γ concentrations were significantly higher in individuals tested less than 6 months from the time of positive PCR (Fig. 32B).

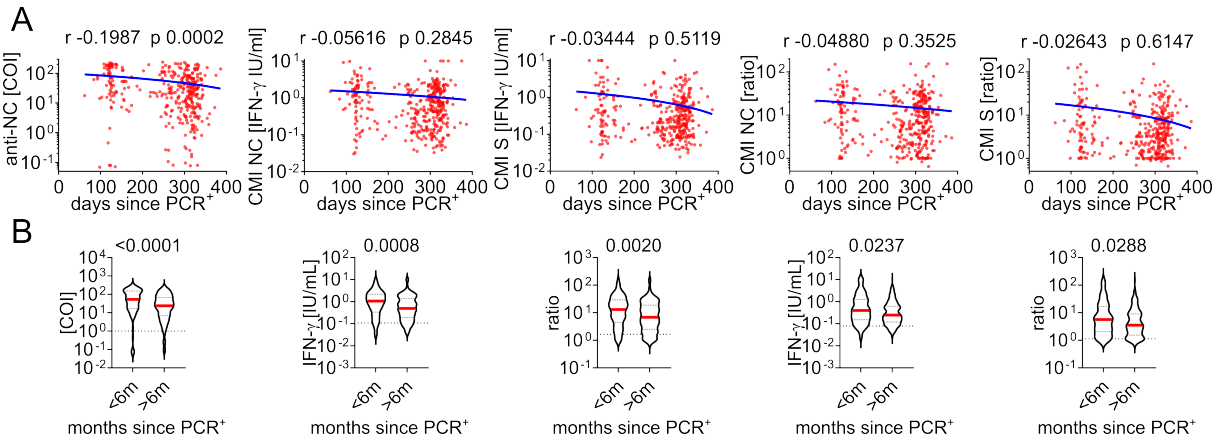

Figure 32. Impact of time on cell-mediated immunity and antibody tests for past SARS-CoV-2 infections. (A) Correlation between days from positive PCR test (provided by the HCHS) and CMI test results or anti-NC antibodies. Blue lines indicate simple non-linear regressions and Spearman correlation results are provided for each graph. (B) Comparative analysis of immunity in individuals infected less or more than six months before sample acquisitions. Statistical differences were calculated with Mann-Whitney U tests and the corresponding p-values are provided above each graph. Adapted from Fonseca Brito et al.[200].

4.3.4 Correlation with clinical features

Next, CMI test results were correlated to the self-reported clinical features of the donors. Interestingly, spike values were significantly higher in donors who were hospitalized as compared to those who only suffered from mild disease, whereas asymptomatic donors had significantly lower nucleocapsid CMI values than those of previously hospitalized donors (Fig. 33A). Similarly, donors who suffered from severe disease or were hospitalized showed higher anti-nucleocapsid values than those with mild disease (Fig. 33A). The presence of symptoms did not impact CMI test results, contrary to the antibody tests (Fig. 33B and C). However, hair loss was significantly more reported by donors who suffered from severe disease. Accordingly, anti-nucleocapsid antibody tests were significantly higher in patients who suffered from hair loss compared to asymptomatic individuals, while no significant differences were found in the CMI tests (Fig. 33D). Together, these data indicate that more severe disease was associated with an elevated IFN-γ release, but the presence of symptoms had little impact on CMI tests, contrary to the commercially available serologic test.

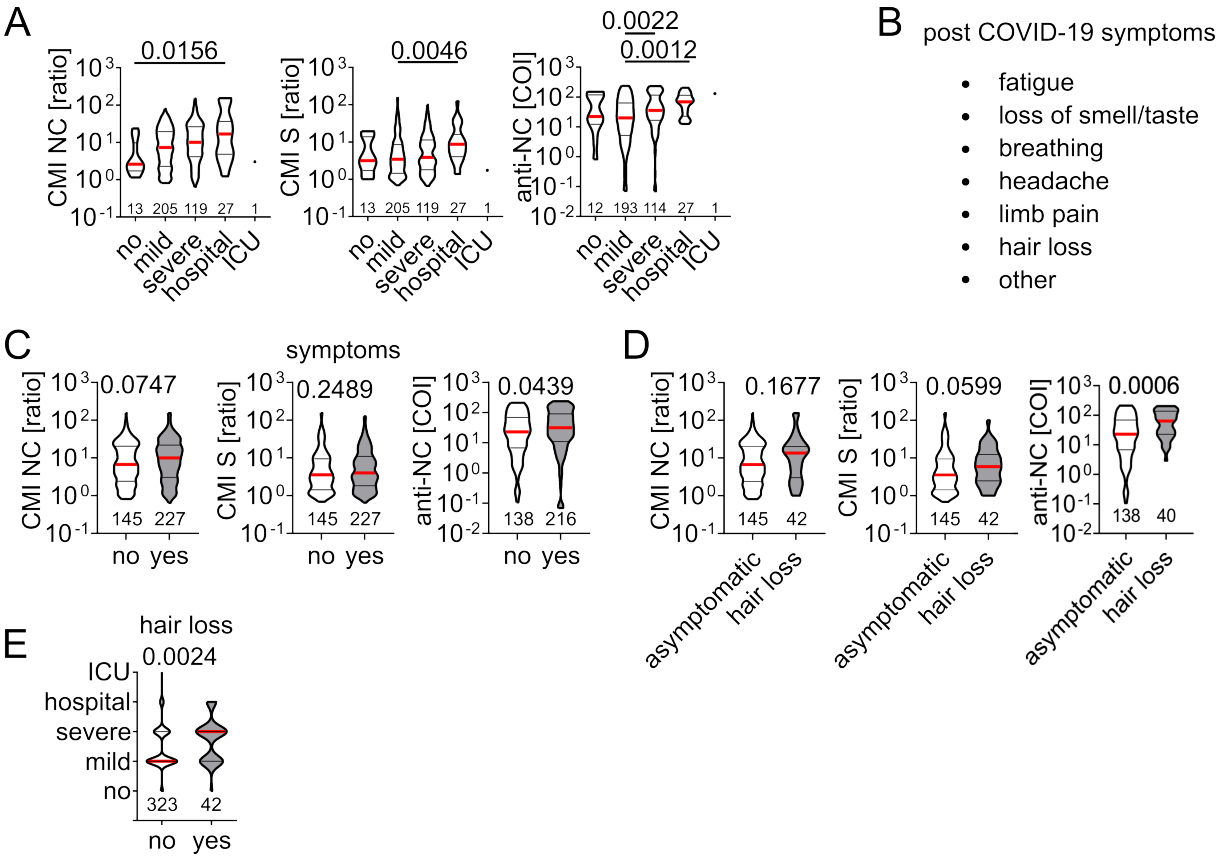

Figure 33. Association of CMI and antibody tests with acute and chronical clinical course. (A) Clinical course during acute SARS-CoV-2 infection with the corresponding NC and S CMI tests or antibody titers. (B) Post-COVID-19 symptoms retrieved from the questionnaires at the time of sample acquisition and (C) test results according to absence (no) or presence (yes) of symptoms. (D) Anti-NC titers and CMI test results of asymptomatic individuals and those who developed post-COVID-19 hair loss. (E) Clinical course during acute SARS-CoV-2 infection of individuals with absence (no) or presence (yes) of hair loss. Statistical differences in (A) were calculated with Kruskal-Wallis tests with Dunn's multiple comparisons and p-values >0.05 are provided for each comparison. Differences in (C-E) were calculated with Mann-Whitney U tests and the p-values are provided above each graph. Clinical course and symptom information were provided by the HCHS. Adapted from Fonseca Brito et al.[200].

4.3.5 Applications of CMI tests

Early in the SARS-CoV-2 pandemic, the possibility of a vertical transmission of the virus during pregnancy was heavily discussed[202-205]. Importantly, as SARS-CoV-2-specific IgG antibodies can be transmitted from mother to fetus during pregnancy[206], and IgM tests show relatively lower sensitivity, serological tests alone are not sufficient to assess previous infection of the fetus. Moreover, SARS-CoV-2 does not establish latency and negative PCR results do not exclude the possibility of previous infection. As T cell responses can be generated during fetal development[135], CMI tests in this context were a suitable candidate to assess previous infection. Thus, women with a

primary SARS-CoV-2 infection during pregnancy were recruited and, after birth, cord blood from nine newborn babies and peripheral blood from the respective mothers were collected and stimulated with SARS-CoV-2 nucleocapsid, spike, and membrane peptides. In this case, all mothers exhibited positive absolute values and ratios for at least one of the peptide stimulations, whereas no babies showed an increase in IFN-γ upon stimulation, indicating no infection of the fetus during pregnancy (Fig. 34A). In summary, CMI tests are straightforward, cost-effective tests that can be used to assess previous SARS-CoV-2 infection, in particular in cases where serologic testing is not possible.

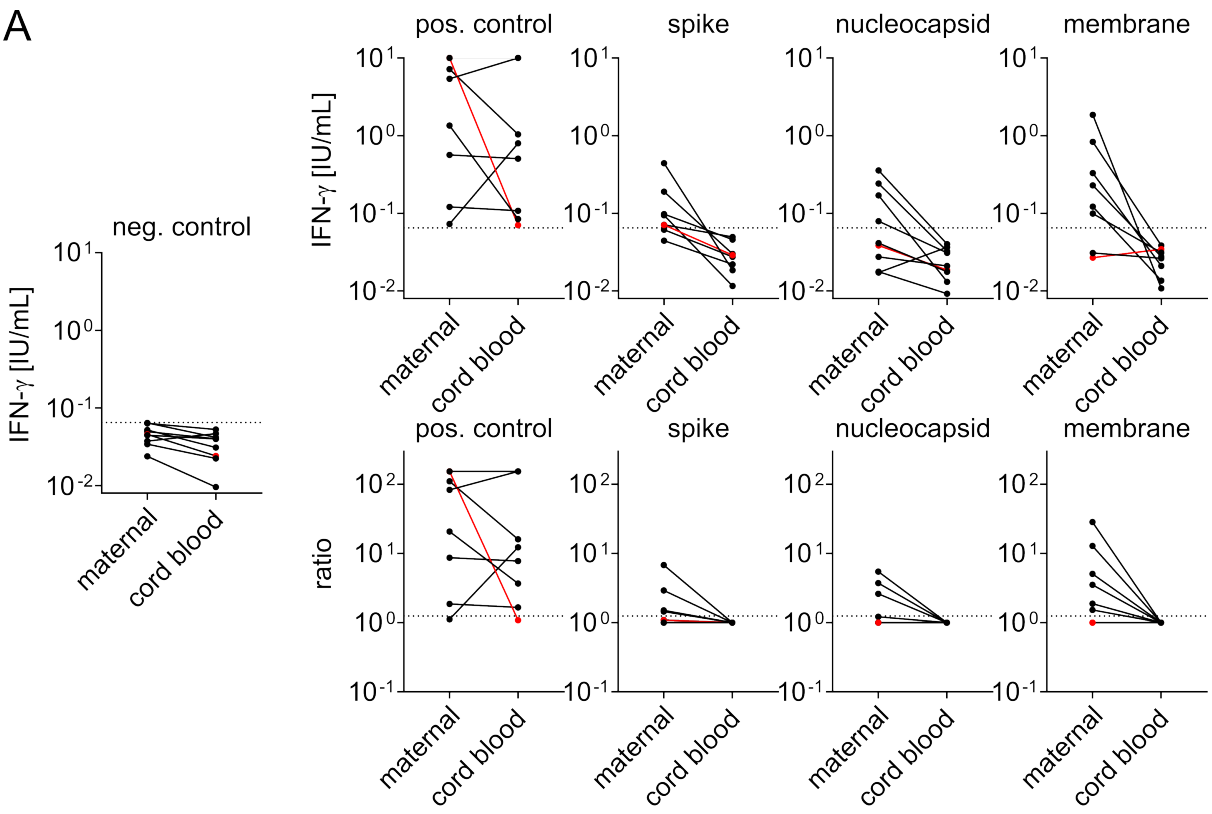

Figure 34. SARS-CoV-2 cell-mediated immunity tests to assess mother-to-fetus transmission. (A) Absolute measurements (negative control and upper row) and according ratios to the negative controls (lower row). Red dots indicate a mother-baby pair where CMI was tested two days after positive PCR test. Dotted lines indicate the limit of detection of the assay. Mother-baby pairs were recruited by Dr. Ann-Christin Tallarek. Adapted from Tallarek et al.[207].

5 Discussion

5.1 Low susceptibility of cells of the materno-fetal barrier to MCMV infection is associated with NRP1 expression

Congenital CMV infection is the major non-genetic cause of permanent disabilities and children and places a great burden on public health systems[39]. Infection of mice with MCMV is the most commonly used model to study CMV infection and disease, but transmission to the fetus through the placenta does not occur in these animals, limiting the possibility to investigate interactions between the fetus and the virus. Here, I addressed the determinants of *in utero* vertical transmission to understand the protection of mouse fetuses to MCMV infection and identified a low susceptibility of SM9-1 placental trophoblasts and cells isolated from the materno-fetal barrier to MCMV infection, which was associated with a low expression of neuropilin-1.

Several mechanisms have been proposed to enable congenital infection with CMVs and include i) infection of trophoblast cells and infection of other fetal cells via cell-to-cell spread, ii) transcytosis, iii) leakage of cell-free virus across the materno-fetal barrier, and iv) virus-infected maternal cells transmigrating into the fetus[208]. Our results indicate that cells from the materno-fetal barrier exhibit low susceptibility to MCMV infection, and that this barrier is crucial in the characteristic protection of mouse the fetus against congenital infection. The different anatomy of the materno-fetal barrier has long been proposed to be determinant in blocking fetal infection[99]. Cytomegaloviruses can congenitally infect humans, primates and guinea pigs, while CMVs do not cross the placenta in mice and rats. Interestingly, humans, primates, and guinea pigs have hemomonochorial placentas, i.e., one layer of trophoblast cells separates the fetal chorion from the maternal blood. By contrast, placentas in mice and rats are hemotrichorial, and maternal blood is separated from the chorion by two additional trophoblastic layers[209]. Accordingly, cell-free virus particles or virus-infected cells would need to cross two additional layers of cells to infect the fetus. The gestation period might additionally influence transmission into the fetus, as gestational time in mice lasts for three weeks in comparison to approximately nine or 40 weeks in guinea pigs and humans, respectively. Collectively, a low susceptibility to MCMV infection in combination with anatomical differences and shorter gestational periods could explain the lack of congenital CMV infection in mice.

Neuropilin-1 has recently been identified as a host factor facilitating MCMV entry into endothelial cells, fibroblasts, and macrophages, and deletion of this gene severely impaired infection rates and led to slower gene expression kinetics[86]. In this project, NRP1 was shown to be expressed at low levels in the SM9-1 placental trophoblast cell line and primary placenta cells. Accordingly, these cells showed lower susceptibility to MCMV infection and overexpression of NRP1 led to an increase in the frequency of infected SM9-1 cells. Neuropilins (NRPs) are a widely conserved family of transmembrane proteins comprising NRP1 and splice variants of neuropilin-2 (NRP2). These molecules can interact with several ligands, e.g., vascular endothelial growth factor (VEGF), transforming growth factor β (TGF-β), and platelet-derived growth factor B[210], playing crucial roles in regulating cells from the nervous and vascular systems. Interestingly, NRPs have been reported to act as host factors for several other viruses such as SARS-CoV-2, Epstein-Barr virus and human T-lymphotropic virus type 1[211-214]. Notably, NRP2 is a host factor for HCMV through interaction with members of the viral envelope glycoprotein pentameric complex[81]. By contrast, the MCMV-encoded chemokine 2 (MCK2) protein, part of the MCMV gH-gL-MCK2 glycoprotein complex homologous to the HCMV pentameric complex, has been reported to not interact with NRP1[85]. A question that remains open is whether the expression of NRP1 in trophoblasts in vivo or in primary placenta cells can increase MCMV infection. Of note, experiments were performed to assess this question in primary placenta cells. Cells were transduced with NRP1-expressing lentivirus and infected 24h post transduction. However, after 24h in culture, a portion of non-transduced cells acquired a susceptibility to MCMV infection and resembled fibroblasts in culture. Alternatively, in cultures lacking these fibroblasts-like cells, cells were additionally resistant to lentiviral transduction and hindered the artificial expression of NRP1 in this setting. In conclusion, the results of these experiments were inconsistent and did not allow for interpretation (data not shown). Experiments using different vectors for expression of NRP1 or different cell types (e.g. trophoblasts differentiated from murine trophoblast stem cells) can likely be alternative strategies to address this question. Moreover, further studies will be needed to address how MCMV interacts with NRP1 and how this interaction can be modulated. The human placenta seems to be infected *in vitro* and *in vivo*[215-217] and future studies will need to address whether NRP2 can mediate HCMV infection at the materno-fetal barrier, and whether blocking this interaction can protect against congenital infection. Additionally, whether NRP1-expressing mouse

trophoblasts can produce infectious MCMV particles remains to be investigated. In summary, a deeper understanding of CMV infection at the materno-fetal barrier can both help in the design of new experimental models and, in the long term, contribute to the development of tools for preventing congenital HCMV infections.

5.2 Delayed MCMV-specific T cell response in early-life MCMV infection

T cell responses to congenital CMV infection differ from those in immunocompetent adult individuals, potentially contributing to the higher susceptibility to disease in early life. However, the underlying mechanisms driving these mechanisms are not clear. Here, I confirmed a delayed MCMV-specific T cell response in early life associated with a low frequency of naïve MCMV-specific cells. As a result, control of viral infection was equally delayed, coinciding with an increase in the number of T cells.

The functionality of the immune system against foreign agents is related to the diversity of the T cell receptor pool, as higher diversity results in higher chances of recognizing different pathogen-derived antigens[218]. The number of T cells in early life is significantly lower, resulting in low TCR diversity[36]. This limited T cell repertoire in neonates may lead to a delayed expansion of virus-specific T cells upon infection, as the chances of MCMV-specific T cells being present at the time of infection are extremely low. Accordingly, after infection with MCMV, expansion of MCMV-specific CD8 T cells was delayed in neonates. This translated into a delayed control of MCMV infection, as adults were able to decrease lung viral loads at day 7 of infection while in neonates this happened first at 10 dpi. Notably, this delayed reduction in viral loads happened only after the most robust increase in the number of T cells per gram of body weight in the first week of life and coincides with the first detection of MCMV-specific CD8 T cells in neonates, supporting the role of T cells in controlling MCMV infection (Fig. 9 and 10). Likewise, the risk of developing long-lasting symptoms after congenital HCMV infection greatly decreases with the advancing gestational age[219-221], whereas T cell numbers in the fetus steadily increase[33].

The distribution of major lymphocyte populations dynamically changes in early life, with T, B, and NK cells increasing in number within the first weeks in mice. T cells play a multitude of roles after being activated and can interact with other cells, such as B and NK cells[222,223]. While B cells are not essential in eliminating acute infection[138,224], they

are necessary to reduce the chances of reinfection[225]. Activation of B cells specific to protein antigens requires T cell help[226]. Thus, delayed virus-specific B cell and T cell responses in this context are to be expected. Indeed, antibody responses are delayed in neonatal mice upon challenge with e.g. RSV[227] and influenza[228]. The role of NK cells in the control of congenital CMV infection is not well understood. Even though the number of NK cells remained fairly stable within the first 4 weeks of life of a mouse, it has been reported that expression of activating NK cell receptors in early-life is reduced, in particular the activating Ly49H receptor which recognizes the m157 peptide of MCMV[229,230]. However, though adoptive transfer of NK cells seems to improve control of MCMV infection in neonatal DAP12$^{-/-}$ mice (deficient in NK cell activation signaling)[231], it remains unclear to what extent the differences between adult and neonatal NK cells contribute to an increased susceptibility to disease development.

5.3 Non-protective features of T cells primed in the early life immune system

T cell lymphopenia plays a significant role in the higher susceptibility to MCMV disease in early life. Although CMV-specific T cell responses are generated in both humans [135] and mice[95,129] during early life, they do not effectively protect against CMV disease, suggesting differences in the phenotype of antiviral T cells in early life. Here, I employed different models of adoptive T cell transfer to explore how the neonatal environment influences the T cell phenotype upon MCMV infection. Adult T cells adoptively transferred into infected neonates acquired an effector phenotype, proliferated robustly in an antigen-specific manner, and localized to sites of infection, but failed to reduce viral loads after early life MCMV infection. Importantly, these sets of experiments are indicative of antigen presentation in early life MCMV infection, as TCR signalling after antigen recognition is required to induce differentiation into effector cells and to induce T cell clonal proliferation[232,233]. Instead, the overall priming of T cells seems to be altered. Previously, it has been reported that 100 T cells/NIF are sufficient to significantly reduce MCMV infection in adult lymphopenia models[138], while the up to 250 OT-I that were present in NIFs of neonatal mice infected with MCMV-4DR failed to provide robust control of viral infection (Fig. 14), indicating that the antiviral function of these cells in the early-life environment is impaired. Notably, OT-I cells have been shown to protect neonates against an MCMV recombinant lacking the

genes encoding the viral regulators of antigen presentation (vRAP) in early life[95], indicating that at least a fraction of T cells primed in early life can exhibit antiviral capabilities.

Accordingly, phenotyping of T cells isolated from adult and neonatal lungs after MCMV infection enabled the detection of an excess of cytotoxicity-deficient effector CD8 T cells after priming in the early-life system. Indeed, at steady state effector CD8 T cells isolated from neonates showed a preferential differentiation into low-cytotoxicity $T_{eff}1$ cells (Fig. 19C). Cytotoxic phenotypes in effector CD8 T cells are induced through well-coordinated sequences of signals conferred by TCR engagement, co-stimulation, and cytokines. After receiving these signals, transcription factors such as T-BET (encoded by the *Tbx21* gene), BLIMP1 (*Prdm1*), ZEB2 (*Zeb2*), and ID2 (*Id2*) cooperate to induce production of cytotoxicity-related molecules such as granzyme A, granzyme B, perforin and, in humans, granulysin[234-237]. During this process, transcription factors like TCF1 (encoded by *Tcf7*), LEF1 (*Lef1*), BACH-2 (*Bach2*), ZEB1 (*Zeb1*) and FOXO1 (*Foxo1*) must be repressed. Notably, the overall expression of *Zeb2* and *Id2* was significantly lower in effector CD8 cells isolated from infected neonates compared to adults. Accordingly, fewer cells in neonatal lungs differentiated into $T_{eff}3$ and $T_{eff}4$, while those who did differentiate into $T_{eff}2$ expressed significantly lower levels of granzymes than in infected adults. Thus, priming signals provided by neonatal systems seem to be insufficient to drive terminal differentiation of CD8 T cells into cytotoxic phenotypes.

Recently, CX3CR1 expression has been linked to T cell differentiation, making this a good marker for assessing differentiation states[238]. Higher expression of *Cx3cr1* is associated with an increase in *Zeb2* and, consecutively *Gzma* expressions in LCMV infection[234]. Thus, the low frequency of *Cx3cr1*-encoding $T_{eff}4$ cells in infected neonates supports the hypothesis that a highly differentiated state was not achieved.

Surprisingly, early-life MCMV infection elicited a stronger CD4 T cell response, with more adoptively transferred CD4 T cells exhibiting clonal expansion. Additionally, Th1 cells in neonates exhibited higher expression of cytotoxic molecules. MCMV infection has been previously reported to lead to a cytotoxic CD4 response, which is particularly important in controlling MCMV infection in salivary glands[123,239]. Importantly, these cells appear to exert their effector functions through secretion of IFN-γ[239], which is here shown to be expressed at higher levels in CD4 T cells isolated from infected neonates than adults. Salivary glands are CMV reservoirs that lack cross-presenting cells,

leading to weaker CD8 T cell responses[123]. Thus, the increased cytotoxicity of CD4 T cells in this organ is likely a compensatory mechanism for the reduced antiviral CD8 response. In fact, control of salivary gland MCMV infection is dependent on CD4 T cells[240-242]. Similarly, in the absence of a weak cytotoxic CD8 response in neonates, lung CD4 T cells exhibited enhanced cytotoxicity after MCMV infection. However, these cells are insufficient in reducing lung MCMV infection in adult mice, as adoptive transfer of CD4 T cells in T- and B cell-deficient *Rag2*$^{-/-}$ mice after lung infection does not provide extra protection[138]. Moreover, it is not known whether the higher expression of cytotoxic molecules in CD4 cells enhances MCMV control or lung pathophysiology in this situation.

Altogether, CD4 T cells primed in early life exhibit higher cytotoxic phenotypes, while CD8 T cell priming in neonatal systems seems to be incomplete and leads to less differentiated effector CD8 T cells. It would be of interest to investigate whether modulating priming signals in early life can rescue the low cytotoxicity phenotype observed in neonates. Moreover, whether T cells primed in neonatal systems have an impaired killing capability remains to be validated.

5.4 Impaired priming of CD8 T cells in early-life MCMV infection

Differentiation of T cells depends on the strength of each of the priming signals received. Thus, while the strength of the TCR signal is dependent on its affinity to the cognate antigen[243,244], signals 2 and 3 are dependent on the expression of co-stimulatory molecules, cytokines and their respective receptors on the T cell surfaces. By investigating age-related differences in lung APCs, I found that non-infected neonatal lungs exhibited higher frequencies of CD103-expressing, cross-presenting cDC1. However, these cells expressed lower levels of the co-stimulatory molecules CD80 and CD86. Recently, a subset of DCs expressing CD103 has been described to cause apoptotic waves in the early-life lung[245]. Accordingly, these cells can interfere with lung CD8 T cells and consequently lead to altered differentiation into cytotoxic T cells[245]. A limitation of this study is that activation of dendritic cells by pathogens leads to overexpression of co-stimulatory molecules, while expression of co-stimulatory molecules was only analyzed in uninfected animals. Though experiments were performed to compare DC subpopulations after activation in infected neonates and adults (not shown), the highly inflammatory conditions led to extremely different immune cell subpopulations present in the lungs which did not allow for a fair

comparison between lung DCs of different ages. However, upon RSV infection at PND 7, lung-draining cDC1 seem to be less responsive to type I interferon signalling than adult mice, indicating that co-stimulation of T cells might be impaired in early life[246]. Thus, future studies should address whether neonatal DCs can upregulate co-stimulatory molecules to the same levels as adults after MCMV infection. Nevertheless, the initially lower levels of co-stimulatory molecules may constitute a disadvantageous setting for CD8 T cell priming.

Cytokine signals further optimize the differentiated phenotype acquired by effector T cells[247], and differentiation of CD8 T cells into highly cytotoxic subsets depends on timely cooperation between several transcription factors[248]. Accordingly, there was a remarkable shift in the cytokine response after MCMV infection, with adults highly expressing IL-2, IL-7, and IL-15, whereas neonates upregulated IL-6, IFN-γ, and IFN-β. Importantly, cytokines upregulated in adults belong to the common receptor γ-chain family and their signalling induces ID2, ZEB2, T-bet, and BLIMP-1 upregulation to drive the CD8 T cell phenotype into cytotoxic-granule-producing cells[249-252]. In line with this, the single-cell transcriptomics revealed the genes encoding for these proteins (*Id2*, *Zeb2*, *Tbx21,* and *Prdm1*, respectively) to be less expressed in effector CD8 T cells isolated from MCMV-infected neonates. γ-chain cytokines concurrently lead to the downregulation of differentiation-repressing transcription factors such as ZEB1, ID3, and TCF1[249-252]). Importantly, *ex vivo* IL-15 treatment can increase the expression of CXCR6 and CCL5[252], marker genes of T_{eff} 3 and T_{eff} 4. Thus, these cytokines are involved in driving terminal differentiation and cytotoxic phenotypes of effector CD8 T cells, suggesting that the lower concentration of these molecules strongly impacts early-life MCMV pathology.

Additionally, IL-27, IL-33, and IFN-α were present in adult lungs but remained largely undetected in neonates. IFN-α signalling affects the activation and differentiation of T cells[253] and its absence results in fewer granzyme-producing cells[254]. Moreover, this molecule is crucial in the activation and correct localization of antigen-presenting cells and the lack thereof can interfere with co-stimulation through decreased frequencies of antigen-specific cells[255,256], decreased expression of co-stimulatory molecules, and impaired generation of cross-presenting inflammatory DCs[257]. IL-33 can promote antiviral T cell immunity[258,259], while IL-27 is able to upregulate effector genes to promote a $CD44^{+}CD62L^{-}$ effector phenotype in tumor settings[260]. In summary, the lack

of these cytokines during priming of CD8 T cells seems to impair differentiation of these cells in early life MCMV infection, leading to a preferential $T_{eff}2$ phenotype. Surprisingly, neonatal lungs exhibited higher concentrations of IFN-γ than adults. While these higher concentrations are not enough to drive a cytotoxic program in effector CD8 T cells in neonates, it is known that IFN-γ is necessary to control lung MCMV infection[138] and the meaning of these disparities will need to be addressed. Moreover, only cytokines important for the priming of CD8 T cells were analyzed, and other molecules can be differentially expressed in an age-dependent manner. As NIFs are possible sites of antigen presentation and priming, further studies will need to assess whether these differences exist and what the consequences might be.

In adults, T cells are efficiently primed leading to effective control of MCMV infection within days[261,262]. Consequently, transfer of effector T cells from MCMV-infected adults into neonates led to improved control of viral infection, supporting the hypothesis that T cell priming in early life is impaired. Of note, no adoptive transfer from T cells derived from infected neonates into non-infected neonates was performed, as the number of cells that can be isolated from very young mice is a limiting factor. Therefore, this question will need to be addressed in future studies using other systems, e.g. cell culture killing assays. Furthermore, strategies to improve T cell priming in early life upon CMV infection should be investigated. Recently, an antibody targeting CD8 coupled to an IL-2 molecule has been successively used to improve the priming of CD8 T cells in the liver, resulting in improved control of hepatitis B virus infection in adult mice[263]. Alternatively, cytokine-antibody complexes have been used to improve the differentiation of T cells into effector phenotypes[264,265]. These approaches might be viable in improving T cell priming after early-life MCMV infection and should be addressed in future studies.

5.5 Low frequency of antiviral CD8 T cells in congenital HCMV infection

In humans, a high-dimensional flow cytometry-based phenotyping of the main leukocyte populations in the peripheral blood of HCMV-exposed babies revealed T cells to be the most affected by infection. Additionally, NK cells and γδT cells were expressed at higher frequencies in infected newborns (Fig. 24), indicating a role of these cells in the control of congenital HCMV infection. In fact, HCMV has been shown

to lead to adaptive-like expansion of vδ1$^+$ T cells[266-268] and NKG2C$^+$ NK cells[269,270], and these cells might also play a role in control of congenital infection[271].

T cell phenotypes represented most of the differences between control and congenitally infected newborns, supporting the findings from the mouse model. Importantly, HCMV infection has been shown to lead to the accumulation of CD8$^+$TEMRA cells in adults, which constitute most of the HCMV-specific CD8 T cells[111,134]. These cells are characterized by a highly differentiated state exhibiting high expression of CX3CR1[238], and high lysis capacity through high expression of e.g. granzyme B and perforin[272,273]. Similarly, expression of the CD57 marker on CD8 T cells is also increased during HCMV infection[109], primarily on CD8+TEMRA[274] where it seems to be associated with better control of viremia[110]. Most of these cells additionally co-express the NKG2C receptor and exhibit higher cytotoxicity upon several stimuli, including HCMV peptides[275]. Thus, control of congenital HCMV infection likely depends on the quantity and cytotoxic potential of CD57$^+$ CD8 T cells and CD8 TEMRA cells. Notably, a median of 9% of CD8 T cells from HCMV$^+$ neonates exhibited CD57 expression, in comparison to 42% in HCMV$^+$ adults. Similarly, in the mouse model, approximately 10% of T cells isolated from infected neonates showed positive cytotoxicity scores, while in adults around 40% CD8 T cells were above this threshold. While HCMV-specific T cells are known to produce cytotoxic molecules upon stimulation[135], their cytotoxic potential remains to be addressed. Additionally, with the recent rise of multiomics approaches, future studies will be better positioned to investigate the presence and quality of CD8 T cell priming signals in early-life infection.

In conclusion, a low precursor frequency in early life greatly increases susceptibility to CMV. However, when higher frequencies of T cells are achieved, a deficient CD8 T cell priming environment characterized by a lower γ-chain cytokine signalling skews CD8 T cell differentiation towards less cytotoxic phenotypes, adding to the increased susceptibility to CMV disease (Fig. 35).

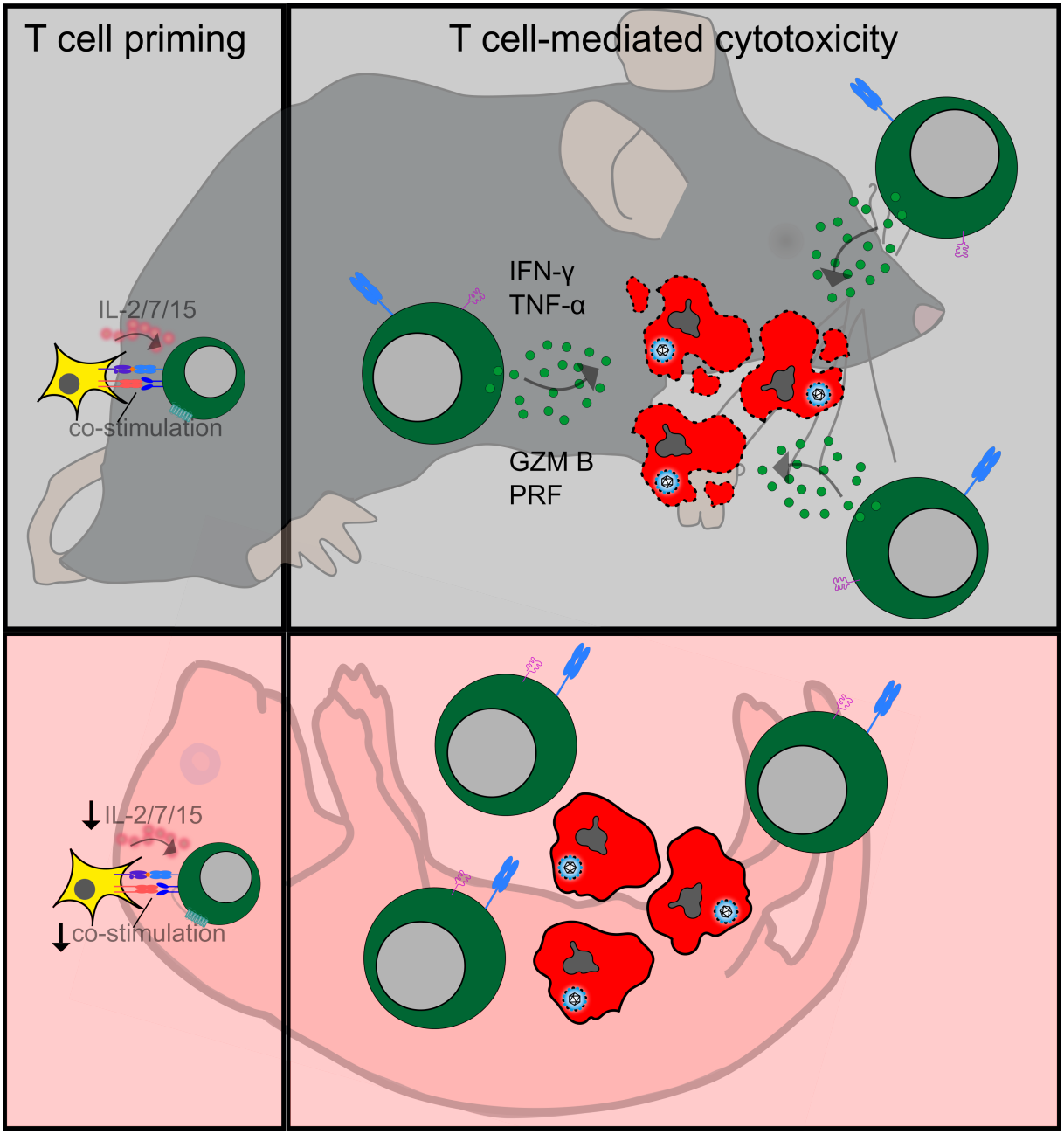

Figure 35. Graphical summary of age-related differences in the T cell response against MCMV infection. CD8 T cells are efficiently primed in adults (upper panel) through IL-2, IL-7, IL-15 and co-stimulation, driving the differentiation program into highly cytotoxic effector CD8 T cells that efficiently eliminate virus-infected cells. In neonates (lower panel), lower levels of priming signals 2 and 3 impair the generation of cytotoxic CD8 T cells and MCMV-infected cells persist longer in these systems.

5.6 Performance of an Interferon-γ test to assess cell-mediated immunity to SARS-CoV-2

Several diagnostic tests are currently employed to assess current and past infection with SARS-CoV-2. In this study, the performance of CMI tests for SARS-CoV-2

infection was evaluated using a large cohort of 522 blood donors with a known history of SARS-CoV-2 infection. In addition, a high interval between infection and data acquisition allowed to emphasize the potential of IGRA in assessing SARS-CoV-2 CMI a year after infection, to compare the strength of the response between different epitopes, and to correlate these findings to clinical data.

Importantly, the blood samples were tested before the establishment of the main vaccination program in Germany that was made available to the general public in April 2021. Furthermore, at the time when the last test was performed, only approximately 4% (71,465 cases) of the population in Hamburg had experienced a past SARS-CoV-2 infection, reducing the likelihood of asymptomatic individuals making part of the negative control group and improving the resolution of the calculated cut-off values.

To date, several studies have reported the use of IGRA to assess SARS-CoV-2 cell-mediated immunity[276-279]. These tests can be of special importance for individuals who do not develop humoral immunity[280] or individuals with acquired immune defects, where antibody responses cannot be used to assess SARS-CoV-2 immunity. Indeed, neonates are at higher risk for false negative tests due to lower antibody responses, but similarly to false positive responses, as antibodies can be transmitted to the newborn *in utero*[206] or through breast milk[281,282]. Thus, as T cell immunity can be developed already during fetal development, CMI tests might constitute a more reliable approach to assess past SARS-CoV-2 infection. Accordingly, IGRAs revealed no CMI to SARS-CoV-2 in neonates born to mothers with acute or resolved SARS-CoV-2 infection (Fig. 34). By contrast, within the same study, higher levels of IgG were found in cord blood than in maternal serum[207], indicating possible transplacental IgG transfer from mother to fetus[283]. Thus, while in these neonates it cannot be distinguished whether IgG is derived from the mothers or the fetus, a positive CMI result would indicate likely congenital infection with SARS-CoV-2. Importantly, despite no congenital SARS-CoV-2 infections being detected in our study, these events have been circumstantially reported and appear to be rare events[284].

The baseline IFN-γ values in convalescent donors were significantly higher than those of control donors. Though these differences are of a small effect size, the implications arising from them are unknown and need to be addressed by further studies. It is to be expected that higher IFN-γ values are observed in the context of latent infections, e.g. HCMV, where low-grade reactivation events occur and repeatedly stimulate T cells. By

contrast, SARS-CoV-2 does not establish latency and can be cleared, in most cases, within weeks of infection, making it unclear why higher IFN-γ values are observed in these donors almost one year after recovery.

Nucleocapsid stimulations elicited higher IFN-γ release in convalescent patients and exhibited better performance than tests using spike. It has been reported that most SARS-CoV-2 immunodominant T cell epitopes are derived from NC[285], which might explain the higher performance of this protein. Moreover, several variants of SARS-CoV-2 have emerged since the virus was first detected. Mutations within the spike sequence make up most of the single nucleotide polymorphisms that define these variants[286,287], indicating that this protein might be subject to higher selective pressures. Thus, with the use of peptide sequences derived from the first-sequences SARS-CoV-2, it is likely that more epitopes from spike have mutated and can no longer be recognized by T cells within these tests, leading to lower supernatant IFN-γ values.

Anti-nucleocapsid antibody tests were more affected by the time between positive PCR result and sample collection, indicating that CMI tests might be at an advantage when assessing past infection over longer periods. Indeed, it has been reported that T cells responses against SARS-CoV-2 variants are more conserved as compared to antibody epitopes[288-290]. Further studies will need to assess in more detail how sensitive CMI tests are to the appearance of new variants, as it has been extensively reported that antibody tests might fail to recognize epitopes from different variants[291-294].

Tests with spike yielded several false positive tests, in contrast to CMI tests with NC or anti-NC antibody tests, contributing to a better performance of tests involving nucleocapsid. Cross-reactive T cells can be generated upon infection with other related human coronaviruses[197], with a great proportion of these recognizing spike epitopes[295]. Thus, it is possible that infections with other human coronaviruses can influence SARS-CoV-2 CMI results, in particular tests with spike. Similarly, a smaller proportion of donors with negative PCR and antibody tests exhibited positive nucleocapsid CMI results, or both S and NC.

A small proportion of donors were positive for SARS-CoV-2 PCR and anti-NC antibody results, but negative S and NC CMI. In these donors, a higher number of white blood cells was detected, and future studies will need to assess whether there is a direct connection between these two results. No differential blood counts were obtained in

this study, and it would be interesting to investigate which cells are responsible for higher numbers of leukocytes in this context. However, an increase in the white blood cell count is usually a result of higher numbers of neutrophils, whose role in regulating T cell responses is under discussion[296]. Importantly, if high WBC counts can generally interfere with CMI results, it is recommendable that these numbers are assessed when using CMI tests established in routine diagnostics.

Taken together, this study suggests that CMI tests are simple, cost-effective tests that can be used both to investigate antigen-specific T cell responses against SARS-CoV-2 and in routine diagnostics to assess the generation of virus-specific T cells upon infection or vaccination.

5.7 Concluding remarks

Mothers infected with HCMV can transmit the virus to the fetus; however, this is not true for mice infected with MCMV, even at high infection doses of immunocompromised mothers. This work elucidates a mechanism of resistance to MCMV infection at the murine materno-fetal interface. Cells at this interface express low levels of NRP1, and artificial expression of this protein can increase infection of these cells. These data suggest that an increased susceptibility to infection of cells from the materno-fetal interface could facilitate cell-to-cell spread and potentially lead to fetal infection, allowing for the development of a mouse model where congenital infection with MCMV is possible.

Congenital CMV infection is associated with a higher risk for CMV disease. While T cells can rapidly clear infection in immunocompetent adults, neonates shed the virus for prolonged periods, in great part due to a low precursor frequency of CMV-specific T cells in early life. The work presented in this thesis additionally suggests that T cells in early life do not differentiate into highly cytotoxic phenotypes, delaying the control of CMV infection. This defect in differentiation is linked to deficient priming signals that are crucial for the establishment of antiviral CD8 T cells.

To leverage the potent T cell responses generated upon viral infections, I established a diagnostic test to assess previous SARS-CoV-2 infection. This test reliably distinguished healthy from convalescent donors. Altogether, CMI tests are simple and cost-effective, with the potential to be used in routine diagnostic labs.

6 Materials

6.1 Animals

Strain	Reference
C57BL/6J	JAX stock #000664
Rag2-/-Il2rg-/-	JAX stock #008449
β-actin-eGFP	JAX stock #006567
β-actin-eCFP	JAX stock #004218
OT-I	JAX stock #003831
OT-II	JAX stock #004194

6.2 Cells

Cell line	Tissue	Reference
10.1	Murine embryo fibroblasts	Harvey et al.[297]
M2-10B4	Bone marrow/stroma fibroblasts	Lemoine et al.[298]
SM9-1	Swiss mouse trophoblasts	Hunt et al.[299]
SM9-1 GFP	Swiss mouse trophoblasts transduced with eGFP-encoding lentivirus	This study, generated by Dr. Eleonore Ostermann
SM9-1 NRP1-GFP	Swiss mouse trophoblasts transduced with eGFP-encoding lentivirus	This study, generated by Dr. Eleonore Ostermann
Primary placenta cells	Primary placenta cells derived from C57BL/6 mice	This study

6.3 Viruses

Virus	Description	Reference
MCMV-2DR	mMIEP-mCherry-*Gaussia* luciferase -polyA cassette inserted within m157; MCK2 repaired	Bošnjak et al.[85]
MCMV-3DR	mMIEP-mCherry-*Gaussia* luciferase -polyA cassette inserted within m157; OVA257-264 sequence within m164; MCK2 repaired	Lemmermann et al, Marquardt et al. And Stahl et al.[83,300,301]
MCMV-4DR	Based on MCMV-3DR with hMIEP-TfR-OVA299-385-BGH-PolyA sequence inserted within m128	This study

mMIEP; MCMV major immediate early promoter; MCK2, MCMV-encoded chemokine 2; ; hMIEP, HCMV major immediate early promoter; TfR, transferrin receptor; BGH-PolyA; bovine growth hormone polyadenylation

6.4 Primers and probes

Name	Sequence
OT-I TCRα F	CAGCAGCAGGTGAGACAAAGT
OT-I TCRα R	GGCTTTATAATTAGCTTGGTCC
OT-I TCRβ F	AAGGTGGAGAGAGACAAAGGATTC
OT-I TCRβ R	TTGAGAGCTGTCTCC
OT-I internal positive control F	CAAATGTTGCTTGTCTGGTG
OT-I internal positive control R	GTCAGTCGAGTGCACAGTTT
OT-II TCRα F	AAAGGGAGAAAAAGCTCTCC
OT-II TCRα R	ACACAGCAGGTTCTGGGTTC
OT-II TCRβ F	GCTGCTGCACAGACCTACT
OT-II TCRβ R	CAGCTCACCTAACACGAGGA

(continued)

OT-II internal positive control F	CTAGGCCACAGAATTGAAAGATCT
OT-II internal positive control R	GTAGGTGGAAATTCTAGCATCATCC
eGFP F (PCR)	AAGTTCATCTGCACCACCG
eGFP R (PCR)	TCCTTGAAGAAGATGGTGCG
eGFP internal positive control F	CTAGGCCACAGAATTGAAAGATCT
eGFP internal positive control R	GTAGGTGGAAATTCTAGCATCATCC
eGFP F (qPCR)	TACCCCGACCACATGAAGCAGC
eGFP R (qPCR)	GTCGTCCTTGAAGAAGATGGTGCG
eGFP probe	FAM-TTCAAGTCCGCCATGCCCGAA-TAMRA

6.5 Antibodies

Antigen	**Clone**	**Target species**	**Fluorophore**	**Dilution**	**Source/RRID**
NRP1	3E12	Mouse	PE	1:20	Biolegend, AB_2561928
CD3	17A2	Mouse	Alexa Fluor 647	FC: 1:100 IF:1:200	BioLegend, AB_389323
CD3	17A2	Mouse	Brilliant Violet 711	FC: 1:100	BioLegend, AB_312966
CD3	17A2	Mouse	FITC	FC: 1:100	BioLegend, AB_312661
CD3	REA641	Human	PE	FC: 1:100	Miltenyi Biotec, AB_2657081
CD4	REA604	Human	PE-Vio770	FC: 1:100	Miltenyi Biotec, AB_2657967
CD4	GK1.5	Human	PerCP	FC: 1:100	BioLegend, AB_2657967

(continued)

CD8b	YTS156.7.7	Rat	APC	FC: 1:100	BioLegend, AB_2562774
CD8b	REA 793	Human	APC-Vio770	FC: 1:100	Miltenyi Biotec, AB_2659548
CD44	IM7	Rat/Mouse	APC	FC: 1:100	BioLegend, AB_312963
CD44	IM7	Rat/Mouse	PE	FC: 1:100	BioLegend, AB_312959
CD44	IM7	Rat/Mouse	Pacific Blue	FC: 1:100	BioLegend, AB_493683
CD44	REA664	Human	PE-Vio770	FC: 1:100	Miltenyi Biotec, AB_2733233
CD45	30-F11	Rat	APC	FC: 1:100 IF:1:100	BioLegend, AB_312977
CD45	30-F11	Rat	Alexa Fluor 750	FC: 1:100 IF:1:100	R&D Systems, AB_3065245
CD62L	Mel-14	Rat	Alexa Fluor 488	FC: 1:100	BioLegend, AB_493376
B220	REA755	Human	FITC	FC: 1:100	Miltenyi Biotec, AB_2658273
B220	RA3-6B2	Rat/Mouse	PE	FC: 1:100 IF:1:200	Invitrogen, AB_465672
CXCR6	SA051D1	Rat/Mouse	Brilliant Violet 711	FC: 1:100	BioLegend, AB_2721558
KLRG1	2F1/KLRG1	Syrian Hamster	APC-Cyanine7	FC: 1:100	BioLegend, AB_2566554

(continued)

NK1.1	PK136	Mouse	APC	FC: 1:100	Miltenyi Biotec, AB_2727927
TCRvα2	B20.1	Rat	PE	FC: 1:100	BioLegend, AB_1134183
TCRβ	REA318	Human	PerCP-Vio700	FC: 1:100	Miltenyi Biotec, AB_2654028
CD3	OKT3	Mouse	Brilliant Violet 510	FC: 1:100	BioLegend, AB_2561943
CD4	OKT4	Mouse	Alexa Fluor 700	FC: 1:100	BioLegend, AB_571942
CD8	RPA-T8	Mouse	Brilliant Violet 605	FC: 1:100	BioLegend, AB_2563185
CD25	BV 96	Mouse	Brilliant Violet 421	FC: 1:100	BioLegend, AB_11126749
CD31	WM59	Mouse	APC-Cyanine7	FC: 1:100	BioLegend, AB_10640734
CD39	A1	Mouse	PE-Cyanine7	FC: 1:100	BioLegend, AB_2293623
CD45RA	HI100	Mouse	PE-Dazzle 594	FC: 1:100	BioLegend, AB_2564079
CD73	AD2	Mouse	PE	FC: 1:100	BioLegend, AB_2298698
CD127	A019D5	Mouse	Brilliant Violet 650	FC: 1:100	BioLegend, AB_2562095
HLA-DR	L243	Mouse	Brilliant Violet 711	FC: 1:100	BioLegend, AB_2562913
CCR4	TG6	Mouse	PerCP-Cyanine5.5	FC: 1:100	BioLegend, N/A
CD4	RPA-T4	Mouse	PE-Dazzle 594	FC: 1:100	BioLegend, AB_2563565

(continued)

CD8	HIT8a	Mouse	Alexa Fluor 700	FC: 1:100	BioLegend, AB_528884
CD27	O323	Mouse	Brilliant Violet 650	FC: 1:100	BioLegend, AB_2562096
CD45RO	UCHL1	Mouse	Brilliant Violet 785	FC: 1:100	BioLegend, AB_2563819
CD69	FN50	Mouse	APC-Cyanine7	FC: 1:100	BioLegend, AB_314849
CD161	HP-3G10	Mouse	Brilliant Violet 605	FC: 1:100	BioLegend, AB_2563607
CCR6	G034E3	Mouse	PerCP-Cyanine5.5	FC: 1:100	BioLegend, AB_10918985
CCR7	G043H7	Mouse	Brilliant Violet 711	FC: 1:100	BioLegend, AB_2563865
TCR γδ	11F2	Mouse	PE-Cyanine7	FC: 1:100	BD Biosciences, AB_2870377
TCR Vδ1	TS-1	Mouse	FITC	FC: 1:100	Thermo Fisher Scientific, AB_223619
TCR Vδ2	123R3	Mouse	APC	FC: 1:100	Miltenyi Biotec, AB_10831200
TCR vδ9	IMMU 360	Mouse	FITC	FC: 1:100	Beckman Coulter, AB_130871
CD3	OKT3	Mouse	Brilliant Violet 785	FC: 1:100	BioLegend, AB_2563507
CD4	RPA-T4	Mouse	APC-Cyanine7	FC: 1:100	BioLegend, AB_314086

(continued)

CD8	RPA-T8	Mouse	Brilliant Violet 510	FC: 1:100	BioLegend, AB_2561942
CD25	2A3	Mouse	PE	FC: 1:100	BD Biosciences, AB_2783790
CD28	CD28.2	Mouse	PE-Cyanine7	FC: 1:100	BioLegend, AB_10644005
CD38	HIT2	Mouse	Alexa Fluor 700	FC: 1:100	BioLegend, AB_2072781
CD57	HCD57	Mouse	FITC	FC: 1:100	BioLegend, AB_535992
CD95	DX2	Mouse	Brilliant Violet 421	FC: 1:100	BioLegend, AB_2561830
CCR7	G043H7	Mouse	APC	FC: 1:100	BioLegend, AB_10917385
TCR Vδ7.2	3C10	Mouse	APC-Cyanine7	FC: 1:100	BioLegend, AB_2561995
CD107a	REA792	Human	PE	FC: 1:100	Miltenyi Biotec, AB_2654474
NKG2A	REA110	Human	PE-Vio770	FC: 1:100	Miltenyi Biotec, AB_2726172
NKG2C	REA205	Human	APC	FC: 1:100	Miltenyi Biotec, AB_2727933
NKG2D	1D11	Mouse	Brillian Violet 785	FC: 1:100	Biolegend, AB_2728271
TruStain FcX™	93	Mouse	unconjugated	FC: 1:100	Biolegend, AB_1574975

FITC, fluorescein isothicyanate; PE, R-phycoerythrin; PerCP, Peridin-Chlorophyll-Protein; APC, allophycocyanin; FC, flow cytometry; IF, immunofluorescence; RRID, Research Resource Identifier

6.6 Tetramers

Antigen	MHC allele	Sequence	Dilution	Source
M38	H-2K^b	SSPPMFRV	1:200	Ramon Arens
M45	H-2D^b	HGIRNASFI	1:200	Ramon Arens
m139	H-2K^b	TVYGFCLL	1:200	Ramon Arens
M25	I-A^b	NHLYETPISATAMVI	1:100	NIH Tetramer Facility

6.7 Peptides

Peptide	Virus	Source
Nucleocapsid (NC)	SARS-CoV-2	Miltenyi Biotec
Spike (S)	SARS-CoV-2	Miltenyi Biotec
Membrane (M)	SARS-CoV-2	Miltenyi Biotec

6.8 Chemicals and reagents

Name	Source
Ketamidor 10%	WDT
Xylazine	WDT
Tween-20	Sigma-Aldrich
Paraformaldehyde (PFA)	Merck
Phorbol 12-myristate 13-acetate (PMA)	Sigma-Aldrich
Ionomycin	Sigma-Aldrich
Tissue-Tek O.C.T. Compound	Sakura Finetek
Coelenterazine	Synchem
Zombie Violet viability dye	Biolegend
Zombie NIR viability dye	Biolegend
eFluor 450 proliferation dye	Thermo Fisher Scientific
eFluor 670 proliferation dye	Thermo Fisher Scientific
DAPI	Sigma-Aldrich
Normal rat serum	Life Technologies GmbH
Trypan Blue	Thermo Fisher Scientific

6.9 Cell culture media

Name	Source
Dulbecco's Modified Eagle's Medium (DMEM) with glucose	Sigma-Aldrich
Dulbecco's Phosphate Buffered Saline	Sigma-Aldrich
Trypsin-EDTA (1x)	Sigma-Aldrich
Fetal calf serum (FCS)	Pan Biotech Gmbh
Penicillin/streptomycin (100x)	Sigma-Aldrich
DMEM Mixture F-12 (DMEM/F12)	Thermo Fisher Scientific
2-mercaptoethanol	Thermo Fisher Scientific
Sodium pyruvate	Thermo Fisher Scientific

6.10 Buffers

Name	Components	Source
FACS Buffer	5% FCS in PBS	Pan Biotech Gmbh
	3 mM EDTA	Sigma-Aldrich
MACS Buffer	5% FCS in PBS	Pan Biotech Gmbh
	6 mM EDTA	Sigma-Aldrich
10X Erythrocyte lysis buffer	1.5M NH4Cl	Merck
	100 mM KHCO3	Merck
	10 mM EDTA	Sigma-Aldrich
Fixation buffer for histology, pH 7.4	4% (w/v) PFA	Merck
	30% (w/v) sucrose	Merck
Fixation buffer for flow cytometry, pH 7.4	2% (w/v) PFA in PBS	Merck
TBS-T, pH 7.5	1 mM Tris-HCl	Sigma-Aldrich
	0.15 mM NaCl	Merck
	0.1% Tween 20	Sigma-Aldrich
Mowiol mounting medium, pH 8.5	100 mM Tris	Sigma-Aldrich
	5.5M Mowiol 4-88	Sigma-Aldrich
	25% (v/v) glycerol	Sigma-Aldrich

(continued)

50x TAE buffer, pH 8.0	2M Tris-Hcl	Sigma-Aldrich
	50 mM EDTA	Sigma-Aldrich
	5.5% (v/v) acetic acid	Merck
Virus standard buffer/sucrose, pH 7.8	50 mM Tris-Hcl	Merck
	12 mM KCl	Merck
	5 mM Na2 EDTA	Sigma-Aldrich
	15% (w/v) sucrose	Merck
Methylcellulose	2.5% (w/v) Methylcellulose	Th. Geyer GmbG & Co. KG
	10 (v/v) Modified Eagle's Medium	Sigma-Aldrich
	1% (v/v) Penicillin/Streptomycin	Sigma-Aldrich
	1.5% (v/) L-Glutamine	Sigma-Aldrich
	10 mM NaHCO3	Merck
	5% (v/v) FCS	Pan Biotech Gmbh

6.11 Commercial kits

Name	**Source**
blackPREP Rodent Tail DNA Kit	Analytik Jena AG
Pan T Cell Isolation Kit II, mouse	Miltenyi Biotec
Naive CD4+ T Cell Isolation Kit, mouse	Miltenyi Biotec
Naïve CD8a+ T Cell Isolation Kit, mouse	Miltenyi Biotec
CD3ε MicroBead Kit, mouse	Miltenyi Biotec
Pan Dendritic Cell Isolation Kit, mouse	Miltenyi Biotec
eBioscience™ Intracellular Fixation & Permeabilization Buffer Set	Invitrogen
LEGENDplex™Custom Mouse 14 Plex Panel	Biolegend
Chromium Next GEM Single Cell 5' Kit v2	10x Genomics
Library Construction Kit	10x Genomics
Chromium Next GEM Chip K Single Cell Kit	10x Genomics
Chromium Single Cell Mouse TCR Amplification Kit	10x Genomics

6.12 Devices and equipment

Name	Source
NanoDrop ND-2000 Spectrophotometer	Peqlab
QuantStudio 5	Thermo Fischer
MJ Research PTC-200 Thermal Cycler	Bio-Rad
HeraSafe Safety Cabinet	Heraeus
Hera Cell 150 CO2 incubator	Heraeus
Centro LB 960 XS3 Microplate	Berthold
TissueLyser II	Qiagen
Sorvall RC6 Plus centrifuge	Thermo Fisher
CryoStar NX70 cryostat	Epredia
Beckman Optima L-70 Ultracentrifuge	Beckman Coulter
MACS Multistand	Miltenyi Biotec
QuadroMACS Separator	Miltenyi Biotec
Zeiss AxioObserver w/ Apotome widefield microscope	Carl Zeiss
Leica TCS SP8 X confocal microscope	Leica
AxioScan Z.1 slide scanner	Carl Zeiss
FACSCanto flow cytometer	BD Biosciences
LSRFortessa flow cytometer	BD Biosciences
FACSSymphony A3 flow cytometer	BD Biosciences
FACS Aria Fusion cell sorter	BD Biosciences
LIAISON XL chemiluminescence analyzer	Diasorin

6.13 Bioinformatic tools

Name	Source
GraphPad Prism 8, 9, and 10	GraphPad
WinList v9 and v10	Verity Software House
Microsoft Office 2016	Microsoft
Image Lab Software	Bio-Rad
FACSDiva	BD Biosciences

(continued)

ImageJ	National Institutes of Health
Inkscape	Inkscape
Endnote	Clarivate
Leica Application Suite C	Leica
Zen v2 and v3 blue edition	Carl Zeiss
AxioVision SE64 Rel 4.9	Carl Zeiss
FlowJo V10	BD
R	R development team
Rstudio	Posit
ggplot2 v3	Wickham[302]
Seurat v4	Satija Lab[303]
palmerpenguins	Horst et al.[304]
Rtsne	Van der Maaten and van der Maaten[305] [306]
pheatmap	Kolde[307]
tidyverse	Wickham et al.[308]

7 Methods

7.1 Viruses

Infection experiments were performed with MCMV-3DR[83,300,301] unless otherwise stated. This recombinant encodes for an mCherry-P2A-Gaussia luciferase reporter within the m157 ORF of MCMV under the major IE promoter. Additionally, a chicken ovalbumin SIINFEKL (OVA257-264) was inserted within the m164 ORF. A previously described spontaneous mutation within the m129 ORF[309] has been repaired to encode the full-length MCK2. MCMV-4DR was created by Prof. Felix Stahl and Dr. Eleonore Ostermann and is a modification of MCMV-3DR, where the sequence for a fusion protein made of the first 118 residues of the human transferrin receptor linked to residues 299-385 of chicken ovalbumin was inserted within the m128 ORF under the human major immediate early promotor (Fig. 13). MCMV-2DR[85] does not encode for any of the chicken ovalbumin sequences (Fig. 13). All recombinants derived from the pSM3fr Smith strain and were modified by bacterial artificial chromosome mutagenesis using the *en passant* protocol[310].

7.2 Production of virus stocks

For virus stock production, 6 x 10^7 10.1 fibroblast cells were infected with a multiplicity of infection (MOI) of 0.015 in complete medium and distributed equally through thirty 150 mm cell culture dishes. At 3 and 5 dpi, supernatants were transferred to fresh tubes and centrifuged at 6,000 x *g* for 10 minutes at 4° C. The supernatants were transferred to fresh tubes and centrifuged at 25,800 x *g* for 3 hours at 4° C. The supernatants were then discarded and the pellets resuspended overnight in PBS on ice. Next, the resuspended pellet was loaded onto a sucrose/virus standard buffer cushion and ultracentrifuged at 70,000 x *g* for 90 min at 4° C. The supernatant was discarded, the pellet resuspended in PBS overnight on ice and aliquoted into fresh tubes the following day.

7.3 Virus titration

Virus titers were determined by plaque assay. In summary, 4 x 10^4 M2-10B4 fibroblasts were seeded overnight with DMEM containing 3% FCS and 1% P/S on a 48-well plate. Next, independent quadruplicates of 10-fold serial dilutions ranging from 10^{-3} to 10^{-8} were prepared and added to different wells. The plates were incubated for 3 hours at

37°C and 5% CO_2, after which 400 µL of methylcellulose were added to each well. After 4-5 days, plaques were counted to calculate the virus titers.

7.4 Animals

C57BL/6J mice were purchased from Charles River Laboratories, kept at the animal facility of the University Medical Center Hamburg-Eppendorf and bred in individually ventilated cages under pathogen-free conditions. β-actin eGFP[311], β-actin eCFP[312], *Rag2*$^{-/-}$*IL2rg*$^{-/-}$[313,314] and ovalbumin-transgenic TCR (OT-I and OT-II) mice[315,316] were all from a C57BL/6 background. OT-I mice were crossed with β-actin eCFP to generate OTIxCFP mice and OT-II mice with β-actin eGFP to generate OTIIxGFP mice. Experiments were performed according to the guidelines of the FELASA and Society of Laboratory Animals (GV-SOLAS) and approved by the local authorities (Behörde für Gesundheit und Verbraucherschutz, Amt für Verbraucherscutz, Freie und Hansestadt Hamburg, reference numbers 06/16, 39/17, 45/19, 04/20, and ORG1059).

7.5 Genotyping of transgenic mice

Mice tails were collected within the first weeks of life by animal technicians from the animal facility of the UKE and stored at -20° C until further processing. Genotyping was performed using the blackPREP Rodent Tail DNA Kit according to the manufacturer's instructions. In short, tails were lysed in Lysis Solution QPT with Proteinase K at 37°C for up to 3h. The lysed tails were centrifuged at 10,000 x *g* for 30s and the supernatant was transferred to a fresh tube containing SBS Binding Solution. The DNA-containing solution were vortexed, added to a spin filter and centrifuged for 2 min at 10,000 x *g*. Next, MS Washing Solution were added to the spin filter, which was centrifuged for 2 min at 10,000 x *g*. This washing step was performed one more time and the empty spin filter was centrifuged at 15,000 x *g* for 2 min to remove residual ethanol. The DNA was then eluted after incubation with ddH2O and the spin filter was centrifuged for 1 min at 8,000 x *g*. Genotypes were then assessed by polymerase chain reaction (PCR) or, for act-eGFP mice, quantitative PCR.

7.6 Mouse infections

Neonatal mice were infected intratracheally within 24h of birth (PND 0) with 10^4 plaque-forming units (PFU) MCMV diluted in 10 µL PBS. Adult mice (6-36 weeks) were

infected intranasally with either $2x10^5$ or 10^6 PFU MCMV diluted in 40 µL PBS under anesthesia (100 mg/kg body weight ketamine and 5 mg/kg body weight xylazine, i.p.).

7.7 T cell isolation for adoptive cell transfers

Naive T cells were isolated from secondary lymphoid organs of adult *wt*, OT-I or OT-II mice. Collected organs were mashed through a 100 µm cell strainer, rinsed with FACS buffer and centrifuged for 15 min at 500 x *g*. The pellet was then resuspended in FACS buffer and the cell suspension passed through a 40 µm cell strainer. The cells were then counted and T cells were isolated with either a Pan T Cell Isolation Kit (for wildtype T cells), CD4 T Cell Isolation Kit (for OT-II cells) or CD8 T Cell Isolation kit (OT-I cells) according to manufacturer's instructions. In brief, the cells were resuspended in MACS buffer containing biotin-antibody cocktail, mixed and incubated for 5 min on ice. Next, magnetically-labelled anti-biotin antibodies suspended in MACS buffer were added to the cell suspension, which was then mixed and incubated 10 min on ice. Cells were then passed through a LS column previously placed on a magnetic MACS separator. The column was washed twice and the flow-through containing the isolated T cells was centrifuged 15 min at 500 x *g*. OT-I and OT-II were subsequently stained with the proliferation dye eFluor 670 and, in some cases, isolated wildtype T cells were stained with eFluor 450 according to the manufacturer's instructions with minor changes. Briefly, cells were washed twice with PBS and incubated 10 min at 37°C in a concentration of 10^7 cells/ml with 10 µM proliferation dye. Labelling was then stopped by adding 5 volumes of stopping buffer and incubating 5 min on ice.

Effector T cells were isolated from the lungs of MCMV-infected adult wildtype mice. Mice were infected with $2x10^5$ PFU MCMV-3DR and, at 7 dpi, lungs were collected and digested with a Lung Dissociation Kit according to the manufacturer's instructions. In short, lungs were placed in a C Tube containing Dissociation Buffer, Enzyme D and Enzyme A. The C Tube was attached to a gentleMACS Dissociator and lungs were dissociated using the preset m_lung_01 program. C Tubes were incubated at 37°C for 30 min and shaken every 5-10 min. Then, C Tubes were again attached to the gentleMACS Dissociator and the program m_lung_02 was run for a final dissociation. Cells were then run through a 100 µm cell strainer and stained with Zombie NIR, BV771-labelled anti-CD3 (clone 17A2) and PE-labelled anti-CD44 (clone IM7) antibodies. The cells were then resuspended in FACS Buffer and living CD3+CD44+ effector T cells were sorted in a FACS Aria III cell sorter.

Isolated cells were always washed twice with PBS and counted before application into the recipient animals. Adoptive transfers were always performed with 50 µL PBS containing different cell numbers as specified in the experiments.

7.8 Cell culture

All cell culture work was performed under a laminar flow hood. M2-10B4 and 10.1 fibroblasts were cultured in 150 mm tissue culture dishes with Dulbecco's modified Eagle medium (DMEM) complemented with 10% fetal calf serum (FCS) and 100 IU Penicillin/100 µg Streptomycin (P/S) (altogether, complete DMEM) at 37°C and 5% CO_2. At around 90% confluence, cells were washed once with PBS and 0.25% Trypsin-EDTA solution was added to the cell monolayer. After 5 minutes, complete DMEM was added and 10% of the cells were transferred to a new cell culture dish. For plaque assays, cells numbers were calculated on an automated cell counter after loading 10 µL cell suspension into counting slide. Wildtype SM9-1 and transduced cells were cultured in 100 mm tissue culture dishes with DMEM Mixture F-12 (DMEM/F12) complemented with 10% FCS, 100 IU / 100 µg P/S, and 50 µM 2-mercaptoethanol (complete DMEM/F12) at 37°C and 5% CO_2.

7.9 Polymerase chain reaction

PCRs were performed using 2 µL eluted DNA in 1X KAPPA2G Fast ReadyMix according to the manufacturer's instructions. PCR products were analyzed on 1% agarose TAE gels for 45 min at 120 V.

7.10 Isolation of placenta cells

Placenta cells were isolated as previously described[317,318]**.** Briefly, placentas were macroscopically dissociated from the fetuses, cut into small fragments and digested in collagenase Type II-S until the tissue could pass through a 10 mL serological pipette. The digested tissue was passed through a 70 µm cell strainer, separated in a discontinuous Percoll gradient (0-70%), and cells were collected from the 20-50% layers. Primary placenta cells were then washed and cultured in complete DMEM/F12.

7.11 Single cell suspensions from spleens, lymph nodes and blood for flow cytometry

Mouse blood was obtained by retro-orbital bleeding into EDTA-coated tubes and stored at room temperature until further processing. Red blood cells were lysed in 10 volumes of erythrocyte lysis buffer for 15 min at room temperature. Cells were then centrifuged for 5 min at 500 x *g* and resuspended in FACS buffer. Lung-draining lymph nodes were gently mashed between two glass slides and the resulting cell suspension was collected in FACS buffer. Cells were then centrifuged for 5 min at 500 x *g* and resuspended in FACS buffer. Spleens were cut into four pieces and gently mashed on a 100 µm cell strainer. Cells were centrifuged for 15 min at 500 x *g* and resuspended in FACS buffer.

7.12 Isolation of lung T cells

Animals were perfused with PBS and lungs collected and digested as described in section 7.7. Next, T cells were isolated with a CD3ε MicroBead Kit according to the manufacturer's instructions with changes. Briefly, every 10^7 cells were resuspended in 100 µL MACS buffer with 10 µL CD3ε-Biotin antibody and incubated for 10 min on ice. Next, 80 µL MACS buffer per 10^7 cells were added together with 20 µL anti-Biotin MicroBeads and incubated for 15 min on ice. Cells were centrifuged at 500 x *g* for 5 min, resuspended in 500 µL MACS buffer and loaded onto a LS column. The column was washed twice with MACS buffer, placed on a 15 mL tube, and magnetically-labeled $CD3^+$ T cells were plunged from the column in 5 mL MACS buffer. The cell suspension was centrifuged for 5 min at 500 x *g*, the cells were resuspended in FACS buffer and stored on ice until further processing.

7.13 Single-cell RNA sequencing

For single-cell RNA sequencing, lung T cells were isolated as described in section 7.12. and were subjected to an additional purification step through staining T cells with a BV711-labeled αCD3 antibody and cell sorting in a BD FACSAria Fusion (see section 7.18). Isolated cells were then given to the Next-Generation Sequencing technology platform of the Leibniz Institute for Virology for further processing. Single-cell RNA libraries were prepared using the Chromium Next GEM Single Cell 5' Kit v2 and T cell

receptor libraries were constructed with the Chromium Single Cell Mouse TCR Amplification Kit according to the manufacturer's instructions.

7.14 Isolation of lung dendritic cells

Lungs were collected and digested as described in section 7.7. Next, dendritic cells were enriched from the lung cell suspension using a Pan Dendritic Cell Isolation Kit according to the manufacturer's instructions with changes. In short, 10^8 cells were resuspended in 350 µL MACS buffer and blocked with 50 µL FcR Blocking Reagent for 5 min on ice. Next, 100 µL Pan Dendritic Cell Biotin-Antibody Cocktail was added, the suspension was mixed and incubated on ice for 10 min. Cells were centrifuged 5 min at 500 x *g*, resuspended in 800 µL MACS buffer and 200 µL Anti-Biotin Microbeads and incubated for 10 min on ice. Cells were then loaded onto an LS column, the column washed twice with MACS buffer and the flow-through containing DCs was centrifuged for 5 min at 500 x *g*. The cell pellet was resuspended in FACS buffer and stored on ice until further processing.

7.15 Organ processing for determination of viral loads and luciferase assay

One to four right lung lobes were collected and lysed on a TissueLyser II in 1 mL PBS containing a 7 mm stainless steel bead for 2 min at 25 Hz. Lung lysates were then centrifuged at 20,000 x *g* and the supernatants were used for a luciferase assay. Briefly, 10 µL of lysed lung supernatant were added to 90 µL PBS onto a black 96-well plate with white wells. Luciferase activity was analyzed on a Centro LB 960 XS3 automated luminometer. For this, 10 µL 1 µg/mL coelenterazine was automatically added to each well and luminescence was measured 10 s later. Luciferase values from non-infected animals were used to determine the limit of detection.

7.16 Organ processing for histology and image acquisition

Left lung lobes were collected and fixed overnight in 2% PFA with 30% sucrose. The lungs were subsequently washed twice with PBS and incubated for 30 min in O.C.T. embedding compound. Up to 7 lungs were then placed on a cryomold, frozen on dry ice and stored at -20° C until further processing. Sections of 7 to 20 µm were made on a cryostat and stored overnight in the dark at room temperature. Slides were either immediately process or stored at -20° C for further processing. Next, slides were

hydrated in TBS-T and placed on a slide rack with a disposable immunostaining slide. Tissues were blocked with TBS-T containing 5% rat serum for 30 min at room temperature. Next, 200 µL antibody cocktails in TBS-T were added per slide an incubated for 1h at room temperature. Nuclei were then stained with DAPI for 1 min and the tissue was washed three times with TBS-T. Then, slides were allowed to dry and slides were mounted with Mowiol Mounting Media. Slides were stored at 4° C and measured within the next two days. Images were acquired with either a ZEISS Axioscan 7 Microscope Slide Scanner or a Leica TCS SP8 confocal microscope. Images were processed with ZEN 2.6 or LAS AF Lite 4.0.

7.17 Quantification of histology data

NIFs were identified by accumulation of $CD45^+$ cells and/or accumulation of DAPI-stained nuclei. NIF sizes were calculated using the processing software. Infected cells were identified based on their mCherry expression in combination with a single nucleus. OT-I and OT-II cells were identified based on their expression of eCFP or eGFP, respectively, in combination with a single nucleus. Cells and NIFs were counted manually.

7.18 Flow cytometry and cell sorting

Flow cytometry is a powerful technique that allows for the analysis of protein expression at the single-cell level. This method can measure thousands of cells per second, offering high-throughput and multiparametric results. As cells pass through laser beams, they scatter light and emit fluorescence. The forward-scattered light (FSC) and side-scattered light (SSC) are measured when a cell passes a laser beam, and their values inform cell size (FSC) and cellular granularity or internal complexity (SSC). Flow cytometers can also detect fluorescence, making it possible to label cells with fluorescently tagged antibodies that bind to specific cellular markers. The expression level of target molecules is then associated with the intensity of the fluorescence signal, enabling comparison of protein expression levels between different cell types.

After generation of single cell suspensions cell surface stainings were performed in combination with Fc receptor blocking. For this, 100 µL FACS buffer containing 5% normal rat serum were added to the cell suspensions with the according concentration of each antibody. The cells were incubated for 15 min in the dark on ice, centrifuged

for 5 min at 500 x *g* and the cell pellet was resuspended in FACS buffer. For intracellular stainings, cells were centrifuged for 5 min at 500 x *g*, resuspended in 2% fixation solution and incubated for 30 min in the dark on ice. Next, cells were washed twice with Permeabilization Buffer with 5 min centrifugations at 500 x *g*. Next, cells were incubated with Permeablization buffer containing 5% normal rat serum and the according concentration of the antibodies. Cells were then washed two more times with Permeabilization Buffer with 5 min centrifugations at 500 x *g*. In some cases, cells were fixed overnight in 2% PFA. Before measurement, cells were washed once with FACS Buffer and resuspended in the same buffer. Samples were measured either on a BD FACSCanto, a BD FACS LSRFortessa, a BD FACSymphony A1, or a BD FACSymphony A3. For cell sorting, cells were stained as described above. Cells were then sorted on a BD FACSAria Fusion with a 100 µm nozzle.

Stainings of samples from the HCMV study were performed by Romy Hackbusch. Briefly, antibodies were previously titrated and an antibody cocktails with the according antibody concentrations was prepared (Table 3). Cell surfaces were stained by adding 50 µL antibody cocktail to 50 µL whole blood. Samples were incubated for 10 min in the dark at room temperature. Live/dead stainings were added to the according tubes and samples were additionally incubated for 20 min in the dark at room temperature. Then, 1 mL erythrocyte lysis buffer was added and the samples were incubated for 10 min in the dark at room temperature. Cell suspensions were incubated for 5 min at 500 x *g* and supernatants were discarded. Samples were then washed twice with PBS and resuspended with 1 mL FACS Buffer until measurement.

7.18.1 Gating strategy for primary placenta cells

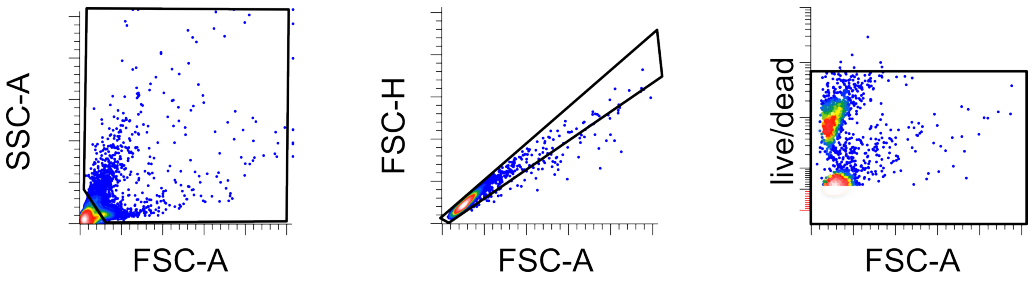

Figure 36. Gating strategy for primary placenta cells. Cell debris was gated out based on low forward and side scatter area (FSC-A and SSC-A, respectively) pulse values (left panel). Single cells were selected based on FSC-A and forward scatter height (FSC-H) values (middle panel). Next, live/dead$^-$ cells were selected as living cells. The live/dead threshold was set based on unstained primary placenta cells. Relative to Figures 5 and 8.

7.18.2 Gating strategy for tetramer-labeled blood T cells

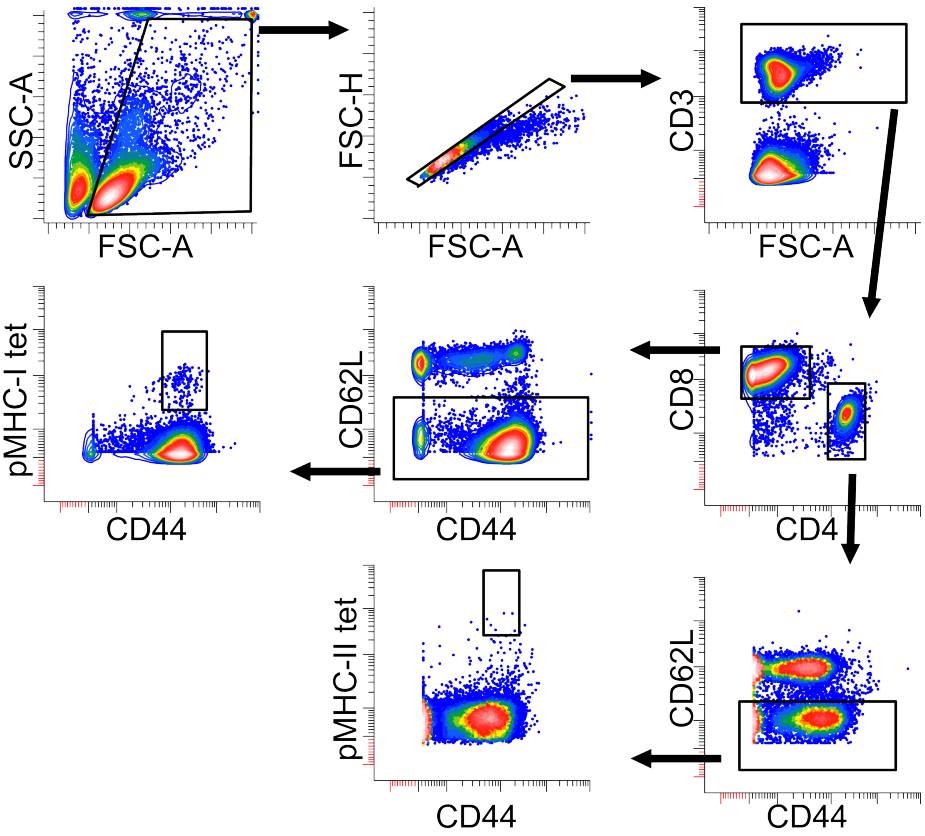

Figure 37. Gating strategy for tetramer-labeled blood cells. Major leukocyte populations were gated based on FSC-A and SSC-A. From these, single cells were gated based on FSC-A and FSC-H values. T cells ($CD3^+$) were then selected and subsequently separated into CD4 and CD8 T cells. Non-naïve populations of both CD4 and CD8 T cell populations were selected based on the lack of CD62L expression. Out of these gated cells, pMHC-I and pMHC-II tetramer signals were then evaluated on effector ($CD44^+$) CD4 and CD8 T cell subpopulations. Relative to Figures 8 and 9.

7.18.3 Gating strategy for adoptively transferred eGFP⁺ T cells

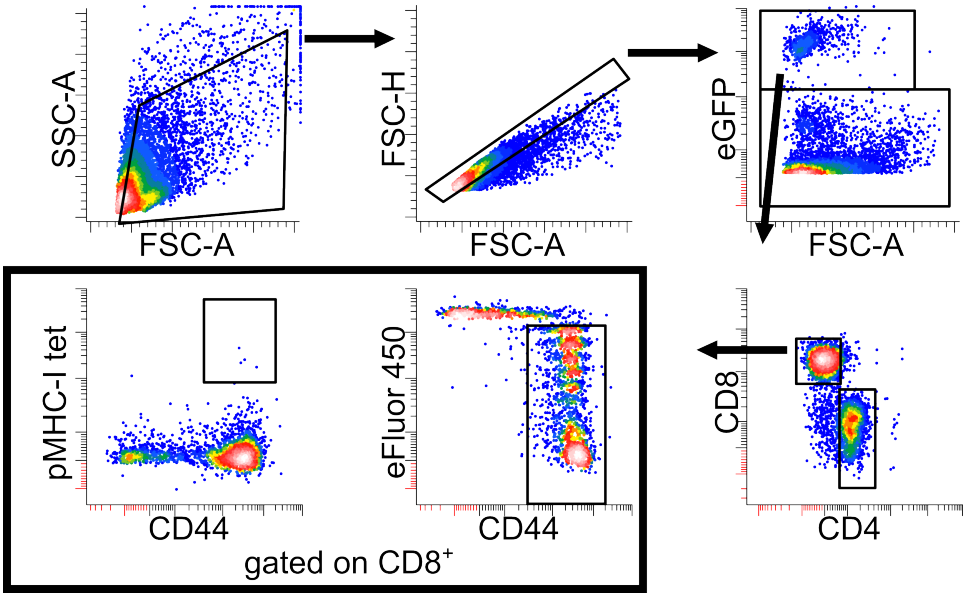

Figure 38. Gating strategy for adoptively transferred lung T cells. Major cell populations were gated based on FSC-A and SSC-A. From these, single cells were gated based on FSC-A and FSC-H values. Adoptively transferred (eGFP⁺) T cells were then selected and further separated into CD4 and CD8 subsets. The frequency of pMHC-I tetramer⁺ cells was only evaluated on CD8+ T cells. Relative to Figure 11.

7.18.4 Gating strategy for lymph node OT-I and OT-II T cells

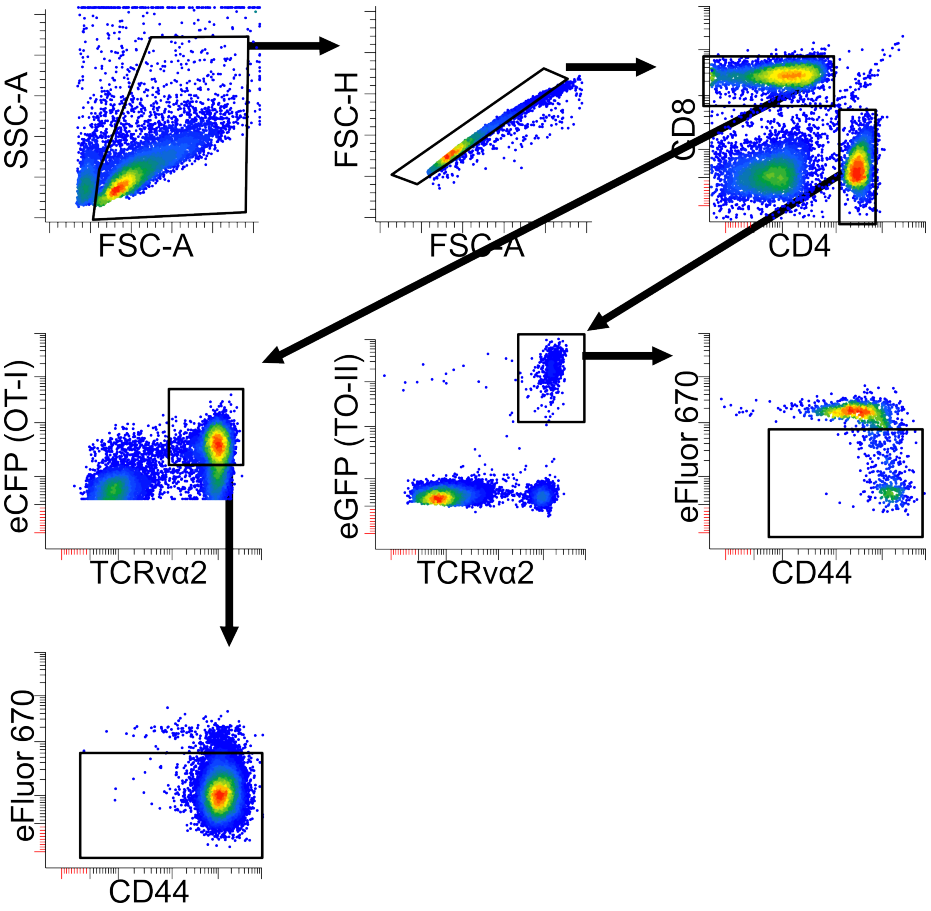

Figure 39. Gating strategy for adoptively transferred OT-I and OT-II T cells in lymph nodes. Major lymphocyte populations were gated based on FSC-A and SSC-A values and single cells were gated with FSC-A and FSC-H. $CD4^+$ cells were subsequently gated and OT-II T cells were gated based on expression of TCRvα2 and eGFP. Additionally, $CD8^+$ cells were gated and OT-I cells were selected as $TCRv\alpha2^+eCFP^+$ cells. Expression of CD44 and loss of eFluor 670 proliferation dye were analyzed for both OT-I and OT-II cells. Relative to Figure 13.

7.19 Cytokine multiplex assay

Organ supernatants were prepared by Silvia Tödter. Lungs were collected after perfusion with PBS, weighed, and lysed with a TissueLyser II in 200 µL PBS. Supernatants were frozen at -80° C until further processing. Supernatants were thawed on ice and processed with a custom-made LEGENDplex panel targeting IFN-α, IFN-β, IFN-γ, IL-10, IL-12p70, IL-15, IL-18, IL-1β, IL-2, IL-27, IL-33, IL-6, IL-7 and TGF-β1 (free active) according to the manufacturer's instructions. In short, 25 µL of sample or standard were added to 25 µL Assay Buffer and 25 µL Detection Antibodies on a 96-

well V-bottom plate. The plate was placed on a plate shaker for 2h at room temperature while shaking at 600 rpm. Next, 25 µL SA-PE was added to each tube and the plate was further shaken for 30 min at room temperature. The plate was centrifuged at 1,000 x *g* for 5 min and the supernatants were discarded. Next, 200 µL Wash Buffer was added to each well and the plate was shaken for 1 min. The plate was then centrifuged for 5 min at 1,000 x *g* and 200 µL Wash Buffer was added. The samples were then measured on a BD FACSCanto.

Table 3. Flow cytometry panels used for phenotyping of peripheral blood cells from HCMV-exposed neonates.

Fluorophore (channel)	Peripheral blood subsets	Effector T cells	CD4 differentiation	Invariant T cells	Tregs	B cells	NK cells
Brilliant Violet 421	CD56	CD95	CRTH2	CD25	CD25	CD20	CD56
Brilliant Violet 500	CD45	CD8	CD3	CD3	CD3	CD45	live/dead
Brilliant Violet 605	CD16	-	CD161	CD161	CD8	-	-
Brilliant Violet 650	CD3	CD127	CD127	CD27	CD127	-	CD3
Brilliant Violet 711	CD14	HLA-DR	CD45RA	CCR7	HLA-DR	CD10	-
Brilliant Violet 785	HLA-DR	CD3	CD25	CD45RO	-	CD19	NKG2D
FITC	-	CD57	CXCR3	Vδ1+Vγ9	-	CD38	CD69
PerCP-Cy5.5	CD15	-	CCR6	CCR6	CCR4	CD24	-
PE	CD127	CD25	TCRγδ	CD8β	CD73	sIgD	CD107a
PE-Texas Red	CD11c	CD45RA	CXCR5	CD4	CD45RA	CD5	CD57
PE-Cy7	CD123	CD28	CCR4	TCRγδ	CD39	CD43	NKG2A
APC	CD141	CCR7	CCR10	Vα7.2+Vδ2	-	CD21	NKG2C
Alexa Fluor 700	CD20	CD38	CD4	CD8α	CD4		CD14
APC-Cy7	CD1c	CD4	-	CD69	CD31	CD27	CD16

FITC, fluorescein isothiocyanate; PerCP-Cy5.5, Peridinin-chlorophyll-protein complex-Cyanine5.5; PE, R-phycoerythrin; APC, allophycocyanin;

7.20 Single cell and single nuclei RNA sequencing analyses

The single nuclei RNA sequencing dataset (GSE152248)[178] was reanalyzed with R using the Seurat package (v4.2.0)[303]. The cell subsets were annotated according to the original report. Only placentas isolated from gestational day 12.5 were considered for the analysis.

Data analysis of the single-cell RNA sequencing was performed by Sanamjeet Virdi using the Seurat package (v4.2.0)[303]. All analyses, plots, and tables were generated in R version 4.1.15 [319] with ggplot2 version 3.3.6 [302].

7.21 Interferon-γ release assay

Peptide pools containing overlapping 15-mer sequences spanning the entirety of the SARS-CoV-2 nucleocapsid (PepTivator SARS-CoV-2 Prot_N) and predicted immunodominant sequence domains of the SARS-CoV-2 spike (PepTivator SARS-CoV-2 Prot_S), HCMV IE1 (PepTivator CMV IE-1), and pp65 (PepTivator CMV pp65) proteins were used to stimulate peripheral blood T cells. Following blood collection, heparinized whole blood (800µL) was incubated with (i) PBS), (ii) a combination of phorbol-12-myristate-13-acetate (PMA, 50 ng/mL) and ionomycin (positive control, 500 ng/mL), (iii) SARS-CoV-2 peptides (1 µg/mL), or (iv) a mix of HCMV IE1 and HCMV pp65 peptides (0.5 µg/mL each) for 24 hours at 37°C. The concentration of IFN-γ in the supernatants was quantified by Kathrin Cermann and Anthea Spier with supervision of Dr. Marc Lütgehetmann using a chemiluminescence immunoassay (QuantiFERON) on a LIAISON XL analyzer (DiaSorin) as per the manufacturer's recommendations. In the study assessing CMI at the feto-maternal interface, 400 µL whole blood was stimulated with the same concentrations and the supernatants were diluted 1:2 with PBS before analysis. Optimal thresholds were selected by calculating the maximum Youden index (J) with the formula:

$$J_{max} = \max_t(\text{sensitivity}(t) + \text{specificity}\ (t) - 1)$$

where *t* represents the threshold value for which J is maximal.

7.22 Statistical analysis

Statistical analyses were performed with GraphPad Prism versions 8, 9, and 10. Dimensionality reduction of the IGRA dataset was performed with R (version 4.2.1)[319] using the Rtsne package (version 0.16)[305,306].

7.23 Clinical cohorts

In the human CMV cohort pregnant women with an HCMV infection were enrolled by Dr. Anna Perez. All participants signed an informed consent form and the study was approved by the Hamburg Chamber of Medical Practitioners. Positive HCMV status was confirmed by PCR from urine and serology testing. Peripheral blood was collected from the newborns within the first three days of life, with the exception of one sample that was collected after 12 days. CMV status was assessed through PCR from urine samples collected within the first day.

For evaluating the performance of the IGRA study participants were recruited from the 16th of November 2020 to the 28th of April 2021 as previously described[198,199]. In this period seroprevalence for SARS-CoV-2 was reported to be 4% in Hamburg[142]. Individuals with a positive PCR test for SARS-CoV-2 at least 2 months prior to recruitment were enrolled. Negative controls were participants of the Hamburg City Health Study (HCHS) with no history of positive PCR for SARS-CoV-2. All participants were examined through the HCHS program with a questionnaire to assess severity at time of infection and long COVID-19 symptoms. Additionally, blood was drawn for the different analyses. All participants provided written informed consent. The recruitment of participants was approved by the State of Hamburg Chamber of Medical Practitioners under the license number PV5131 and the study was conducted in compliance with the Declaration of Helsinki.

For assessment of T cell responses at the feto-maternal interface, study subjects with a SARS-CoV-2 infection during pregnancy were recruited after signing informed consent. This study was approved by the Hamburg Chamber of Medical Practitioners under the license number PV7312 and recruitment was done by Ann-Christin Tallarek under the supervision of Dr. Anke Diemert and Prof. Dr. Petra Arck. SARS-CoV-2 status was confirmed by qPCR.

8 References

1. Warnock, R.A., Askari, S., Butcher, E.C., and von Andrian, U.H. (1998). Molecular mechanisms of lymphocyte homing to peripheral lymph nodes. J Exp Med *187*, 205-216. 10.1084/jem.187.2.205.
2. Shah, K., Al-Haidari, A., Sun, J., and Kazi, J.U. (2021). T cell receptor (TCR) signaling in health and disease. Signal Transduct Target Ther *6*, 412. 10.1038/s41392-021-00823-w.
3. Chen, L., and Flies, D.B. (2013). Molecular mechanisms of T cell co-stimulation and co-inhibition. Nat Rev Immunol *13*, 227-242. 10.1038/nri3405.
4. Curtsinger, J.M., Lins, D.C., and Mescher, M.F. (2003). Signal 3 determines tolerance versus full activation of naive CD8 T cells: dissociating proliferation and development of effector function. J Exp Med *197*, 1141-1151. 10.1084/jem.20021910.
5. Sckisel, G.D., Bouchlaka, M.N., Monjazeb, A.M., Crittenden, M., Curti, B.D., Wilkins, D.E., Alderson, K.A., Sungur, C.M., Ames, E., Mirsoian, A., et al. (2015). Out-of-Sequence Signal 3 Paralyzes Primary CD4(+) T-Cell-Dependent Immunity. Immunity *43*, 240-250. 10.1016/j.immuni.2015.06.023.
6. Koh, C.H., Lee, S., Kwak, M., Kim, B.S., and Chung, Y. (2023). CD8 T-cell subsets: heterogeneity, functions, and therapeutic potential. Exp Mol Med *55*, 2287-2299. 10.1038/s12276-023-01105-x.
7. Curtsinger, J.M., Agarwal, P., Lins, D.C., and Mescher, M.F. (2012). Autocrine IFN-gamma promotes naive CD8 T cell differentiation and synergizes with IFN-alpha to stimulate strong function. J Immunol *189*, 659-668. 10.4049/jimmunol.1102727.
8. Mehta, A.K., Gracias, D.T., and Croft, M. (2018). TNF activity and T cells. Cytokine *101*, 14-18. 10.1016/j.cyto.2016.08.003.
9. Maecker, H.T., McCoy, J.P., and Nussenblatt, R. (2012). Standardizing immunophenotyping for the Human Immunology Project. Nat Rev Immunol *12*, 191-200. 10.1038/nri3158.
10. Sallusto, F., Lenig, D., Forster, R., Lipp, M., and Lanzavecchia, A. (1999). Two subsets of memory T lymphocytes with distinct homing potentials and effector functions. Nature *401*, 708-712. 10.1038/44385.
11. Farber, D.L., Yudanin, N.A., and Restifo, N.P. (2014). Human memory T cells: generation, compartmentalization and homeostasis. Nat Rev Immunol *14*, 24-35. 10.1038/nri3567.
12. Eickhoff, S., Brewitz, A., Gerner, M.Y., Klauschen, F., Komander, K., Hemmi, H., Garbi, N., Kaisho, T., Germain, R.N., and Kastenmuller, W. (2015). Robust Anti-viral Immunity Requires Multiple Distinct T Cell-Dendritic Cell Interactions. Cell *162*, 1322-1337. 10.1016/j.cell.2015.08.004.
13. Voskoboinik, I., Whisstock, J.C., and Trapani, J.A. (2015). Perforin and granzymes: function, dysfunction and human pathology. Nat Rev Immunol *15*, 388-400. 10.1038/nri3839.
14. Simon, A.K., Hollander, G.A., and McMichael, A. (2015). Evolution of the immune system in humans from infancy to old age. Proc Biol Sci *282*, 20143085. 10.1098/rspb.2014.3085.
15. United Nations Children's Fund (UNICEF) (2023). Levels & Trends in Child Mortality - Report 2022. World Health Organization. 978-92-806-5422-6.
16. Perin, J., Mulick, A., Yeung, D., Villavicencio, F., Lopez, G., Strong, K.L., Prieto-Merino, D., Cousens, S., Black, R.E., and Liu, L. (2022). Global, regional, and national causes of under-5 mortality in 2000-19: an updated systematic analysis with implications for the Sustainable Development Goals. Lancet Child Adolesc Health *6*, 106-115. 10.1016/S2352-4642(21)00311-4.
17. Bhutta, Z.A., and Black, R.E. (2013). Global maternal, newborn, and child health--so near and yet so far. N Engl J Med *369*, 2226-2235. 10.1056/NEJMra1111853.
18. Olin, A., Henckel, E., Chen, Y., Lakshmikanth, T., Pou, C., Mikes, J., Gustafsson, A., Bernhardsson, A.K., Zhang, C., Bohlin, K., and Brodin, P. (2018). Stereotypic Immune System Development in Newborn Children. Cell *174*, 1277-1292 e1214. 10.1016/j.cell.2018.06.045.

19. Adkins, B., Leclerc, C., and Marshall-Clarke, S. (2004). Neonatal adaptive immunity comes of age. Nat Rev Immunol *4*, 553-564. 10.1038/nri1394.
20. Levy, O. (2007). Innate immunity of the newborn: basic mechanisms and clinical correlates. Nat Rev Immunol *7*, 379-390. 10.1038/nri2075.
21. Prendergast, A.J., Klenerman, P., and Goulder, P.J. (2012). The impact of differential antiviral immunity in children and adults. Nat Rev Immunol *12*, 636-648. 10.1038/nri3277.
22. Park, J.E., Botting, R.A., Dominguez Conde, C., Popescu, D.M., Lavaert, M., Kunz, D.J., Goh, I., Stephenson, E., Ragazzini, R., Tuck, E., et al. (2020). A cell atlas of human thymic development defines T cell repertoire formation. Science *367*. 10.1126/science.aay3224.
23. Kollmann, T.R., Marchant, A., and Way, S.S. (2020). Vaccination strategies to enhance immunity in neonates. Science *368*, 612-615. 10.1126/science.aaz9447.
24. Yockey, L.J., Lucas, C., and Iwasaki, A. (2020). Contributions of maternal and fetal antiviral immunity in congenital disease. Science *368*, 608-612. 10.1126/science.aaz1960.
25. Megli, C.J., and Coyne, C.B. (2022). Infections at the maternal-fetal interface: an overview of pathogenesis and defence. Nat Rev Microbiol *20*, 67-82. 10.1038/s41579-021-00610-y.
26. Fitzpatrick, D., Holmes, N.E., and Hui, L. (2022). A systematic review of maternal TORCH serology as a screen for suspected fetal infection. Prenat Diagn *42*, 87-96. 10.1002/pd.6073.
27. Neu, N., Duchon, J., and Zachariah, P. (2015). TORCH infections. Clin Perinatol *42*, 77-103, viii. 10.1016/j.clp.2014.11.001.
28. Rasti, S., Ghasemi, F.S., Abdoli, A., Piroozmand, A., Mousavi, S.G., and Fakhrie-Kashan, Z. (2016). ToRCH "co-infections" are associated with increased risk of abortion in pregnant women. Congenit Anom (Kyoto) *56*, 73-78. 10.1111/cga.12138.
29. Devaraju, M., Li, A., Ha, S., Li, M., Shivakumar, M., Li, H., Nishiguchi, E.P., Gerardin, P., Waldorf, K.A., and Al-Haddad, B.J.S. (2023). Beyond TORCH: A narrative review of the impact of antenatal and perinatal infections on the risk of disability. Neurosci Biobehav Rev *153*, 105390. 10.1016/j.neubiorev.2023.105390.
30. Song, X., Li, Q., Diao, J., Li, J., Li, Y., Zhang, S., Chen, L., Wei, J., Shu, J., Liu, Y., et al. (2022). Association Between First-Trimester Maternal Cytomegalovirus Infection and Stillbirth: A Prospective Cohort Study. Front Pediatr *10*, 803568. 10.3389/fped.2022.803568.
31. Dudley, D.M., Van Rompay, K.K., Coffey, L.L., Ardeshir, A., Keesler, R.I., Bliss-Moreau, E., Grigsby, P.L., Steinbach, R.J., Hirsch, A.J., MacAllister, R.P., et al. (2018). Miscarriage and stillbirth following maternal Zika virus infection in nonhuman primates. Nat Med *24*, 1104-1107. 10.1038/s41591-018-0088-5.
32. Elkan Miller, T., Weisz, B., Yinon, Y., Weissbach, T., De Castro, H., Avnet, H., Hoffman, C., Katorza, E., and Lipitz, S. (2021). Congenital Cytomegalovirus Infection Following Second and Third Trimester Maternal Infection Is Associated With Mild Childhood Adverse Outcome Not Predicted by Prenatal Imaging. J Pediatric Infect Dis Soc *10*, 562-568. 10.1093/jpids/piaa154.
33. Wang, Z., Wu, Z., Wang, H., Feng, R., Wang, G., Li, M., Wang, S.Y., Chen, X., Su, Y., Wang, J., et al. (2023). An immune cell atlas reveals the dynamics of human macrophage specification during prenatal development. Cell *186*, 4454-4471 e4419. 10.1016/j.cell.2023.08.019.
34. Hussain, T., Murtaza, G., Kalhoro, D.H., Kalhoro, M.S., Yin, Y., Chughtai, M.I., Tan, B., Yaseen, A., and Rehman, Z.U. (2022). Understanding the Immune System in Fetal Protection and Maternal Infections during Pregnancy. J Immunol Res *2022*, 7567708. 10.1155/2022/7567708.
35. Raaphorst, F.M., van Bergen, J., van den Bergh, R.L., van der Keur, M., de Krijger, R., Bruining, J., van Tol, M.J., Vossen, J.M., and van den Elsen, P.J. (1994). Usage of TCRAV and TCRBV gene families in human fetal and adult TCR rearrangements. Immunogenetics *39*, 343-350. 10.1007/BF00189231.
36. Rechavi, E., Lev, A., Lee, Y.N., Simon, A.J., Yinon, Y., Lipitz, S., Amariglio, N., Weisz, B., Notarangelo, L.D., and Somech, R. (2015). Timely and spatially regulated maturation of B and T cell repertoire during human fetal development. Sci Transl Med *7*, 276ra225. 10.1126/scitranslmed.aaa0072.

37. Park, J.E., Jardine, L., Gottgens, B., Teichmann, S.A., and Haniffa, M. (2020). Prenatal development of human immunity. Science *368*, 600-603. 10.1126/science.aaz9330.
38. Schonland, S.O., Zimmer, J.K., Lopez-Benitez, C.M., Widmann, T., Ramin, K.D., Goronzy, J.J., and Weyand, C.M. (2003). Homeostatic control of T-cell generation in neonates. Blood *102*, 1428-1434. 10.1182/blood-2002-11-3591.
39. Rawlinson, W.D., Boppana, S.B., Fowler, K.B., Kimberlin, D.W., Lazzarotto, T., Alain, S., Daly, K., Doutre, S., Gibson, L., Giles, M.L., et al. (2017). Congenital cytomegalovirus infection in pregnancy and the neonate: consensus recommendations for prevention, diagnosis, and therapy. Lancet Infect Dis *17*, e177-e188. 10.1016/S1473-3099(17)30143-3.
40. Fowler, K.B., and Boppana, S.B. (2018). Congenital cytomegalovirus infection. Semin Perinatol *42*, 149-154. 10.1053/j.semperi.2018.02.002.
41. Marshall, B.C., and Koch, W.C. (2009). Antivirals for cytomegalovirus infection in neonates and infants: focus on pharmacokinetics, formulations, dosing, and adverse events. Paediatr Drugs *11*, 309-321. 10.2165/11316080-000000000-00000.
42. Razonable, R.R., Inoue, N., Pinninti, S.G., Boppana, S.B., Lazzarotto, T., Gabrielli, L., Simonazzi, G., Pellett, P.E., and Schmid, D.S. (2020). Clinical Diagnostic Testing for Human Cytomegalovirus Infections. J Infect Dis *221*, S74-S85. 10.1093/infdis/jiz601.
43. Stephan, A.J., de Lepper, M., Wolle, R., Luzak, A., Wang, W., Jacob, C., Schneider, K.M., Buxmann, H., Goelz, R., Hamprecht, K., et al. (2023). Healthcare costs of congenital cytomegalovirus (cCMV) disease in infants during the first two years of life: a retrospective German claims database analysis. Cost Eff Resour Alloc *21*, 8. 10.1186/s12962-022-00411-x.
44. Grosse, S.D., Dollard, S.C., and Ortega-Sanchez, I.R. (2021). Economic assessments of the burden of congenital cytomegalovirus infection and the cost-effectiveness of prevention strategies. Semin Perinatol *45*, 151393. 10.1016/j.semperi.2021.151393.
45. Zuhair, M., Smit, G.S.A., Wallis, G., Jabbar, F., Smith, C., Devleesschauwer, B., and Griffiths, P. (2019). Estimation of the worldwide seroprevalence of cytomegalovirus: A systematic review and meta-analysis. Rev Med Virol *29*, e2034. 10.1002/rmv.2034.
46. Fowler, K., Mucha, J., Neumann, M., Lewandowski, W., Kaczanowska, M., Grys, M., Schmidt, E., Natenshon, A., Talarico, C., Buck, P.O., and Diaz-Decaro, J. (2022). A systematic literature review of the global seroprevalence of cytomegalovirus: possible implications for treatment, screening, and vaccine development. BMC Public Health *22*, 1659. 10.1186/s12889-022-13971-7.
47. Stagno, S., Pass, R.F., Dworsky, M.E., and Alford, C.A., Jr. (1982). Maternal cytomegalovirus infection and perinatal transmission. Clin Obstet Gynecol *25*, 563-576. 10.1097/00003081-198209000-00014.
48. Sinzger, C., Digel, M., and Jahn, G. (2008). Cytomegalovirus cell tropism. Curr Top Microbiol Immunol *325*, 63-83. 10.1007/978-3-540-77349-8_4.
49. Nangle, S., Mitra, S., Roskos, S., and Havlichek, D. (2018). Cytomegalovirus infection in immunocompetent adults: Is observation still the best strategy? IDCases *14*, e00442. 10.1016/j.idcr.2018.e00442.
50. Ramanan, P., and Razonable, R.R. (2013). Cytomegalovirus infections in solid organ transplantation: a review. Infect Chemother *45*, 260-271. 10.3947/ic.2013.45.3.260.
51. Tang, Y., Guo, J., Li, J., Zhou, J., Mao, X., and Qiu, T. (2022). Risk factors for cytomegalovirus infection and disease after kidney transplantation: A meta-analysis. Transpl Immunol *74*, 101677. 10.1016/j.trim.2022.101677.
52. Hakimi, Z., Aballea, S., Ferchichi, S., Scharn, M., Odeyemi, I.A., Toumi, M., and Saliba, F. (2017). Burden of cytomegalovirus disease in solid organ transplant recipients: a national matched cohort study in an inpatient setting. Transpl Infect Dis *19*. 10.1111/tid.12732.
53. Harvala, H., Stewart, C., Muller, K., Burns, S., Marson, L., MacGilchrist, A., and Johannessen, I. (2013). High risk of cytomegalovirus infection following solid organ transplantation despite prophylactic therapy. J Med Virol *85*, 893-898. 10.1002/jmv.23539.

54. Azevedo, L.S., Pierrotti, L.C., Abdala, E., Costa, S.F., Strabelli, T.M., Campos, S.V., Ramos, J.F., Latif, A.Z., Litvinov, N., Maluf, N.Z., et al. (2015). Cytomegalovirus infection in transplant recipients. Clinics (Sao Paulo) *70*, 515-523. 10.6061/clinics/2015(07)09.
55. Cantoni, N., Hirsch, H.H., Khanna, N., Gerull, S., Buser, A., Bucher, C., Halter, J., Heim, D., Tichelli, A., Gratwohl, A., and Stern, M. (2010). Evidence for a bidirectional relationship between cytomegalovirus replication and acute graft-versus-host disease. Biol Blood Marrow Transplant *16*, 1309-1314. 10.1016/j.bbmt.2010.03.020.
56. Teira, P., Battiwalla, M., Ramanathan, M., Barrett, A.J., Ahn, K.W., Chen, M., Green, J.S., Saad, A., Antin, J.H., Savani, B.N., et al. (2016). Early cytomegalovirus reactivation remains associated with increased transplant-related mortality in the current era: a CIBMTR analysis. Blood *127*, 2427-2438. 10.1182/blood-2015-11-679639.
57. Broers, A.E., van Der Holt, R., van Esser, J.W., Gratama, J.W., Henzen-Logmans, S., Kuenen-Boumeester, V., Lowenberg, B., and Cornelissen, J.J. (2000). Increased transplant-related morbidity and mortality in CMV-seropositive patients despite highly effective prevention of CMV disease after allogeneic T-cell-depleted stem cell transplantation. Blood *95*, 2240-2245.
58. Skipper, C.P., Hullsiek, K.H., Cresswell, F.V., Tadeo, K.K., Okirwoth, M., Blackstad, M., Hernandez-Alvarado, N., Fernandez-Alarcon, C., Walukaga, S., Martyn, E., et al. (2022). Cytomegalovirus viremia as a risk factor for mortality in HIV-associated cryptococcal and tuberculous meningitis. Int J Infect Dis *122*, 785-792. 10.1016/j.ijid.2022.07.035.
59. Deayton, J.R., Prof Sabin, C.A., Johnson, M.A., Emery, V.C., Wilson, P., and Griffiths, P.D. (2004). Importance of cytomegalovirus viraemia in risk of disease progression and death in HIV-infected patients receiving highly active antiretroviral therapy. Lancet *363*, 2116-2121. 10.1016/S0140-6736(04)16500-8.
60. Manicklal, S., Emery, V.C., Lazzarotto, T., Boppana, S.B., and Gupta, R.K. (2013). The "silent" global burden of congenital cytomegalovirus. Clin Microbiol Rev *26*, 86-102. 10.1128/CMR.00062-12.
61. Kenneson, A., and Cannon, M.J. (2007). Review and meta-analysis of the epidemiology of congenital cytomegalovirus (CMV) infection. Rev Med Virol *17*, 253-276. 10.1002/rmv.535.
62. Ssentongo, P., Hehnly, C., Birungi, P., Roach, M.A., Spady, J., Fronterre, C., Wang, M., Murray-Kolb, L.E., Al-Shaar, L., Chinchilli, V.M., et al. (2021). Congenital Cytomegalovirus Infection Burden and Epidemiologic Risk Factors in Countries With Universal Screening: A Systematic Review and Meta-analysis. JAMA Netw Open *4*, e2120736. 10.1001/jamanetworkopen.2021.20736.
63. Grosse, S.D., Ross, D.S., and Dollard, S.C. (2008). Congenital cytomegalovirus (CMV) infection as a cause of permanent bilateral hearing loss: a quantitative assessment. J Clin Virol *41*, 57-62. 10.1016/j.jcv.2007.09.004.
64. Bristow, B.N., O'Keefe, K.A., Shafir, S.C., and Sorvillo, F.J. (2011). Congenital cytomegalovirus mortality in the United States, 1990-2006. PLoS Negl Trop Dis *5*, e1140. 10.1371/journal.pntd.0001140.
65. Dollard, S.C., Grosse, S.D., and Ross, D.S. (2007). New estimates of the prevalence of neurological and sensory sequelae and mortality associated with congenital cytomegalovirus infection. Rev Med Virol *17*, 355-363. 10.1002/rmv.544.
66. Cannon, M.J., Griffiths, P.D., Aston, V., and Rawlinson, W.D. (2014). Universal newborn screening for congenital CMV infection: what is the evidence of potential benefit? Rev Med Virol *24*, 291-307. 10.1002/rmv.1790.
67. Das, R., Blazquez-Gamero, D., Bernstein, D.I., Gantt, S., Bautista, O., Beck, K., Conlon, A., Rosenbloom, D.I.S., Wang, D., Ritter, M., et al. (2023). Safety, efficacy, and immunogenicity of a replication-defective human cytomegalovirus vaccine, V160, in cytomegalovirus-seronegative women: a double-blind, randomised, placebo-controlled, phase 2b trial. Lancet Infect Dis *23*, 1383-1394. 10.1016/S1473-3099(23)00343-2.
68. Revello, M.G., Lazzarotto, T., Guerra, B., Spinillo, A., Ferrazzi, E., Kustermann, A., Guaschino, S., Vergani, P., Todros, T., Frusca, T., et al. (2014). A randomized trial of hyperimmune globulin

to prevent congenital cytomegalovirus. N Engl J Med *370*, 1316-1326. 10.1056/NEJMoa1310214.

69. Hughes, B.L., Clifton, R.G., Rouse, D.J., Saade, G.R., Dinsmoor, M.J., Reddy, U.M., Pass, R., Allard, D., Mallett, G., Fette, L.M., et al. (2021). A Trial of Hyperimmune Globulin to Prevent Congenital Cytomegalovirus Infection. N Engl J Med *385*, 436-444. 10.1056/NEJMoa1913569.
70. Wang, J., Loveland, A.N., Kattenhorn, L.M., Ploegh, H.L., and Gibson, W. (2006). High-molecular-weight protein (pUL48) of human cytomegalovirus is a competent deubiquitinating protease: mutant viruses altered in its active-site cysteine or histidine are viable. J Virol *80*, 6003-6012. 10.1128/JVI.00401-06.
71. Kalejta, R.F. (2008). Tegument proteins of human cytomegalovirus. Microbiol Mol Biol Rev *72*, 249-265, table of contents. 10.1128/MMBR.00040-07.
72. Saffert, R.T., and Kalejta, R.F. (2006). Inactivating a cellular intrinsic immune defense mediated by Daxx is the mechanism through which the human cytomegalovirus pp71 protein stimulates viral immediate-early gene expression. J Virol *80*, 3863-3871. 10.1128/JVI.80.8.3863-3871.2006.
73. Tomtishen, J.P., 3rd (2012). Human cytomegalovirus tegument proteins (pp65, pp71, pp150, pp28). Virol J *9*, 22. 10.1186/1743-422X-9-22.
74. Trgovcich, J., Cebulla, C., Zimmerman, P., and Sedmak, D.D. (2006). Human cytomegalovirus protein pp71 disrupts major histocompatibility complex class I cell surface expression. J Virol *80*, 951-963. 10.1128/JVI.80.2.951-963.2006.
75. Close, W.L., Anderson, A.N., and Pellett, P.E. (2018). Betaherpesvirus Virion Assembly and Egress. In Human Herpesviruses, Y. Kawaguchi, Y. Mori, and H. Kimura, eds. (Springer Singapore), pp. 167-207. 10.1007/978-981-10-7230-7_9.
76. Stern-Ginossar, N., Weisburd, B., Michalski, A., Le, V.T., Hein, M.Y., Huang, S.X., Ma, M., Shen, B., Qian, S.B., Hengel, H., et al. (2012). Decoding human cytomegalovirus. Science *338*, 1088-1093. 10.1126/science.1227919.
77. Dunn, W., Chou, C., Li, H., Hai, R., Patterson, D., Stolc, V., Zhu, H., and Liu, F. (2003). Functional profiling of a human cytomegalovirus genome. Proc Natl Acad Sci U S A *100*, 14223-14228. 10.1073/pnas.2334032100.
78. Hein, M.Y., and Weissman, J.S. (2022). Functional single-cell genomics of human cytomegalovirus infection. Nat Biotechnol *40*, 391-401. 10.1038/s41587-021-01059-3.
79. Jean Beltran, P.M., and Cristea, I.M. (2014). The life cycle and pathogenesis of human cytomegalovirus infection: lessons from proteomics. Expert Rev Proteomics *11*, 697-711. 10.1586/14789450.2014.971116.
80. Vanarsdall, A.L., and Johnson, D.C. (2012). Human cytomegalovirus entry into cells. Curr Opin Virol *2*, 37-42. 10.1016/j.coviro.2012.01.001.
81. Martinez-Martin, N., Marcandalli, J., Huang, C.S., Arthur, C.P., Perotti, M., Foglierini, M., Ho, H., Dosey, A.M., Shriver, S., Payandeh, J., et al. (2018). An Unbiased Screen for Human Cytomegalovirus Identifies Neuropilin-2 as a Central Viral Receptor. Cell *174*, 1158-1171 e1119. 10.1016/j.cell.2018.06.028.
82. Yunis, J., Farrell, H.E., Bruce, K., Lawler, C., Wyer, O., Davis-Poynter, N., Brizic, I., Jonjic, S., Adler, B., and Stevenson, P.G. (2019). Murine Cytomegalovirus Glycoprotein O Promotes Epithelial Cell Infection In Vivo. J Virol *93*. 10.1128/JVI.01378-18.
83. Stahl, F.R., Keyser, K.A., Heller, K., Bischoff, Y., Halle, S., Wagner, K., Messerle, M., and Forster, R. (2015). Mck2-dependent infection of alveolar macrophages promotes replication of MCMV in nodular inflammatory foci of the neonatal lung. Mucosal Immunol *8*, 57-67. 10.1038/mi.2014.42.
84. Wagner, F.M., Brizic, I., Prager, A., Trsan, T., Arapovic, M., Lemmermann, N.A., Podlech, J., Reddehase, M.J., Lemnitzer, F., Bosse, J.B., et al. (2013). The viral chemokine MCK-2 of murine cytomegalovirus promotes infection as part of a gH/gL/MCK-2 complex. PLoS Pathog *9*, e1003493. 10.1371/journal.ppat.1003493.

85. Bosnjak, B., Henze, E., Lueder, Y., Do, K.T.H., Rezalotfi, A., Cuvalo, B., Ritter, C., Schimrock, A., Willenzon, S., Georgiev, H., et al. (2023). MCK2-mediated MCMV infection of macrophages and virus dissemination to the salivary gland depends on MHC class I molecules. Cell Rep *42*, 112597. 10.1016/j.celrep.2023.112597.
86. Lane, R.K., Guo, H., Fisher, A.D., Diep, J., Lai, Z., Chen, Y., Upton, J.W., Carette, J., Mocarski, E.S., and Kaiser, W.J. (2020). Necroptosis-based CRISPR knockout screen reveals Neuropilin-1 as a critical host factor for early stages of murine cytomegalovirus infection. Proc Natl Acad Sci U S A *117*, 20109-20116. 10.1073/pnas.1921315117.
87. Li, J., Wellnitz, S., Chi, X.S., Yue, Y., Schmidt, K.A., Nguyen, N., Chen, W., Yurgelonis, I., Rojas, E., Liu, Y., et al. (2022). Horizontal Transmission of Cytomegalovirus in a Rhesus Model Despite High-Level, Vaccine-Elicited Neutralizing Antibody and T-Cell Responses. J Infect Dis *226*, 585-594. 10.1093/infdis/jiac129.
88. Brizic, I., Lisnic, B., Krstanovic, F., Brune, W., Hengel, H., and Jonjic, S. (2022). Mouse Models for Cytomegalovirus Infections in Newborns and Adults. Curr Protoc *2*, e537. 10.1002/cpz1.537.
89. Choi, K.Y., El-Hamdi, N.S., and McGregor, A. (2021). A trimeric capable gB CMV vaccine provides limited protection against a highly cell associated and epithelial tropic strain of cytomegalovirus in guinea pigs. J Gen Virol *102*. 10.1099/jgv.0.001579.
90. Farrell, H.E., Bruce, K., Lawler, C., and Stevenson, P.G. (2019). Murine Cytomegalovirus Spread Depends on the Infected Myeloid Cell Type. J Virol *93*. 10.1128/JVI.00540-19.
91. Forte, E., Zhang, Z., Thorp, E.B., and Hummel, M. (2020). Cytomegalovirus Latency and Reactivation: An Intricate Interplay With the Host Immune Response. Front Cell Infect Microbiol *10*, 130. 10.3389/fcimb.2020.00130.
92. Kavanagh, D.G., Gold, M.C., Wagner, M., Koszinowski, U.H., and Hill, A.B. (2001). The multiple immune-evasion genes of murine cytomegalovirus are not redundant: m4 and m152 inhibit antigen presentation in a complementary and cooperative fashion. J Exp Med *194*, 967-978. 10.1084/jem.194.7.967.
93. Saederup, N., Aguirre, S.A., Sparer, T.E., Bouley, D.M., and Mocarski, E.S. (2001). Murine cytomegalovirus CC chemokine homolog MCK-2 (m131-129) is a determinant of dissemination that increases inflammation at initial sites of infection. J Virol *75*, 9966-9976. 10.1128/JVI.75.20.9966-9976.2001.
94. Oduro, J.D., Redeker, A., Lemmermann, N.A.W., Ebermann, L., Marandu, T.F., Dekhtiarenko, I., Holzki, J.K., Busch, D.H., Arens, R., and Cicin-Sain, L. (2016). Murine cytomegalovirus (CMV) infection via the intranasal route offers a robust model of immunity upon mucosal CMV infection. J Gen Virol *97*, 185-195. 10.1099/jgv.0.000339.
95. Stahl, F.R., Heller, K., Halle, S., Keyser, K.A., Busche, A., Marquardt, A., Wagner, K., Boelter, J., Bischoff, Y., Kremmer, E., et al. (2013). Nodular inflammatory foci are sites of T cell priming and control of murine cytomegalovirus infection in the neonatal lung. PLoS Pathog *9*, e1003828. 10.1371/journal.ppat.1003828.
96. Wu, C.A., Paveglio, S.A., Lingenheld, E.G., Zhu, L., Lefrancois, L., and Puddington, L. (2011). Transmission of murine cytomegalovirus in breast milk: a model of natural infection in neonates. J Virol *85*, 5115-5124. 10.1128/JVI.01934-10.
97. Farrell, H.E., Bruce, K., Lawler, C., Oliveira, M., Cardin, R., Davis-Poynter, N., and Stevenson, P.G. (2017). Murine Cytomegalovirus Spreads by Dendritic Cell Recirculation. mBio *8*. 10.1128/mBio.01264-17.
98. Medearis, D.N., Jr. (1964). Mouse Cytomegalovirus Infection. 3. Attempts to Produce Intrauterine Infections. Am J Hyg *80*, 113-120.
99. Johnson, K.P. (1969). Mouse cytomegalovirus: placental infection. J Infect Dis *120*, 445-450. 10.1093/infdis/120.4.445.
100. Woolf, N.K., Jaquish, D.V., and Koehrn, F.J. (2007). Transplacental murine cytomegalovirus infection in the brain of SCID mice. Virol J *4*, 26. 10.1186/1743-422X-4-26.

101. Li, R.Y., and Tsutsui, Y. (2000). Growth retardation and microcephaly induced in mice by placental infection with murine cytomegalovirus. Teratology *62*, 79-85. 10.1002/1096-9926(200008)62:2<79::AID-TERA3>3.0.CO;2-S.
102. Chen, J., Feng, Y., Chen, L., Xiao, J., Liu, T., Yin, Z., and Chen, S. (2011). Long-term impact of intrauterine MCMV infection on development of offspring nervous system. J Huazhong Univ Sci Technolog Med Sci *31*, 371. 10.1007/s11596-011-0383-6.
103. Schleiss, M.R., Bourne, N., Stroup, G., Bravo, F.J., Jensen, N.J., and Bernstein, D.I. (2004). Protection against congenital cytomegalovirus infection and disease in guinea pigs, conferred by a purified recombinant glycoprotein B vaccine. J Infect Dis *189*, 1374-1381. 10.1086/382751.
104. Choi, K.Y., and McGregor, A. (2021). A Fully Protective Congenital CMV Vaccine Requires Neutralizing Antibodies to Viral Pentamer and gB Glycoprotein Complexes but a pp65 T-Cell Response Is Not Necessary. Viruses *13*. 10.3390/v13081467.
105. Dyson, R.M., Palliser, H.K., Kelleher, M.A., Hirst, J.J., and Wright, I.M. (2012). The guinea pig as an animal model for studying perinatal changes in microvascular function. Pediatr Res *71*, 20-24. 10.1038/pr.2011.9.
106. Rocca, M.S., and Wehner, N.G. (2009). The guinea pig as an animal model for developmental and reproductive toxicology studies. Birth Defects Res B Dev Reprod Toxicol *86*, 92-97. 10.1002/bdrb.20188.
107. Moulden, J., Sung, C.Y.W., Brizic, I., Jonjic, S., and Britt, W. (2021). Murine Models of Central Nervous System Disease following Congenital Human Cytomegalovirus Infections. Pathogens *10*. 10.3390/pathogens10081062.
108. Schwabenland, M., Mossad, O., Sievert, A., Peres, A.G., Ringel, E., Baasch, S., Kolter, J., Cascone, G., Dokalis, N., Vlachos, A., et al. (2023). Neonatal immune challenge poses a sex-specific risk for epigenetic microglial reprogramming and behavioral impairment. Nat Commun *14*, 2721. 10.1038/s41467-023-38373-0.
109. Hoji, A., Popescu, I.D., Pipeling, M.R., Shah, P.D., Winters, S.A., and McDyer, J.F. (2019). Early KLRG1(+) but Not CD57(+)CD8(+) T Cells in Primary Cytomegalovirus Infection Predict Effector Function and Viral Control. J Immunol *203*, 2063-2075. 10.4049/jimmunol.1900399.
110. Ferreira, V.H., Kumar, D., and Humar, A. (2019). Deep Profiling of the CD8+ T-cell Compartment Identifies Activated Cell Subsets and Multifunctional Responses Associated With Control of Cytomegalovirus Viremia. Transplantation *103*, 613-621. 10.1097/TP.0000000000002373.
111. Jackson, S.E., Mason, G.M., Okecha, G., Sissons, J.G., and Wills, M.R. (2014). Diverse specificities, phenotypes, and antiviral activities of cytomegalovirus-specific CD8+ T cells. J Virol *88*, 10894-10908. 10.1128/JVI.01477-14.
112. Sylwester, A.W., Mitchell, B.L., Edgar, J.B., Taormina, C., Pelte, C., Ruchti, F., Sleath, P.R., Grabstein, K.H., Hosken, N.A., Kern, F., et al. (2005). Broadly targeted human cytomegalovirus-specific CD4+ and CD8+ T cells dominate the memory compartments of exposed subjects. J Exp Med *202*, 673-685. 10.1084/jem.20050882.
113. Lubke, M., Spalt, S., Kowalewski, D.J., Zimmermann, C., Bauersfeld, L., Nelde, A., Bichmann, L., Marcu, A., Peper, J.K., Kohlbacher, O., et al. (2020). Identification of HCMV-derived T cell epitopes in seropositive individuals through viral deletion models. J Exp Med *217*. 10.1084/jem.20191164.
114. Klenerman, P., and Oxenius, A. (2016). T cell responses to cytomegalovirus. Nat Rev Immunol *16*, 367-377. 10.1038/nri.2016.38.
115. Jackson, S.E., Sedikides, G.X., Mason, G.M., Okecha, G., and Wills, M.R. (2017). Human Cytomegalovirus (HCMV)-Specific CD4(+) T Cells Are Polyfunctional and Can Respond to HCMV-Infected Dendritic Cells In Vitro. J Virol *91*. 10.1128/JVI.02128-16.
116. Chiu, Y.L., Lin, C.H., Sung, B.Y., Chuang, Y.F., Schneck, J.P., Kern, F., Pawelec, G., and Wang, G.C. (2016). Cytotoxic polyfunctionality maturation of cytomegalovirus-pp65-specific CD4 + and CD8 + T-cell responses in older adults positively correlates with response size. Sci Rep *6*, 19227. 10.1038/srep19227.

117. Costa-Garcia, M., Ataya, M., Moraru, M., Vilches, C., Lopez-Botet, M., and Muntasell, A. (2019). Human Cytomegalovirus Antigen Presentation by HLA-DR+ NKG2C+ Adaptive NK Cells Specifically Activates Polyfunctional Effector Memory CD4+ T Lymphocytes. Front Immunol *10*, 687. 10.3389/fimmu.2019.00687.
118. Casazza, J.P., Betts, M.R., Price, D.A., Precopio, M.L., Ruff, L.E., Brenchley, J.M., Hill, B.J., Roederer, M., Douek, D.C., and Koup, R.A. (2006). Acquisition of direct antiviral effector functions by CMV-specific CD4+ T lymphocytes with cellular maturation. J Exp Med *203*, 2865-2877. 10.1084/jem.20052246.
119. Lauruschkat, C.D., Muchsin, I., Rein, A., Erhard, F., Grathwohl, D., Dolken, L., Kochel, C., Falk, C.S., Einsele, H., Wurster, S., et al. (2023). CD4+ T cells are the major predictor of HCMV control in allogeneic stem cell transplant recipients on letermovir prophylaxis. Front Immunol *14*, 1148841. 10.3389/fimmu.2023.1148841.
120. Zhang, W., Morris, A.B., Peek, E.V., Karadkhele, G., Robertson, J.M., Kissick, H.T., and Larsen, C.P. (2021). CMV Status Drives Distinct Trajectories of CD4+ T Cell Differentiation. Front Immunol *12*, 620386. 10.3389/fimmu.2021.620386.
121. van Leeuwen, E.M., Remmerswaal, E.B., Heemskerk, M.H., ten Berge, I.J., and van Lier, R.A. (2006). Strong selection of virus-specific cytotoxic CD4+ T-cell clones during primary human cytomegalovirus infection. Blood *108*, 3121-3127. 10.1182/blood-2006-03-006809.
122. Walton, S.M., Wyrsch, P., Munks, M.W., Zimmermann, A., Hengel, H., Hill, A.B., and Oxenius, A. (2008). The dynamics of mouse cytomegalovirus-specific CD4 T cell responses during acute and latent infection. J Immunol *181*, 1128-1134. 10.4049/jimmunol.181.2.1128.
123. Walton, S.M., Mandaric, S., Torti, N., Zimmermann, A., Hengel, H., and Oxenius, A. (2011). Absence of cross-presenting cells in the salivary gland and viral immune evasion confine cytomegalovirus immune control to effector CD4 T cells. PLoS Pathog *7*, e1002214. 10.1371/journal.ppat.1002214.
124. Lachmann, R., Bajwa, M., Vita, S., Smith, H., Cheek, E., Akbar, A., and Kern, F. (2012). Polyfunctional T cells accumulate in large human cytomegalovirus-specific T cell responses. J Virol *86*, 1001-1009. 10.1128/JVI.00873-11.
125. Cicin-Sain, L. (2019). Cytomegalovirus memory inflation and immune protection. Med Microbiol Immunol *208*, 339-347. 10.1007/s00430-019-00607-8.
126. Sims, S., Bolinger, B., and Klenerman, P. (2015). Increasing inflationary T-cell responses following transient depletion of MCMV-specific memory T cells. Eur J Immunol *45*, 113-118. 10.1002/eji.201445016.
127. Zheng, X., Oduro, J.D., Boehme, J.D., Borkner, L., Ebensen, T., Heise, U., Gereke, M., Pils, M.C., Krmpotic, A., Guzman, C.A., et al. (2019). Mucosal CD8+ T cell responses induced by an MCMV based vaccine vector confer protection against influenza challenge. PLoS Pathog *15*, e1008036. 10.1371/journal.ppat.1008036.
128. Podlech, J., Holtappels, R., Wirtz, N., Steffens, H.P., and Reddehase, M.J. (1998). Reconstitution of CD8 T cells is essential for the prevention of multiple-organ cytomegalovirus histopathology after bone marrow transplantation. J Gen Virol *79 (Pt 9)*, 2099-2104. 10.1099/0022-1317-79-9-2099.
129. Bantug, G.R., Cekinovic, D., Bradford, R., Koontz, T., Jonjic, S., and Britt, W.J. (2008). CD8+ T lymphocytes control murine cytomegalovirus replication in the central nervous system of newborn animals. J Immunol *181*, 2111-2123. 10.4049/jimmunol.181.3.2111.
130. Reddehase, M.J., Mutter, W., Munch, K., Buhring, H.J., and Koszinowski, U.H. (1987). CD8-positive T lymphocytes specific for murine cytomegalovirus immediate-early antigens mediate protective immunity. J Virol *61*, 3102-3108. 10.1128/JVI.61.10.3102-3108.1987.
131. Palav, H.C., Bhonde, G., Padwal, V., Velhal, S., Pereira, J., Singh, A.K., Ghosh, S., Karandikar, K., Satoskar, P., Bhor, V., and Patel, V. (2023). Integrated immune monitoring of HCMV infection in pregnant women with complications and its association with adverse pregnancy outcomes. Microb Pathog *179*, 106109. 10.1016/j.micpath.2023.106109.

132. Tabata, T., Petitt, M., Fang-Hoover, J., and Pereira, L. (2019). Survey of cellular immune responses to human cytomegalovirus infection in the microenvironment of the uterine-placental interface. Med Microbiol Immunol *208*, 475-485. 10.1007/s00430-019-00613-w.
133. Pedron, B., Guerin, V., Jacquemard, F., Munier, A., Daffos, F., Thulliez, P., Aujard, Y., Luton, D., and Sterkers, G. (2007). Comparison of CD8+ T Cell responses to cytomegalovirus between human fetuses and their transmitter mothers. J Infect Dis *196*, 1033-1043. 10.1086/521196.
134. Lilleri, D., Fornara, C., Revello, M.G., and Gerna, G. (2008). Human cytomegalovirus-specific memory CD8+ and CD4+ T cell differentiation after primary infection. J Infect Dis *198*, 536-543. 10.1086/590118.
135. Marchant, A., Appay, V., Van Der Sande, M., Dulphy, N., Liesnard, C., Kidd, M., Kaye, S., Ojuola, O., Gillespie, G.M., Vargas Cuero, A.L., et al. (2003). Mature CD8(+) T lymphocyte response to viral infection during fetal life. J Clin Invest *111*, 1747-1755. 10.1172/JCI17470.
136. Capretti, M.G., Marsico, C., Chiereghin, A., Gabrielli, L., Aceti, A., and Lazzarotto, T. (2021). Immune Monitoring Using QuantiFERON(R)-CMV Assay in Congenital Cytomegalovirus Infection: Correlation With Clinical Presentation and CMV DNA Load. Clin Infect Dis *73*, 367-373. 10.1093/cid/ciaa704.
137. Venturi, V., Nzingha, K., Amos, T.G., Charles, W.C., Dekhtiarenko, I., Cicin-Sain, L., Davenport, M.P., and Rudd, B.D. (2016). The Neonatal CD8+ T Cell Repertoire Rapidly Diversifies during Persistent Viral Infection. J Immunol *196*, 1604-1616. 10.4049/jimmunol.1501867.
138. Lueder, Y., Heller, K., Ritter, C., Keyser, K.A., Wagner, K., Liu, X., Messerle, M., Stahl, F.R., Halle, S., and Forster, R. (2018). Control of primary mouse cytomegalovirus infection in lung nodular inflammatory foci by cooperation of interferon-gamma expressing CD4 and CD8 T cells. PLoS Pathog *14*, e1007252. 10.1371/journal.ppat.1007252.
139. Kucharski, A.J., Klepac, P., Conlan, A.J.K., Kissler, S.M., Tang, M.L., Fry, H., Gog, J.R., Edmunds, W.J., and group, C.C.-w. (2020). Effectiveness of isolation, testing, contact tracing, and physical distancing on reducing transmission of SARS-CoV-2 in different settings: a mathematical modelling study. Lancet Infect Dis *20*, 1151-1160. 10.1016/S1473-3099(20)30457-6.
140. Contreras, S., Dehning, J., Loidolt, M., Zierenberg, J., Spitzner, F.P., Urrea-Quintero, J.H., Mohr, S.B., Wilczek, M., Wibral, M., and Priesemann, V. (2021). The challenges of containing SARS-CoV-2 via test-trace-and-isolate. Nat Commun *12*, 378. 10.1038/s41467-020-20699-8.
141. Girum, T., Lentiro, K., Geremew, M., Migora, B., and Shewamare, S. (2020). Global strategies and effectiveness for COVID-19 prevention through contact tracing, screening, quarantine, and isolation: a systematic review. Trop Med Health *48*, 91. 10.1186/s41182-020-00285-w.
142. World Health Organization (2024). WHO COVID-19 dashboard.
143. Gandhi, R.T., Lynch, J.B., and Del Rio, C. (2020). Mild or Moderate Covid-19. N Engl J Med *383*, 1757-1766. 10.1056/NEJMcp2009249.
144. Berlin, D.A., Gulick, R.M., and Martinez, F.J. (2020). Severe Covid-19. N Engl J Med *383*, 2451-2460. 10.1056/NEJMcp2009575.
145. Huang, C., Wang, Y., Li, X., Ren, L., Zhao, J., Hu, Y., Zhang, L., Fan, G., Xu, J., Gu, X., et al. (2020). Clinical features of patients infected with 2019 novel coronavirus in Wuhan, China. Lancet *395*, 497-506. 10.1016/S0140-6736(20)30183-5.
146. Taylor, C.A., Patel, K., Patton, M.E., Reingold, A., Kawasaki, B., Meek, J., Openo, K., Ryan, P.A., Falkowski, A., Bye, E., et al. (2023). COVID-19-Associated Hospitalizations Among U.S. Adults Aged >/=65 Years - COVID-NET, 13 States, January-August 2023. MMWR Morb Mortal Wkly Rep *72*, 1089-1094. 10.15585/mmwr.mm7240a3.
147. Davis, H.E., McCorkell, L., Vogel, J.M., and Topol, E.J. (2023). Author Correction: Long COVID: major findings, mechanisms and recommendations. Nat Rev Microbiol *21*, 408. 10.1038/s41579-023-00896-0.
148. Jackson, C.B., Farzan, M., Chen, B., and Choe, H. (2022). Mechanisms of SARS-CoV-2 entry into cells. Nat Rev Mol Cell Biol *23*, 3-20. 10.1038/s41580-021-00418-x.
149. Zamorano Cuervo, N., and Grandvaux, N. (2020). ACE2: Evidence of role as entry receptor for SARS-CoV-2 and implications in comorbidities. Elife *9*. 10.7554/eLife.61390.

150. V'Kovski, P., Kratzel, A., Steiner, S., Stalder, H., and Thiel, V. (2021). Coronavirus biology and replication: implications for SARS-CoV-2. Nat Rev Microbiol *19*, 155-170. 10.1038/s41579-020-00468-6.
151. Jamison, D.A., Jr., Anand Narayanan, S., Trovao, N.S., Guarnieri, J.W., Topper, M.J., Moraes-Vieira, P.M., Zaksas, V., Singh, K.K., Wurtele, E.S., and Beheshti, A. (2022). A comprehensive SARS-CoV-2 and COVID-19 review, Part 1: Intracellular overdrive for SARS-CoV-2 infection. Eur J Hum Genet *30*, 889-898. 10.1038/s41431-022-01108-8.
152. Chu, V.T., Schwartz, N.G., Donnelly, M.A.P., Chuey, M.R., Soto, R., Yousaf, A.R., Schmitt-Matzen, E.N., Sleweon, S., Ruffin, J., Thornburg, N., et al. (2022). Comparison of Home Antigen Testing With RT-PCR and Viral Culture During the Course of SARS-CoV-2 Infection. JAMA Intern Med *182*, 701-709. 10.1001/jamainternmed.2022.1827.
153. Binny, R.N., Priest, P., French, N.P., Parry, M., Lustig, A., Hendy, S.C., Maclaren, O.J., Ridings, K.M., Steyn, N., Vattiato, G., and Plank, M.J. (2022). Sensitivity of Reverse Transcription Polymerase Chain Reaction Tests for Severe Acute Respiratory Syndrome Coronavirus 2 Through Time. J Infect Dis *227*, 9-17. 10.1093/infdis/jiac317.
154. Israelow, B., Mao, T., Klein, J., Song, E., Menasche, B., Omer, S.B., and Iwasaki, A. (2021). Adaptive immune determinants of viral clearance and protection in mouse models of SARS-CoV-2. Sci Immunol *6*, eabl4509. 10.1126/sciimmunol.abl4509.
155. Amanat, F., Stadlbauer, D., Strohmeier, S., Nguyen, T.H.O., Chromikova, V., McMahon, M., Jiang, K., Arunkumar, G.A., Jurczyszak, D., Polanco, J., et al. (2020). A serological assay to detect SARS-CoV-2 seroconversion in humans. Nat Med *26*, 1033-1036. 10.1038/s41591-020-0913-5.
156. Scheiblauer, H., Nubling, C.M., Wolf, T., Khodamoradi, Y., Bellinghausen, C., Sonntagbauer, M., Esser-Nobis, K., Filomena, A., Mahler, V., Maier, T.J., and Stephan, C. (2022). Antibody response to SARS-CoV-2 for more than one year - kinetics and persistence of detection are predominantly determined by avidity progression and test design. J Clin Virol *146*, 105052. 10.1016/j.jcv.2021.105052.
157. Long, Q.X., Liu, B.Z., Deng, H.J., Wu, G.C., Deng, K., Chen, Y.K., Liao, P., Qiu, J.F., Lin, Y., Cai, X.F., et al. (2020). Antibody responses to SARS-CoV-2 in patients with COVID-19. Nat Med *26*, 845-848. 10.1038/s41591-020-0897-1.
158. Regev-Yochay, G., Lustig, Y., Joseph, G., Gilboa, M., Barda, N., Gens, I., Indenbaum, V., Halpern, O., Katz-Likvornik, S., Levin, T., et al. (2023). Correlates of protection against COVID-19 infection and intensity of symptomatic disease in vaccinated individuals exposed to SARS-CoV-2 in households in Israel (ICoFS): a prospective cohort study. Lancet Microbe *4*, e309-e318. 10.1016/S2666-5247(23)00012-5.
159. Shrotri, M., Fragaszy, E., Nguyen, V., Navaratnam, A.M.D., Geismar, C., Beale, S., Kovar, J., Byrne, T.E., Fong, W.L.E., Patel, P., et al. (2022). Spike-antibody responses to COVID-19 vaccination by demographic and clinical factors in a prospective community cohort study. Nat Commun *13*, 5780. 10.1038/s41467-022-33550-z.
160. Evans, J.P., Zeng, C., Carlin, C., Lozanski, G., Saif, L.J., Oltz, E.M., Gumina, R.J., and Liu, S.L. (2022). Neutralizing antibody responses elicited by SARS-CoV-2 mRNA vaccination wane over time and are boosted by breakthrough infection. Sci Transl Med *14*, eabn8057. 10.1126/scitranslmed.abn8057.
161. Patel, R., Kaki, M., Potluri, V.S., Kahar, P., and Khanna, D. (2022). A comprehensive review of SARS-CoV-2 vaccines: Pfizer, Moderna & Johnson & Johnson. Hum Vaccin Immunother *18*, 2002083. 10.1080/21645515.2021.2002083.
162. Vergidis, P., Levy, E.R., Ristagno, E.H., Iyer, V.N., O'Horo, J.C., and Joshi, A.Y. (2022). COVID-19 in patients with B cell immune deficiency. J Immunol Methods *510*, 113351. 10.1016/j.jim.2022.113351.
163. Apostolidis, S.A., Kakara, M., Painter, M.M., Goel, R.R., Mathew, D., Lenzi, K., Rezk, A., Patterson, K.R., Espinoza, D.A., Kadri, J.C., et al. (2021). Cellular and humoral immune responses following SARS-CoV-2 mRNA vaccination in patients with multiple sclerosis on anti-CD20 therapy. Nat Med *27*, 1990-2001. 10.1038/s41591-021-01507-2.

164. Choi, B., Choudhary, M.C., Regan, J., Sparks, J.A., Padera, R.F., Qiu, X., Solomon, I.H., Kuo, H.H., Boucau, J., Bowman, K., et al. (2020). Persistence and Evolution of SARS-CoV-2 in an Immunocompromised Host. N Engl J Med *383*, 2291-2293. 10.1056/NEJMc2031364.
165. Bacher, P., Rosati, E., Esser, D., Martini, G.R., Saggau, C., Schiminsky, E., Dargvainiene, J., Schroder, I., Wieters, I., Khodamoradi, Y., et al. (2020). Low-Avidity CD4(+) T Cell Responses to SARS-CoV-2 in Unexposed Individuals and Humans with Severe COVID-19. Immunity *53*, 1258-1271 e1255. 10.1016/j.immuni.2020.11.016.
166. Grifoni, A., Weiskopf, D., Ramirez, S.I., Mateus, J., Dan, J.M., Moderbacher, C.R., Rawlings, S.A., Sutherland, A., Premkumar, L., Jadi, R.S., et al. (2020). Targets of T Cell Responses to SARS-CoV-2 Coronavirus in Humans with COVID-19 Disease and Unexposed Individuals. Cell *181*, 1489-1501 e1415. 10.1016/j.cell.2020.05.015.
167. Braun, J., Loyal, L., Frentsch, M., Wendisch, D., Georg, P., Kurth, F., Hippenstiel, S., Dingeldey, M., Kruse, B., Fauchere, F., et al. (2020). SARS-CoV-2-reactive T cells in healthy donors and patients with COVID-19. Nature *587*, 270-274. 10.1038/s41586-020-2598-9.
168. Rydyznski Moderbacher, C., Ramirez, S.I., Dan, J.M., Grifoni, A., Hastie, K.M., Weiskopf, D., Belanger, S., Abbott, R.K., Kim, C., Choi, J., et al. (2020). Antigen-Specific Adaptive Immunity to SARS-CoV-2 in Acute COVID-19 and Associations with Age and Disease Severity. Cell *183*, 996-1012 e1019. 10.1016/j.cell.2020.09.038.
169. Sette, A., and Crotty, S. (2021). Adaptive immunity to SARS-CoV-2 and COVID-19. Cell *184*, 861-880. 10.1016/j.cell.2021.01.007.
170. Meckiff, B.J., Ramirez-Suastegui, C., Fajardo, V., Chee, S.J., Kusnadi, A., Simon, H., Eschweiler, S., Grifoni, A., Pelosi, E., Weiskopf, D., et al. (2020). Imbalance of Regulatory and Cytotoxic SARS-CoV-2-Reactive CD4(+) T Cells in COVID-19. Cell *183*, 1340-1353 e1316. 10.1016/j.cell.2020.10.001.
171. Wagner, K.I., Mateyka, L.M., Jarosch, S., Grass, V., Weber, S., Schober, K., Hammel, M., Burrell, T., Kalali, B., Poppert, H., et al. (2022). Recruitment of highly cytotoxic CD8(+) T cell receptors in mild SARS-CoV-2 infection. Cell Rep *38*, 110214. 10.1016/j.celrep.2021.110214.
172. Bange, E.M., Han, N.A., Wileyto, P., Kim, J.Y., Gouma, S., Robinson, J., Greenplate, A.R., Hwee, M.A., Porterfield, F., Owoyemi, O., et al. (2021). CD8(+) T cells contribute to survival in patients with COVID-19 and hematologic cancer. Nat Med *27*, 1280-1289. 10.1038/s41591-021-01386-7.
173. Painter, M.M., Johnston, T.S., Lundgreen, K.A., Santos, J.J.S., Qin, J.S., Goel, R.R., Apostolidis, S.A., Mathew, D., Fulmer, B., Williams, J.C., et al. (2023). Prior vaccination promotes early activation of memory T cells and enhances immune responses during SARS-CoV-2 breakthrough infection. Nat Immunol *24*, 1711-1724. 10.1038/s41590-023-01613-y.
174. Sotgiu, G., Saderi, L., Petruccioli, E., Aliberti, S., Piana, A., Petrone, L., and Goletti, D. (2019). QuantiFERON TB Gold Plus for the diagnosis of tuberculosis: a systematic review and meta-analysis. J Infect *79*, 444-453. 10.1016/j.jinf.2019.08.018.
175. Reusing, J.O., Jr., Agena, F., Kotton, C.N., Campana, G., Pierrotti, L.C., and David-Neto, E. (2023). QuantiFERON-CMV as a Predictor of CMV Events During Preemptive Therapy in CMV-seropositive Kidney Transplant Recipients. Transplantation. 10.1097/TP.0000000000004870.
176. Valle-Arroyo, J., Aguado, R., Paez-Vega, A., Perez, A.B., Gonzalez, R., Fornes, G., Torre-Cisneros, J., and Cantisan, S. (2020). Lack of cytomegalovirus (CMV)-specific cell-mediated immune response using QuantiFERON-CMV assay in CMV-seropositive healthy volunteers: fact not artifact. Sci Rep *10*, 7194. 10.1038/s41598-020-64133-x.
177. Walker, S., Fazou, C., Crough, T., Holdsworth, R., Kiely, P., Veale, M., Bell, S., Gailbraith, A., McNeil, K., Jones, S., and Khanna, R. (2007). Ex vivo monitoring of human cytomegalovirus-specific CD8+ T-cell responses using QuantiFERON-CMV. Transpl Infect Dis *9*, 165-170. 10.1111/j.1399-3062.2006.00199.x.
178. Marsh, B., and Blelloch, R. (2020). Single nuclei RNA-seq of mouse placental labyrinth development. Elife *9*. 10.7554/eLife.60266.

179. McInnes, L., Healy, J., and Melville, J. (2018). UMAP: Uniform Manifold Approximation and Projection for Dimension Reduction. arXiv:1802.03426. 10.48550/arXiv.1802.03426.
180. Munks, M.W., Cho, K.S., Pinto, A.K., Sierro, S., Klenerman, P., and Hill, A.B. (2006). Four distinct patterns of memory CD8 T cell responses to chronic murine cytomegalovirus infection. J Immunol *177*, 450-458. 10.4049/jimmunol.177.1.450.
181. Arens, R., Wang, P., Sidney, J., Loewendorf, A., Sette, A., Schoenberger, S.P., Peters, B., and Benedict, C.A. (2008). Cutting edge: murine cytomegalovirus induces a polyfunctional CD4 T cell response. J Immunol *180*, 6472-6476. 10.4049/jimmunol.180.10.6472.
182. Fonseca Brito, L., Ostermann, E., Perez, A., Toedter, S., Virdi, S., Indenbirken, D., Glau, L., Gieras, A., Brixel, R., Arens, R., et al. (2024). Limited protection against early-life cytomegalovirus infection results from deficiency of cytotoxic CD8 T cells. bioRxiv, 2024.2007.2010.602923. 10.1101/2024.07.10.602923.
183. Blattman, J.N., Antia, R., Sourdive, D.J., Wang, X., Kaech, S.M., Murali-Krishna, K., Altman, J.D., and Ahmed, R. (2002). Estimating the precursor frequency of naive antigen-specific CD8 T cells. J Exp Med *195*, 657-664. 10.1084/jem.20001021.
184. Ciucci, T., Vacchio, M.S., Chen, T., Nie, J., Chopp, L.B., McGavern, D.B., Kelly, M.C., and Bosselut, R. (2022). Dependence on Bcl6 and Blimp1 drive distinct differentiation of murine memory and follicular helper CD4+ T cells. J Exp Med *219*. 10.1084/jem.20202343.
185. Andreatta, M., Tjitropranoto, A., Sherman, Z., Kelly, M.C., Ciucci, T., and Carmona, S.J. (2022). A CD4(+) T cell reference map delineates subtype-specific adaptation during acute and chronic viral infections. Elife *11*. 10.7554/eLife.76339.
186. Rouse, B.T., and Sehrawat, S. (2010). Immunity and immunopathology to viruses: what decides the outcome? Nat Rev Immunol *10*, 514-526. 10.1038/nri2802.
187. Sandu, I., Cerletti, D., Oetiker, N., Borsa, M., Wagen, F., Spadafora, I., Welten, S.P.M., Stolz, U., Oxenius, A., and Claassen, M. (2020). Landscape of Exhausted Virus-Specific CD8 T Cells in Chronic LCMV Infection. Cell Rep *32*, 108078. 10.1016/j.celrep.2020.108078.
188. Carmona, S.J., Siddiqui, I., Bilous, M., Held, W., and Gfeller, D. (2020). Deciphering the transcriptomic landscape of tumor-infiltrating CD8 lymphocytes in B16 melanoma tumors with single-cell RNA-Seq. Oncoimmunology *9*, 1737369. 10.1080/2162402X.2020.1737369.
189. Wiesel, M., and Oxenius, A. (2012). From crucial to negligible: functional CD8(+) T-cell responses and their dependence on CD4(+) T-cell help. Eur J Immunol *42*, 1080-1088. 10.1002/eji.201142205.
190. Bevan, M.J. (2004). Helping the CD8(+) T-cell response. Nat Rev Immunol *4*, 595-602. 10.1038/nri1413.
191. Si, Y., Wang, Y., Tian, Q., Wang, Q., Pollard, J.M., Srivastava, P.K., Esser-Kahn, A.P., Collier, J.H., Sperling, A.I., and Chong, A.S. (2023). Lung cDC1 and cDC2 dendritic cells priming naive CD8(+) T cells in situ prior to migration to draining lymph nodes. Cell Rep *42*, 113299. 10.1016/j.celrep.2023.113299.
192. Embgenbroich, M., and Burgdorf, S. (2018). Current Concepts of Antigen Cross-Presentation. Front Immunol *9*, 1643. 10.3389/fimmu.2018.01643.
193. Misharin, A.V., Morales-Nebreda, L., Mutlu, G.M., Budinger, G.R., and Perlman, H. (2013). Flow cytometric analysis of macrophages and dendritic cell subsets in the mouse lung. Am J Respir Cell Mol Biol *49*, 503-510. 10.1165/rcmb.2013-0086MA.
194. Enders, G., Daiminger, A., Bader, U., Exler, S., and Enders, M. (2011). Intrauterine transmission and clinical outcome of 248 pregnancies with primary cytomegalovirus infection in relation to gestational age. J Clin Virol *52*, 244-246. 10.1016/j.jcv.2011.07.005.
195. Wang, E.C., and Borysiewicz, L.K. (1995). The role of CD8+, CD57+ cells in human cytomegalovirus and other viral infections. Scand J Infect Dis Suppl *99*, 69-77.
196. Peng, Y., Felce, S.L., Dong, D., Penkava, F., Mentzer, A.J., Yao, X., Liu, G., Yin, Z., Chen, J.L., Lu, Y., et al. (2022). An immunodominant NP(105-113)-B*07:02 cytotoxic T cell response controls viral replication and is associated with less severe COVID-19 disease. Nat Immunol *23*, 50-61. 10.1038/s41590-021-01084-z.

197. Kundu, R., Narean, J.S., Wang, L., Fenn, J., Pillay, T., Fernandez, N.D., Conibear, E., Koycheva, A., Davies, M., Tolosa-Wright, M., et al. (2022). Cross-reactive memory T cells associate with protection against SARS-CoV-2 infection in COVID-19 contacts. Nat Commun *13*, 80. 10.1038/s41467-021-27674-x.
198. Jagodzinski, A., Johansen, C., Koch-Gromus, U., Aarabi, G., Adam, G., Anders, S., Augustin, M., der Kellen, R.B., Beikler, T., Behrendt, C.A., et al. (2020). Rationale and Design of the Hamburg City Health Study. Eur J Epidemiol *35*, 169-181. 10.1007/s10654-019-00577-4.
199. Petersen, E.L., Gossling, A., Adam, G., Aepfelbacher, M., Behrendt, C.A., Cavus, E., Cheng, B., Fischer, N., Gallinat, J., Kuhn, S., et al. (2022). Multi-organ assessment in mainly non-hospitalized individuals after SARS-CoV-2 infection: The Hamburg City Health Study COVID programme. Eur Heart J *43*, 1124-1137. 10.1093/eurheartj/ehab914.
200. Fonseca Brito, L., Todter, S., Kottlau, J., Cermann, K., Spier, A., Petersen, E., Schafer, I., Twerenbold, R., Aepfelbacher, M., Lutgehetmann, M., and Stahl, F.R. (2023). Performance of an interferon-gamma release assay-based test for cell-mediated immunity to SARS-CoV-2. Front Immunol *14*, 1069968. 10.3389/fimmu.2023.1069968.
201. Wu, F., Zhao, S., Yu, B., Chen, Y.M., Wang, W., Song, Z.G., Hu, Y., Tao, Z.W., Tian, J.H., Pei, Y.Y., et al. (2020). A new coronavirus associated with human respiratory disease in China. Nature *579*, 265-269. 10.1038/s41586-020-2008-3.
202. Vivanti, A.J., Vauloup-Fellous, C., Prevot, S., Zupan, V., Suffee, C., Do Cao, J., Benachi, A., and De Luca, D. (2020). Transplacental transmission of SARS-CoV-2 infection. Nat Commun *11*, 3572. 10.1038/s41467-020-17436-6.
203. Hecht, J.L., Quade, B., Deshpande, V., Mino-Kenudson, M., Ting, D.T., Desai, N., Dygulska, B., Heyman, T., Salafia, C., Shen, D., et al. (2020). SARS-CoV-2 can infect the placenta and is not associated with specific placental histopathology: a series of 19 placentas from COVID-19-positive mothers. Mod Pathol *33*, 2092-2103. 10.1038/s41379-020-0639-4.
204. Raschetti, R., Vivanti, A.J., Vauloup-Fellous, C., Loi, B., Benachi, A., and De Luca, D. (2020). Synthesis and systematic review of reported neonatal SARS-CoV-2 infections. Nat Commun *11*, 5164. 10.1038/s41467-020-18982-9.
205. Woodworth, K.R., Olsen, E.O., Neelam, V., Lewis, E.L., Galang, R.R., Oduyebo, T., Aveni, K., Yazdy, M.M., Harvey, E., Longcore, N.D., et al. (2020). Birth and Infant Outcomes Following Laboratory-Confirmed SARS-CoV-2 Infection in Pregnancy - SET-NET, 16 Jurisdictions, March 29-October 14, 2020. MMWR Morb Mortal Wkly Rep *69*, 1635-1640. 10.15585/mmwr.mm6944e2.
206. Zeng, H., Xu, C., Fan, J., Tang, Y., Deng, Q., Zhang, W., and Long, X. (2020). Antibodies in Infants Born to Mothers With COVID-19 Pneumonia. JAMA *323*, 1848-1849. 10.1001/jama.2020.4861.
207. Tallarek, A.C., Urbschat, C., Fonseca Brito, L., Stanelle-Bertram, S., Krasemann, S., Frascaroli, G., Thiele, K., Wieczorek, A., Felber, N., Lutgehetmann, M., et al. (2021). Inefficient Placental Virus Replication and Absence of Neonatal Cell-Specific Immunity Upon Sars-CoV-2 Infection During Pregnancy. Front Immunol *12*, 698578. 10.3389/fimmu.2021.698578.
208. Pass, R.F., and Anderson, B. (2014). Mother-to-Child Transmission of Cytomegalovirus and Prevention of Congenital Infection. J Pediatric Infect Dis Soc *3 Suppl 1*, S2-6. 10.1093/jpids/piu069.
209. DeSesso, J.M., Williams, A.L., Ahuja, A., Bowman, C.J., and Hurtt, M.E. (2012). The placenta, transfer of immunoglobulins, and safety assessment of biopharmaceuticals in pregnancy. Crit Rev Toxicol *42*, 185-210. 10.3109/10408444.2011.653487.
210. Raimondi, C., and Ruhrberg, C. (2013). Neuropilin signalling in vessels, neurons and tumours. Semin Cell Dev Biol *24*, 172-178. 10.1016/j.semcdb.2013.01.001.
211. Cantuti-Castelvetri, L., Ojha, R., Pedro, L.D., Djannatian, M., Franz, J., Kuivanen, S., van der Meer, F., Kallio, K., Kaya, T., Anastasina, M., et al. (2020). Neuropilin-1 facilitates SARS-CoV-2 cell entry and infectivity. Science *370*, 856-860. 10.1126/science.abd2985.

212. Daly, J.L., Simonetti, B., Klein, K., Chen, K.E., Williamson, M.K., Anton-Plagaro, C., Shoemark, D.K., Simon-Gracia, L., Bauer, M., Hollandi, R., et al. (2020). Neuropilin-1 is a host factor for SARS-CoV-2 infection. Science *370*, 861-865. 10.1126/science.abd3072.
213. Wang, H.B., Zhang, H., Zhang, J.P., Li, Y., Zhao, B., Feng, G.K., Du, Y., Xiong, D., Zhong, Q., Liu, W.L., et al. (2015). Neuropilin 1 is an entry factor that promotes EBV infection of nasopharyngeal epithelial cells. Nat Commun *6*, 6240. 10.1038/ncomms7240.
214. Ghez, D., Lepelletier, Y., Lambert, S., Fourneau, J.M., Blot, V., Janvier, S., Arnulf, B., van Endert, P.M., Heveker, N., Pique, C., and Hermine, O. (2006). Neuropilin-1 is involved in human T-cell lymphotropic virus type 1 entry. J Virol *80*, 6844-6854. 10.1128/JVI.02719-05.
215. Mimura, N., Nagamatsu, T., Morita, K., Taguchi, A., Toya, T., Kumasawa, K., Iriyama, T., Kawana, K., Inoue, N., Fujii, T., and Osuga, Y. (2022). Suppression of human trophoblast syncytialization by human cytomegalovirus infection. Placenta *117*, 200-208. 10.1016/j.placenta.2021.12.011.
216. Fisher, S., Genbacev, O., Maidji, E., and Pereira, L. (2000). Human cytomegalovirus infection of placental cytotrophoblasts in vitro and in utero: implications for transmission and pathogenesis. J Virol *74*, 6808-6820. 10.1128/jvi.74.15.6808-6820.2000.
217. Rollman, T.B., Berkebile, Z.W., Okae, H., Bardwell, V.J., Gearhart, M.D., and Bierle, C.J. (2024). Human trophoblast stem cells restrict human cytomegalovirus replication. J Virol, e0193523. 10.1128/jvi.01935-23.
218. Turner, S.J., La Gruta, N.L., Kedzierska, K., Thomas, P.G., and Doherty, P.C. (2009). Functional implications of T cell receptor diversity. Curr Opin Immunol *21*, 286-290. 10.1016/j.coi.2009.05.004.
219. Pass, R.F., Fowler, K.B., Boppana, S.B., Britt, W.J., and Stagno, S. (2006). Congenital cytomegalovirus infection following first trimester maternal infection: symptoms at birth and outcome. J Clin Virol *35*, 216-220. 10.1016/j.jcv.2005.09.015.
220. Stagno, S., Pass, R.F., Cloud, G., Britt, W.J., Henderson, R.E., Walton, P.D., Veren, D.A., Page, F., and Alford, C.A. (1986). Primary cytomegalovirus infection in pregnancy. Incidence, transmission to fetus, and clinical outcome. JAMA *256*, 1904-1908.
221. Ahlfors, K., Forsgren, M., Ivarsson, S.A., Harris, S., and Svanberg, L. (1983). Congenital cytomegalovirus infection: on the relation between type and time of maternal infection and infant's symptoms. Scand J Infect Dis *15*, 129-138. 10.3109/inf.1983.15.issue-2.01.
222. Lanzavecchia, A. (1985). Antigen-specific interaction between T and B cells. Nature *314*, 537-539. 10.1038/314537a0.
223. Sullivan, L.C., Nguyen, T.H.O., Harpur, C.M., Stankovic, S., Kanagarajah, A.R., Koutsakos, M., Saunders, P.M., Cai, Z., Gray, J.A., Widjaja, J.M.L., et al. (2021). Natural killer cell receptors regulate responses of HLA-E-restricted T cells. Sci Immunol *6*. 10.1126/sciimmunol.abe9057.
224. Klenovsek, K., Weisel, F., Schneider, A., Appelt, U., Jonjic, S., Messerle, M., Bradel-Tretheway, B., Winkler, T.H., and Mach, M. (2007). Protection from CMV infection in immunodeficient hosts by adoptive transfer of memory B cells. Blood *110*, 3472-3479. 10.1182/blood-2007-06-095414.
225. Nelson, C.S., Baraniak, I., Lilleri, D., Reeves, M.B., Griffiths, P.D., and Permar, S.R. (2020). Immune Correlates of Protection Against Human Cytomegalovirus Acquisition, Replication, and Disease. J Infect Dis *221*, S45-S59. 10.1093/infdis/jiz428.
226. Parker, D.C. (1993). T cell-dependent B cell activation. Annu Rev Immunol *11*, 331-360. 10.1146/annurev.iy.11.040193.001555.
227. Tregoning, J.S., Wang, B.L., McDonald, J.U., Yamaguchi, Y., Harker, J.A., Goritzka, M., Johansson, C., Bukreyev, A., Collins, P.L., and Openshaw, P.J. (2013). Neonatal antibody responses are attenuated by interferon-gamma produced by NK and T cells during RSV infection. Proc Natl Acad Sci U S A *110*, 5576-5581. 10.1073/pnas.1214247110.
228. Pertmer, T.M., and Robinson, H.L. (1999). Studies on antibody responses following neonatal immunization with influenza hemagglutinin DNA or protein. Virology *257*, 406-414. 10.1006/viro.1999.9666.

229. Rozmanic, C., Lisnic, B., Pribanic Matesic, M., Mihalic, A., Hirsl, L., Park, E., Lesac Brizic, A., Indenbirken, D., Viduka, I., Santic, M., et al. (2023). Perinatal murine cytomegalovirus infection reshapes the transcriptional profile and functionality of NK cells. Nat Commun *14*, 6412. 10.1038/s41467-023-42182-w.
230. Kubota, A., Kubota, S., Lohwasser, S., Mager, D.L., and Takei, F. (1999). Diversity of NK cell receptor repertoire in adult and neonatal mice. J Immunol *163*, 212-216.
231. Sun, J.C., Beilke, J.N., and Lanier, L.L. (2009). Adaptive immune features of natural killer cells. Nature *457*, 557-561. 10.1038/nature07665.
232. Lu, Y., Phillips, C.A., Bjorndahl, J.M., and Trevillyan, J.M. (1994). CD28 signal transduction: tyrosine phosphorylation and receptor association of phosphoinositide-3 kinase correlate with Ca(2+)-independent costimulatory activity. Eur J Immunol *24*, 2732-2739. 10.1002/eji.1830241124.
233. Siefken, R., Kurrle, R., and Schwinzer, R. (1997). CD28-mediated activation of resting human T cells without costimulation of the CD3/TCR complex. Cell Immunol *176*, 59-65. 10.1006/cimm.1996.1066.
234. Omilusik, K.D., Best, J.A., Yu, B., Goossens, S., Weidemann, A., Nguyen, J.V., Seuntjens, E., Stryjewska, A., Zweier, C., Roychoudhuri, R., et al. (2015). Transcriptional repressor ZEB2 promotes terminal differentiation of CD8+ effector and memory T cell populations during infection. J Exp Med *212*, 2027-2039. 10.1084/jem.20150194.
235. Best, J.A., Blair, D.A., Knell, J., Yang, E., Mayya, V., Doedens, A., Dustin, M.L., Goldrath, A.W., and Immunological Genome Project, C. (2013). Transcriptional insights into the CD8(+) T cell response to infection and memory T cell formation. Nat Immunol *14*, 404-412. 10.1038/ni.2536.
236. Dominguez, C.X., Amezquita, R.A., Guan, T., Marshall, H.D., Joshi, N.S., Kleinstein, S.H., and Kaech, S.M. (2015). The transcription factors ZEB2 and T-bet cooperate to program cytotoxic T cell terminal differentiation in response to LCMV viral infection. J Exp Med *212*, 2041-2056. 10.1084/jem.20150186.
237. Xin, A., Masson, F., Liao, Y., Preston, S., Guan, T., Gloury, R., Olshansky, M., Lin, J.X., Li, P., Speed, T.P., et al. (2016). A molecular threshold for effector CD8(+) T cell differentiation controlled by transcription factors Blimp-1 and T-bet. Nat Immunol *17*, 422-432. 10.1038/ni.3410.
238. Zwijnenburg, A.J., Pokharel, J., Varnaite, R., Zheng, W., Hoffer, E., Shryki, I., Comet, N.R., Ehrstrom, M., Gredmark-Russ, S., Eidsmo, L., and Gerlach, C. (2023). Graded expression of the chemokine receptor CX3CR1 marks differentiation states of human and murine T cells and enables cross-species interpretation. Immunity *56*, 1955-1974 e1910. 10.1016/j.immuni.2023.06.025.
239. Xie, W., Lee, B., Bruce, K., Lawler, C., Farrell, H.E., and Stevenson, P.G. (2022). CD4(+) T Cells Control Murine Cytomegalovirus Infection Indirectly. J Virol *96*, e0007722. 10.1128/jvi.00077-22.
240. Campbell, A.E., Cavanaugh, V.J., and Slater, J.S. (2008). The salivary glands as a privileged site of cytomegalovirus immune evasion and persistence. Med Microbiol Immunol *197*, 205-213. 10.1007/s00430-008-0077-2.
241. Jonjic, S., Pavic, I., Lucin, P., Rukavina, D., and Koszinowski, U.H. (1990). Efficacious control of cytomegalovirus infection after long-term depletion of CD8+ T lymphocytes. J Virol *64*, 5457-5464. 10.1128/JVI.64.11.5457-5464.1990.
242. Jonjic, S., Mutter, W., Weiland, F., Reddehase, M.J., and Koszinowski, U.H. (1989). Site-restricted persistent cytomegalovirus infection after selective long-term depletion of CD4+ T lymphocytes. J Exp Med *169*, 1199-1212. 10.1084/jem.169.4.1199.
243. Gallegos, A.M., Xiong, H., Leiner, I.M., Susac, B., Glickman, M.S., Pamer, E.G., and van Heijst, J.W. (2016). Control of T cell antigen reactivity via programmed TCR downregulation. Nat Immunol *17*, 379-386. 10.1038/ni.3386.

244. Allison, K.A., Sajti, E., Collier, J.G., Gosselin, D., Troutman, T.D., Stone, E.L., Hedrick, S.M., and Glass, C.K. (2016). Affinity and dose of TCR engagement yield proportional enhancer and gene activity in CD4+ T cells. Elife *5*. 10.7554/eLife.10134.
245. Silva-Sanchez, A., Meza-Perez, S., Liu, M., Stone, S.L., Flores-Romo, L., Ubil, E., Lund, F.E., Rosenberg, A.F., and Randall, T.D. (2023). Activation of regulatory dendritic cells by Mertk coincides with a temporal wave of apoptosis in neonatal lungs. Sci Immunol *8*, eadc9081. 10.1126/sciimmunol.adc9081.
246. Ruckwardt, T.J., Malloy, A.M., Morabito, K.M., and Graham, B.S. (2014). Quantitative and qualitative deficits in neonatal lung-migratory dendritic cells impact the generation of the CD8+ T cell response. PLoS Pathog *10*, e1003934. 10.1371/journal.ppat.1003934.
247. Cox, M.A., Kahan, S.M., and Zajac, A.J. (2013). Anti-viral CD8 T cells and the cytokines that they love. Virology *435*, 157-169. 10.1016/j.virol.2012.09.012.
248. Urban, S.L., and Welsh, R.M. (2014). Out-of-sequence signal 3 as a mechanism for virus-induced immune suppression of CD8 T cell responses. PLoS Pathog *10*, e1004357. 10.1371/journal.ppat.1004357.
249. Pipkin, M.E., Sacks, J.A., Cruz-Guilloty, F., Lichtenheld, M.G., Bevan, M.J., and Rao, A. (2010). Interleukin-2 and inflammation induce distinct transcriptional programs that promote the differentiation of effector cytolytic T cells. Immunity *32*, 79-90. 10.1016/j.immuni.2009.11.012.
250. Malek, T.R., and Castro, I. (2010). Interleukin-2 receptor signaling: at the interface between tolerance and immunity. Immunity *33*, 153-165. 10.1016/j.immuni.2010.08.004.
251. Yang, C.Y., Best, J.A., Knell, J., Yang, E., Sheridan, A.D., Jesionek, A.K., Li, H.S., Rivera, R.R., Lind, K.C., D'Cruz, L.M., et al. (2011). The transcriptional regulators Id2 and Id3 control the formation of distinct memory CD8+ T cell subsets. Nat Immunol *12*, 1221-1229. 10.1038/ni.2158.
252. Lee, J., Lee, K., Bae, H., Lee, K., Lee, S., Ma, J., Jo, K., Kim, I., Jee, B., Kang, M., and Im, S.J. (2023). IL-15 promotes self-renewal of progenitor exhausted CD8 T cells during persistent antigenic stimulation. Front Immunol *14*, 1117092. 10.3389/fimmu.2023.1117092.
253. Crouse, J., Kalinke, U., and Oxenius, A. (2015). Regulation of antiviral T cell responses by type I interferons. Nat Rev Immunol *15*, 231-242. 10.1038/nri3806.
254. Kohlmeier, J.E., Cookenham, T., Roberts, A.D., Miller, S.C., and Woodland, D.L. (2010). Type I interferons regulate cytolytic activity of memory CD8(+) T cells in the lung airways during respiratory virus challenge. Immunity *33*, 96-105. 10.1016/j.immuni.2010.06.016.
255. Kolumam, G.A., Thomas, S., Thompson, L.J., Sprent, J., and Murali-Krishna, K. (2005). Type I interferons act directly on CD8 T cells to allow clonal expansion and memory formation in response to viral infection. J Exp Med *202*, 637-650. 10.1084/jem.20050821.
256. Brewitz, A., Eickhoff, S., Dahling, S., Quast, T., Bedoui, S., Kroczek, R.A., Kurts, C., Garbi, N., Barchet, W., Iannacone, M., et al. (2017). CD8(+) T Cells Orchestrate pDC-XCR1(+) Dendritic Cell Spatial and Functional Cooperativity to Optimize Priming. Immunity *46*, 205-219. 10.1016/j.immuni.2017.01.003.
257. Bosteels, C., Neyt, K., Vanheerswynghels, M., van Helden, M.J., Sichien, D., Debeuf, N., De Prijck, S., Bosteels, V., Vandamme, N., Martens, L., et al. (2020). Inflammatory Type 2 cDCs Acquire Features of cDC1s and Macrophages to Orchestrate Immunity to Respiratory Virus Infection. Immunity *52*, 1039-1056 e1039. 10.1016/j.immuni.2020.04.005.
258. Brunner, T.M., Serve, S., Marx, A.F., Fadejeva, J., Saikali, P., Dzamukova, M., Duran-Hernandez, N., Kommer, C., Heinrich, F., Durek, P., et al. (2024). A type 1 immunity-restricted promoter of the IL-33 receptor gene directs antiviral T-cell responses. Nat Immunol *25*, 256-267. 10.1038/s41590-023-01697-6.
259. Bonilla, W.V., Frohlich, A., Senn, K., Kallert, S., Fernandez, M., Johnson, S., Kreutzfeldt, M., Hegazy, A.N., Schrick, C., Fallon, P.G., et al. (2012). The alarmin interleukin-33 drives protective antiviral CD8(+) T cell responses. Science *335*, 984-989. 10.1126/science.1215418.

260. Ding, M., Fei, Y., Zhu, J., Ma, J., Zhu, G., Zhen, N., Zhu, J., Mao, S., Sun, F., Wang, F., and Pan, Q. (2022). IL-27 improves adoptive CD8(+) T cells' antitumor activity via enhancing cell survival and memory T cell differentiation. Cancer Sci *113*, 2258-2271. 10.1111/cas.15374.
261. Arens, R., Loewendorf, A., Redeker, A., Sierro, S., Boon, L., Klenerman, P., Benedict, C.A., and Schoenberger, S.P. (2011). Differential B7-CD28 costimulatory requirements for stable and inflationary mouse cytomegalovirus-specific memory CD8 T cell populations. J Immunol *186*, 3874-3881. 10.4049/jimmunol.1003231.
262. Arens, R., Loewendorf, A., Her, M.J., Schneider-Ohrum, K., Shellam, G.R., Janssen, E., Ware, C.F., Schoenberger, S.P., and Benedict, C.A. (2011). B7-mediated costimulation of CD4 T cells constrains cytomegalovirus persistence. J Virol *85*, 390-396. 10.1128/JVI.01839-10.
263. Andreata, F., Moynihan, K.D., Fumagalli, V., Di Lucia, P., Pappas, D.C., Kawashima, K., Ni, I., Bessette, P.H., Perucchini, C., Bono, E., et al. (2024). CD8 cis-targeted IL-2 drives potent antiviral activity against hepatitis B virus. Sci Transl Med *16*, eadi1572. 10.1126/scitranslmed.adi1572.
264. Boyman, O., Kovar, M., Rubinstein, M.P., Surh, C.D., and Sprent, J. (2006). Selective stimulation of T cell subsets with antibody-cytokine immune complexes. Science *311*, 1924-1927. 10.1126/science.1122927.
265. Rubinstein, M.P., Lind, N.A., Purton, J.F., Filippou, P., Best, J.A., McGhee, P.A., Surh, C.D., and Goldrath, A.W. (2008). IL-7 and IL-15 differentially regulate CD8+ T-cell subsets during contraction of the immune response. Blood *112*, 3704-3712. 10.1182/blood-2008-06-160945.
266. Davey, M.S., Willcox, C.R., Joyce, S.P., Ladell, K., Kasatskaya, S.A., McLaren, J.E., Hunter, S., Salim, M., Mohammed, F., Price, D.A., et al. (2017). Clonal selection in the human Vdelta1 T cell repertoire indicates gammadelta TCR-dependent adaptive immune surveillance. Nat Commun *8*, 14760. 10.1038/ncomms14760.
267. Ravens, S., Schultze-Florey, C., Raha, S., Sandrock, I., Drenker, M., Oberdorfer, L., Reinhardt, A., Ravens, I., Beck, M., Geffers, R., et al. (2017). Human gammadelta T cells are quickly reconstituted after stem-cell transplantation and show adaptive clonal expansion in response to viral infection. Nat Immunol *18*, 393-401. 10.1038/ni.3686.
268. McMurray, J.L., von Borstel, A., Taher, T.E., Syrimi, E., Taylor, G.S., Sharif, M., Rossjohn, J., Remmerswaal, E.B.M., Bemelman, F.J., Vieira Braga, F.A., et al. (2022). Transcriptional profiling of human Vdelta1 T cells reveals a pathogen-driven adaptive differentiation program. Cell Rep *39*, 110858. 10.1016/j.celrep.2022.110858.
269. Beziat, V., Dalgard, O., Asselah, T., Halfon, P., Bedossa, P., Boudifa, A., Hervier, B., Theodorou, I., Martinot, M., Debre, P., et al. (2012). CMV drives clonal expansion of NKG2C+ NK cells expressing self-specific KIRs in chronic hepatitis patients. Eur J Immunol *42*, 447-457. 10.1002/eji.201141826.
270. Ruckert, T., Lareau, C.A., Mashreghi, M.F., Ludwig, L.S., and Romagnani, C. (2022). Clonal expansion and epigenetic inheritance of long-lasting NK cell memory. Nat Immunol *23*, 1551-1563. 10.1038/s41590-022-01327-7.
271. Vermijlen, D., Brouwer, M., Donner, C., Liesnard, C., Tackoen, M., Van Rysselberge, M., Twite, N., Goldman, M., Marchant, A., and Willems, F. (2010). Human cytomegalovirus elicits fetal gammadelta T cell responses in utero. J Exp Med *207*, 807-821. 10.1084/jem.20090348.
272. Hamann, D., Baars, P.A., Rep, M.H., Hooibrink, B., Kerkhof-Garde, S.R., Klein, M.R., and van Lier, R.A. (1997). Phenotypic and functional separation of memory and effector human CD8+ T cells. J Exp Med *186*, 1407-1418. 10.1084/jem.186.9.1407.
273. van Aalderen, M.C., van den Biggelaar, M., Remmerswaal, E.B.M., van Alphen, F.P.J., Meijer, A.B., Ten Berge, I.J.M., and van Lier, R.A.W. (2017). Label-free Analysis of CD8(+) T Cell Subset Proteomes Supports a Progressive Differentiation Model of Human-Virus-Specific T Cells. Cell Rep *19*, 1068-1079. 10.1016/j.celrep.2017.04.014.
274. Rousseliere, A., Delbos, L., Bressollette, C., Berthaume, M., and Charreau, B. (2021). Mapping and Characterization of HCMV-Specific Unconventional HLA-E-Restricted CD8 T Cell

Populations and Associated NK and T Cell Responses Using HLA/Peptide Tetramers and Spectral Flow Cytometry. Int J Mol Sci *23*. 10.3390/ijms23010263.

275. Sottile, R., Panjwani, M.K., Lau, C.M., Daniyan, A.F., Tanaka, K., Barker, J.N., Brentjens, R.J., Sun, J.C., Le Luduec, J.B., and Hsu, K.C. (2021). Human cytomegalovirus expands a CD8(+) T cell population with loss of BCL11B expression and gain of NK cell identity. Sci Immunol *6*, eabe6968. 10.1126/sciimmunol.abe6968.
276. Barreiro, P., Sanz, J.C., San Roman, J., Perez-Abeledo, M., Carretero, M., Megias, G., Vinuela-Prieto, J.M., Ramos, B., Canora, J., Martinez-Peromingo, F.J., et al. (2022). A Pilot Study for the Evaluation of an Interferon Gamma Release Assay (IGRA) To Measure T-Cell Immune Responses after SARS-CoV-2 Infection or Vaccination in a Unique Cloistered Cohort. J Clin Microbiol *60*, e0219921. 10.1128/jcm.02199-21.
277. Brand, I., Gilberg, L., Bruger, J., Gari, M., Wieser, A., Eser, T.M., Frese, J., Ahmed, M.I.M., Rubio-Acero, R., Guggenbuehl Noller, J.M., et al. (2021). Broad T Cell Targeting of Structural Proteins After SARS-CoV-2 Infection: High Throughput Assessment of T Cell Reactivity Using an Automated Interferon Gamma Release Assay. Front Immunol *12*, 688436. 10.3389/fimmu.2021.688436.
278. Renaudineau, Y., Abravanel, F., Izopet, J., Bost, C., Treiner, E., Congy, N., and Blancher, A. (2022). Novel T cell interferon gamma release assay (IGRA) using spike recombinant protein for COVID19 vaccine response and Nucleocapsid for SARS-Cov2 response. Clin Immunol *237*, 108979. 10.1016/j.clim.2022.108979.
279. Johnson, S.A., Phillips, E., Adele, S., Longet, S., Malone, T., Mason, C., Stafford, L., Jamsen, A., Gardiner, S., Deeks, A., et al. (2023). Evaluation of QuantiFERON SARS-CoV-2 interferon-gamma release assay following SARS-CoV-2 infection and vaccination. Clin Exp Immunol *212*, 249-261. 10.1093/cei/uxad027.
280. Sekine, T., Perez-Potti, A., Rivera-Ballesteros, O., Stralin, K., Gorin, J.B., Olsson, A., Llewellyn-Lacey, S., Kamal, H., Bogdanovic, G., Muschiol, S., et al. (2020). Robust T Cell Immunity in Convalescent Individuals with Asymptomatic or Mild COVID-19. Cell *183*, 158-168 e114. 10.1016/j.cell.2020.08.017.
281. Stafford, L.S., Valcarce, V., Henry, M., Neu, J., Parker, L., Mueller, M., Vicuna, V., Gowen, T., Cato, E., Kosik, I., et al. (2023). Detection of SARS-CoV-2 IgA and IgG in human milk and breastfeeding infant stool 6 months after maternal COVID-19 vaccination. J Perinatol *43*, 775-781. 10.1038/s41372-022-01581-5.
282. Fox, A., Marino, J., Amanat, F., Oguntuyo, K.Y., Hahn-Holbrook, J., Lee, B., Zolla-Pazner, S., and Powell, R.L. (2022). The IgA in milk induced by SARS-CoV-2 infection is comprised of mainly secretory antibody that is neutralizing and highly durable over time. PLoS One *17*, e0249723. 10.1371/journal.pone.0249723.
283. Edlow, A.G., Li, J.Z., Collier, A.Y., Atyeo, C., James, K.E., Boatin, A.A., Gray, K.J., Bordt, E.A., Shook, L.L., Yonker, L.M., et al. (2020). Assessment of Maternal and Neonatal SARS-CoV-2 Viral Load, Transplacental Antibody Transfer, and Placental Pathology in Pregnancies During the COVID-19 Pandemic. JAMA Netw Open *3*, e2030455. 10.1001/jamanetworkopen.2020.30455.
284. Garcia-Ruiz, I., Sulleiro, E., Serrano, B., Fernandez-Buhigas, I., Rodriguez-Gomez, L., Sanchez-Nieves Fernandez, D., Anton-Pagarolas, A., Esperalba-Esquerra, J., Frick, M.A., Camba, F., et al. (2021). Congenital infection of SARS-CoV-2 in live-born neonates: a population-based descriptive study. Clin Microbiol Infect *27*, 1521 e1521-1521 e1525. 10.1016/j.cmi.2021.06.016.
285. Nelde, A., Bilich, T., Heitmann, J.S., Maringer, Y., Salih, H.R., Roerden, M., Lubke, M., Bauer, J., Rieth, J., Wacker, M., et al. (2021). SARS-CoV-2-derived peptides define heterologous and COVID-19-induced T cell recognition. Nat Immunol *22*, 74-85. 10.1038/s41590-020-00808-x.
286. Harvey, W.T., Carabelli, A.M., Jackson, B., Gupta, R.K., Thomson, E.C., Harrison, E.M., Ludden, C., Reeve, R., Rambaut, A., Consortium, C.-G.U., et al. (2021). SARS-CoV-2 variants, spike mutations and immune escape. Nat Rev Microbiol *19*, 409-424. 10.1038/s41579-021-00573-0.

287. Telenti, A., Hodcroft, E.B., and Robertson, D.L. (2022). The Evolution and Biology of SARS-CoV-2 Variants. Cold Spring Harb Perspect Med *12*. 10.1101/cshperspect.a041390.
288. Geers, D., Shamier, M.C., Bogers, S., den Hartog, G., Gommers, L., Nieuwkoop, N.N., Schmitz, K.S., Rijsbergen, L.C., van Osch, J.A.T., Dijkhuizen, E., et al. (2021). SARS-CoV-2 variants of concern partially escape humoral but not T-cell responses in COVID-19 convalescent donors and vaccinees. Sci Immunol *6*. 10.1126/sciimmunol.abj1750.
289. Tarke, A., Coelho, C.H., Zhang, Z., Dan, J.M., Yu, E.D., Methot, N., Bloom, N.I., Goodwin, B., Phillips, E., Mallal, S., et al. (2022). SARS-CoV-2 vaccination induces immunological T cell memory able to cross-recognize variants from Alpha to Omicron. Cell *185*, 847-859 e811. 10.1016/j.cell.2022.01.015.
290. Tarke, A., Sidney, J., Methot, N., Yu, E.D., Zhang, Y., Dan, J.M., Goodwin, B., Rubiro, P., Sutherland, A., Wang, E., et al. (2021). Impact of SARS-CoV-2 variants on the total CD4(+) and CD8(+) T cell reactivity in infected or vaccinated individuals. Cell Rep Med *2*, 100355. 10.1016/j.xcrm.2021.100355.
291. Hoffmann, M., Arora, P., Gross, R., Seidel, A., Hornich, B.F., Hahn, A.S., Kruger, N., Graichen, L., Hofmann-Winkler, H., Kempf, A., et al. (2021). SARS-CoV-2 variants B.1.351 and P.1 escape from neutralizing antibodies. Cell *184*, 2384-2393 e2312. 10.1016/j.cell.2021.03.036.
292. Planas, D., Saunders, N., Maes, P., Guivel-Benhassine, F., Planchais, C., Buchrieser, J., Bolland, W.H., Porrot, F., Staropoli, I., Lemoine, F., et al. (2022). Considerable escape of SARS-CoV-2 Omicron to antibody neutralization. Nature *602*, 671-675. 10.1038/s41586-021-04389-z.
293. Tuekprakhon, A., Nutalai, R., Dijokaite-Guraliuc, A., Zhou, D., Ginn, H.M., Selvaraj, M., Liu, C., Mentzer, A.J., Supasa, P., Duyvesteyn, H.M.E., et al. (2022). Antibody escape of SARS-CoV-2 Omicron BA.4 and BA.5 from vaccine and BA.1 serum. Cell *185*, 2422-2433 e2413. 10.1016/j.cell.2022.06.005.
294. Planas, D., Veyer, D., Baidaliuk, A., Staropoli, I., Guivel-Benhassine, F., Rajah, M.M., Planchais, C., Porrot, F., Robillard, N., Puech, J., et al. (2021). Reduced sensitivity of SARS-CoV-2 variant Delta to antibody neutralization. Nature *596*, 276-280. 10.1038/s41586-021-03777-9.
295. Tarke, A., Zhang, Y., Methot, N., Narowski, T.M., Phillips, E., Mallal, S., Frazier, A., Filaci, G., Weiskopf, D., Dan, J.M., et al. (2023). Targets and cross-reactivity of human T cell recognition of common cold coronaviruses. Cell Rep Med *4*, 101088. 10.1016/j.xcrm.2023.101088.
296. Li, Y., Wang, W., Yang, F., Xu, Y., Feng, C., and Zhao, Y. (2019). The regulatory roles of neutrophils in adaptive immunity. Cell Commun Signal *17*, 147. 10.1186/s12964-019-0471-y.
297. Harvey, D.M., and Levine, A.J. (1991). p53 alteration is a common event in the spontaneous immortalization of primary BALB/c murine embryo fibroblasts. Genes Dev *5*, 2375-2385. 10.1101/gad.5.12b.2375.
298. Lemoine, F.M., Humphries, R.K., Abraham, S.D., Krystal, G., and Eaves, C.J. (1988). Partial characterization of a novel stromal cell-derived pre-B-cell growth factor active on normal and immortalized pre-B cells. Exp Hematol *16*, 718-726.
299. Hunt, J.S., Banerjee, S., and Pace, J.L. (1998). Differential expression and regulation of a human transgene, HLA-B27, in mouse placental and embryonic cell lines. Mol Hum Reprod *4*, 817-825. 10.1093/molehr/4.8.817.
300. Lemmermann, N.A., Gergely, K., Bohm, V., Deegen, P., Daubner, T., and Reddehase, M.J. (2010). Immune evasion proteins of murine cytomegalovirus preferentially affect cell surface display of recently generated peptide presentation complexes. J Virol *84*, 1221-1236. 10.1128/JVI.02087-09.
301. Marquardt, A., Halle, S., Seckert, C.K., Lemmermann, N.A.W., Veres, T.Z., Braun, A., Maus, U.A., Forster, R., Reddehase, M.J., Messerle, M., and Busche, A. (2011). Single cell detection of latent cytomegalovirus reactivation in host tissue. J Gen Virol *92*, 1279-1291. 10.1099/vir.0.029827-0.
302. Wickham, H. (2016). ggplot2 : Elegant Graphics for Data Analysis. Use R!,. 2nd ed. Springer International Publishing : Imprint: Springer,.

303. Hao, Y., Hao, S., Andersen-Nissen, E., Mauck, W.M., 3rd, Zheng, S., Butler, A., Lee, M.J., Wilk, A.J., Darby, C., Zager, M., et al. (2021). Integrated analysis of multimodal single-cell data. Cell *184*, 3573-3587 e3529. 10.1016/j.cell.2021.04.048.
304. Horst, A.M.H., A.P.; Gorman, K. B. (2020). palmerpenguins: Palmer Archipelago (Antarctica) penguin data. 10.5281/zenodo.3960218.
305. van der Maaten, L.J.P.H., G.E. (2008). Visualizing High-Dimensional Data Using t-SNE. Journal of Machine Learning Research *9*, 2579-2605.
306. van der Maaten, L.J.P. (2014). Accelerating t-SNE using Tree-Based Algorithms. Journal of Machine Learning Research *15*, 3221-3245.
307. Kolde, R. (2019). pheatmap: Pretty Heatmaps.
308. Wickham, H.A., M.; Bryan, J.; Chang, W.; D'Agostino McGowan, L.; François, R.; Grolemund, G.; Hayes, A.; Henry, L.; Hester, J.; Kuhn, M.; Pedersen, T. L.; Miller, E.; Bache, S. M.; Müller, K.; Ooms, J.; Robinson, D.; Seidel, D. P.; Spinu, V.; Takahashi, K.; Vaughan, D.; Wilke, C.; Woo, K.; Yutani, H. (2019). Welcome to the Tidyverse. Journal of Open Source Software *4*, 1686. 10.21105/joss.01686.
309. Jordan, S., Krause, J., Prager, A., Mitrovic, M., Jonjic, S., Koszinowski, U.H., and Adler, B. (2011). Virus progeny of murine cytomegalovirus bacterial artificial chromosome pSM3fr show reduced growth in salivary Glands due to a fixed mutation of MCK-2. J Virol *85*, 10346-10353. 10.1128/JVI.00545-11.
310. Tischer, B.K., Smith, G.A., and Osterrieder, N. (2010). En passant mutagenesis: a two step markerless red recombination system. Methods Mol Biol *634*, 421-430. 10.1007/978-1-60761-652-8_30.
311. Okabe, M., Ikawa, M., Kominami, K., Nakanishi, T., and Nishimune, Y. (1997). 'Green mice' as a source of ubiquitous green cells. FEBS Lett *407*, 313-319. 10.1016/s0014-5793(97)00313-x.
312. Hadjantonakis, A.K., Macmaster, S., and Nagy, A. (2002). Embryonic stem cells and mice expressing different GFP variants for multiple non-invasive reporter usage within a single animal. BMC Biotechnol *2*, 11. 10.1186/1472-6750-2-11.
313. Shinkai, Y., Rathbun, G., Lam, K.P., Oltz, E.M., Stewart, V., Mendelsohn, M., Charron, J., Datta, M., Young, F., Stall, A.M., and et al. (1992). RAG-2-deficient mice lack mature lymphocytes owing to inability to initiate V(D)J rearrangement. Cell *68*, 855-867. 10.1016/0092-8674(92)90029-c.
314. Cao, X., Shores, E.W., Hu-Li, J., Anver, M.R., Kelsall, B.L., Russell, S.M., Drago, J., Noguchi, M., Grinberg, A., Bloom, E.T., and et al. (1995). Defective lymphoid development in mice lacking expression of the common cytokine receptor gamma chain. Immunity *2*, 223-238. 10.1016/1074-7613(95)90047-0.
315. Barnden, M.J., Allison, J., Heath, W.R., and Carbone, F.R. (1998). Defective TCR expression in transgenic mice constructed using cDNA-based alpha- and beta-chain genes under the control of heterologous regulatory elements. Immunol Cell Biol *76*, 34-40. 10.1046/j.1440-1711.1998.00709.x.
316. Hogquist, K.A., Jameson, S.C., Heath, W.R., Howard, J.L., Bevan, M.J., and Carbone, F.R. (1994). T cell receptor antagonist peptides induce positive selection. Cell *76*, 17-27. 10.1016/0092-8674(94)90169-4.
317. Thordarson, G., Folger, P., and Talamantes, F. (1987). Development of a placental cell culture system for studying the control of mouse placental lactogen II secretion. Placenta *8*, 573-585. 10.1016/0143-4004(87)90028-2.
318. Pennington, K.A., Schlitt, J.M., and Schulz, L.C. (2012). Isolation of primary mouse trophoblast cells and trophoblast invasion assay. J Vis Exp, e3202. 10.3791/3202.
319. R Development Core Team (2021). R: A language and environment for statistical computing. (R Foundation for Statistical Computing).

9 Appendix

9.1 CV

Academic Formation

- PhD in Chemistry (University of Hamburg and Leibniz Graduate School "Infections"), 2018 — Present
    - Doctoral thesis: Congenital Cytomegalovirus infection: identification of factors determining vertical transmission and clinical outcome of infected neonates (Center for Diagnostics of the University Medical Center Hamburg-Eppendorf and Department Virus-Host Interactions of the Leibniz Institute of Virology; supervised by Prof. Dr. Felix Stahl, PhD and Prof. Dr. Wolfram Brune)
- MSc in Medical Life Sciences (University of Kiel, Germany), 2016 — 2018
    - Master's thesis: Characterization of intracellular and extracellular vesicles from human T cells (Institute for Immunology of the UKSH, Kiel, Germany; supervised by Prof. Ottmar Janßen and Prof. Andreas Tholey)
- BSc in Biology (University of the Algarve, Faro, Portugal), 2010 — 2014
    - Bachelor's thesis: Characterization of the taxonomy of the algae genus Cystoseira through phylogenetic inference methods (Center of Marine Sciences, Faro, Portugal; supervised by Prof. João Varela and Dr. Carolina Bruno de Sousa)

Publications

- **Fonseca Brito, L.**, Ostermann, E., Perez, A., Tödter, S., Indenbirken, D., Glau, L., Gieras, A., Brixel, R., Arens, R., Grundhoff, A., Arck, P., Diemert, A., Tolosa, E., Brune, W., Stahl, F.R.; Limited protection agains early-life cytomegalovirus infection results from deficiency of cytotoxic CD8 T cells. **bioRxiv. 2024**

- **Fonseca Brito, L.,** Tödter, S., Kottlau, J., Cermann, K., Spier, A., Petersen, E., Schäfer, I., Twerenbold, R., Aepfelbacher, M., Lütgehetmann, M., Stahl, F.R.; Performance of an interferon-γ release assay-based test for cell-mediated immunity to SARS-CoV-2. **Front Immunol. 2023**
- Tallarek, A.C., Urbschat, C., **Fonseca Brito, L**., Stanelle-Bertram, S., Krasemann, S., Frascaroli, G., Thiele, K., Wieczorek, A., Felber, N., Lütgehetmann, M., Markert, U.R., Hecher, K., Brune, W., Stahl, F., Gabriel, G., Diemert, A., Arck, P.C.. Inefficient Placental Virus Replication and Absence of Neonatal Cell-Specific Immunity Upon Sars-CoV-2 Infection During Pregnancy. **Front Immunol. 2021**
- **Fonseca Brito, L.,** Brune, W., Stahl, F.R., Cytomegalovirus (CMV) Pneumonitis: Cell Tropism, Inflammation, and Immunity. **Int. J. Mol. Sci. 2019**
- Bruno de Sousa, C., Cox, C., **Brito, L**., Pavão, M., Pereira, H., Ferreira, A., Ginja, C., Campino, L., Bermejo, R., Parente, M., Varela, J. Improved phylogeny of brown algae *Cystoseira* (Fucales) from the Atlantic-Mediterranean region based on mitochondrial sequences. **PLOS ONE 2019**.
- Bruno de Sousa, C., Lago, J., Macridachis, J., Oliveira, M., **Brito, L.**, Vizetto-Duarte, C., Florindo, C., Hendrickx, S., Maes, L., Morais, T., Uemi, M., Neto, L., Dionísio, L., Cortes, S., Barreira, L., Custódio, L., Alberício, F., Campino, L., Varela, J. Report of *in vitro* antileishmanial properties of Iberian macroalgae. **Nat. Prod. Res. 2018**

Conferences

- **Fonseca Brito, L.**, Ostermann, E., Perez, A., Tödter, S., Indenbirken, D., Glau, L., Gieras, A., Brixel, R., Arens, R., Grundhoff, A., Arck, P., Diemert, A., Tolosa, E., Brune, W., Stahl, F.R.; Defective T cell immunity in congenital cytomegalovirus infection. DEEP-DV International Symposium 2023
- **Fonseca Brito, L.**, Tödter, S., Perez, A., Ostermann, E., Virdi, S., Indenbirken, D., Glau, L., Gieras, A., Diemert, A., Tolosa, E., Brune, W., Stahl, F.R.; Defective early life CD8 T cell priming in congenital cytomegalovirus disease. Joint Meeting DgfI & ÖGAI 2022

- **Fonseca Brito, L.**, Tödter, S., Kottlau, J., Lütgehetmann, M., Stahl, F.R.; Test quality characteristics of an in-house laboratory diagnostic test for anti-SARS-CoV-2 cell-mediated immunity. Joint Meeting DgfI & ÖGAI 2022
- Kehribar, T.E., Urbschat, C., Schepanski, S., Tallarek, A.C., Stahl, F.R., **Fonseca Brito, L.**, Hecher, K., Thiele, K., Diemert, A., Arck, P.C.; Blunted humoral and cellular immune response in pregnant women upon vaccination against SARS-CoV-2 infection. European Society for Reproductive Immunology, 2022
- Bruno de Sousa, C., Macridachis, J., **Brito, L.,** Oliveira, M., Florindo, C., Alberício, F., Campino, L., Barreira, L., Custódio, L., Varela, J.; In vitro inhibitory effect of iberian species of the *Cystoseira* genus upon *Leishmania infantum*. British Society for Parasitology, 2014.

Languages

- Written and verbal fluency in English, Portuguese and Cape Verdean Creole
- Moderate knowledge of Spanish and German
- Basic knowledge of French

9.2 List of abbreviations

ACE2 - Angiotensin-Converting Enzyme 2

AF - Alexa Fluor

APC (fluorophore) - Allophycocyanin

APC - Antigen Presenting Cell

AUC - Area Under the Curve

Bach2 - BTB and CNC Homology 1, Basic Leucine Zipper Transcription Factor 2

BLIMP1 - B-Lymphocyte-Induced Maturation Protein 1

BV - Brilliant Violet

CCL - C-C Motif Chemokine Ligand

CCR - C-C Chemokine Receptor

CD - Cluster of Differentiation

CDR3 - Complementarity-Determining Region 3

con - Conventional

COVID-19 - Coronavirus Disease 2019

CX3CR - C-X3-C Motif Chemokine Receptor

CXCR - C-X-C Motif Chemokine Receptor 3

cCMV - Congenital Cytomegalovirus

cDC1 - Conventional Type 1 Dendritic Cell

CMI - Cell-Mediated Immunity

CM - Central Memory

CMV - Cytomegalovirus

DAPI - 4',6-Diamidino-2-Phenylindole

DMEM - Dulbecco's Modified Eagle Medium

DMEM/F12 - Dulbecco's Modified Eagle Medium/Ham's F-12 Mixture

DN - Double-Negative

DAP12 - DNAX Activating Protein of 12kDa

DC - Dendritic Cell

dpi - Days post-infection

E - Early

EDTA - Ethylenediaminetetraacetic Acid

eCFP - Enhanced Cyan Fluorescent Protein

eGFP - enhanced Green Fluorescent Protein

ELISA - Enzyme-Linked Immunosorbent Assay

ELISpot - Enzyme-Linked Immunospot Assay

EM - Effector Memory

Eomes - Eomesodermin

E- - Early

FACS - Fluorescence-Activated Cell Sorting

FCS - Fetal Calf Serum

FcR - Fc Receptor

FITC - Fluorescein Isothiocyanate

Foxo1 - Forkhead Box O1

Foxp3 - Forkhead Box P3

FSC - Forward Scatter

gpCMV - Guinea Pig Cytomegalovirus

GZM - Granzyme

GVHD - Graft-Versus-Host Disease

HCMV - Human Cytomegalovirus

HIV - Human Immunodeficiency Virus

ICAM-1 - Intercellular Adhesion Molecule-1 I

I**D-1** - Inhibitor of DNA Binding-1

IGRA - Interferon-Gamma Release Assay

IFN - Interferon

Ifit - Interferon-Induced Protein with Tetratricopeptide Repeats

Ifnar1- Interferon Receptor Alpha Chain

IgE - Immunoglobulin E

IgG - Immunoglobulin G

IgM - Immunoglobulin M

IL - Interleukin

Il2ra - Interleukin-2 Receptor Alpha Chain

kbp - Kilobase Pairs

KLRG1 - Killer Cell Lectin-Like Receptor Subfamily G, Member 1

L - Late

Lef1 - Lymphoid Enhancer-Binding Factor 1

LCMV - Lymphocytic Choriomeningitis Virus

MACS - Magnetic-Activated Cell Sorting

MAIT - Mucosa-Associated Invariant T

MCK2 - MCMV Chemokine 2

MdFI - Median Fluorescence Intensity

MHC - Major Histocompatibility Complex

MCMV - Murine Cytomegalovirus

Mtb - Mycobacterium tuberculosis

MOI - Multiplicity of Infection

NIF - Nodular Inflammatory Foci

NKG2C - Natural Killer Group 2C

NK - Natural Killer

NRP1 - Neuropilin-1

NRP2 - Neuropilin-2

NC - Nucleocapsid

ORF - Open Reading Frame

PBS - Phosphate Buffered Saline

PC - Principal Component

PDGFR-α - Platelet-Derived Growth Factor Receptor-Alpha

PE - Phycoerythrin

PFA - Paraformaldehyde

PFU - Plaque-Forming Units

pMHC - Peptide-Major Histocompatibility Complex

PND - Post-Natal Day

PRF - Perforin

Prdm1 - PR Domain Zinc Finger Protein 1 (BLIMP1)

RBD - Receptor Binding Domain

RhCMV - Rhesus Macaque Cytomegalovirus

RLU - Relative Light Units

RT-PCR - Real-Time Polymerase Chain Reaction

SARS-CoV-2 - Severe Acute Respiratory Syndrome Coronavirus 2

Sell - L-Selectin (CD62L)

S1pr5 - Sphingosine-1-Phosphate Receptor 5

SNHL - Sensorineural Hearing Loss

SM9-1 - Mouse Placental Trophoblast Cell Line

SSC - Side Scatter

Tcf7 - Transcription Factor 7

TCR - T Cell Receptor

TEMRA - Terminally Differentiated Effector Memory T Cells

Th - T helper

Tbx21 - T-Box Transcription Factor 21 (T-BET)

TGF-β - Transforming Growth Factor Beta

TNF-α - Tumor Necrosis Factor-Alpha

TORCH - Toxoplasma, Others, Rubella, Cytomegalovirus, and Herpes Simplex

t-SNE - t-distributed stochastic neighbor embedding

UMAP - Uniform Manifold Approximation and Projection

UL - Unique Long

VEGF - Vascular Endothelial Growth Factor

ZEB - Zinc-Finger E-Box Binding Homeobox

9.3 List of hazardous substances

substance	GHS symbol	hazard statements	precautionary statements
2-mercaptoethanol		H317, H361, H402	P261, P201, P273, P280, P272, P202
ammonium chloride		H302, H319	P264. P280, P301+P330+P331, P305+P351+P338, P312
ethanol		H319	P210. P264, P280, P303+P361+P353, P305+P351+P338, P337+P313
staphylococcal enterotoxin b		H300+H310+H330, H315, H319, H335	P262, P264, P280, P302+P352+P310, P304+P340+P310, P305+P351+P338
phorbol- 12-myristate 13-acetate		H301+H310+H330, H314, H317, H333+H304, H340, H352, H351	P202, P260, P280, P303+P361+P353, P304+P340+P310, P305+P351+P338
hydrochloric acid		H314, H335	P280, P303+P361+P353, P304+P340, P305+P351+P338, P310
isopropanol		H319, H336	P210, P240, P261, P280, P305 + P351 + P338
methanol		H301 + H311 + H331, H370	P210, P240, P280, P301 + P310, P302 + P350, P304 + P340
parafomaldehyde	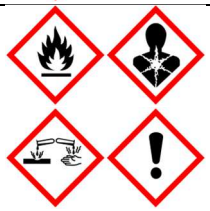	H228, H302 + H332, H315, H317, H318, H335, H341, H350	P210, P280, P301 + P312, P304 + P340 + P312, P305 + P351 + P338, P308 + P313
penicillin/streptomycin		H317, H361	P201, P202, P261, P272, P280
4′,6-diamidino-2-phenylindole		H315, H317, H335	P261, P264, P271, P272, P280, P302 + P352

9.4 Acknowledgments

I would like to first thank my supervisors, Prof. Dr. Felix Stahl and Prof. Dr. Wolfram Brune, for the opportunity to work on this project. Thank you Felix for the several discussions that have greatly stimulated my critical thinking skills and contributed to the development of my scientific mindset.

Thank you Prof. Hans-Willi Mittrücker for agreeing to be one of the reviewers of my thesis, and Professors Kay Grünewald and Hartmut Schlüter for being members of my examining committee.

Thank you Hanna for critically reading my thesis and the helpful feedback.

Thank you Eleonore Ostermann for the support, collaboration and long discussions on the CMV projects. Thank you Silvia Tödter for the assistance, especially during the initial phases of my research here and for introducing me to the key techniques employed in this project.

Additionally, I would like to acknowledge the UKE animal caretakers, particularly Nicole Lüder, for managing the breeding of my mice and ensuring that my worked proceeded smoothly. Thank you to the UKE Flow Cytometry Facility, the UKE Microscopy Imaging Facility, and the UKE Institute of Anatomy for providing critical infrastructure.

Thank you Dr. Samanjeet Virdi, who assisted me in analyzing the single-cell RNA sequencing dataset, as well as Dr. Daniela Indenbirken for her help in processing the samples.

Thank you to Prof. Dr. Eva Tolosa, Romy Hackbusch, Dr. Anna Gieras, and Dr. Kati Tillack for their contributions in processing and analyzing samples from the HCMV study. Thank you to Dr. Anna Perez, Dr. Mirja Pagenkemper, Dr. Anke Diemert, and Prof. Dr. Petra Arck for their efforts in recruiting donors and providing me with such precious samples. I would like to thank the Hamburg City Health Cohort for providing essential samples and data for the SARS-CoV-2 project. Thank you Katrin Cermann, Anthea Spier, and Prof. Dr. Marc Lütgehetmann for their support in processing the CMI test samples.

Thank you to my current and former colleagues in our lab: Silvia, Julian, Lena, Valentina, Lama, and Doro, for their support and assistance. Thank you also to the present and former members of the LIV research unit on virus-host interactions: Elena,

Olha, Kerstin, Renke, Enrico, Giada, Yingqi, Tianyu, Martina, Xuan, Theo, Jiajia, Ina, Michaela, Laura, Laura, Tommaso, and Vicky—for their valuable input and the great moments shared.

Thank you to my (former) colleagues in Campus Forschung, especially Hanna, Chandini, Manasi, Siti, Min, Nina, Stuart, Sandra, Claudia, Marion, Josi, and Kristin for raising a relaxed environment in the lab.

Thank you to my Hamburg family Christina, Edgar, Djemma, Susi, and Sebi for their support in helping me settle in this city.

Finally, my deepest gratitude goes to my family and Irke for their endless love and support throughout this journey.

10 Statement of Authorship

I hereby declare and affirm that this doctoral dissertation is my own work and that I have not used any aids and sources other than those indicated. If electronic resources based on generative artificial intelligence (gAI) were used in the course of writing this dissertation, I confirm that my own work was the main and value-adding contribution and that complete documentation of all resources used is available in accordance with good scientific practice. I am responsible for any erroneous or distorted content, incorrect references, violations of data protection and copyright law or plagiarism that may have been generated by the gAI.

Hamburg, 26.07.2024